Development of antibodies to human transient receptor potential vanilloid 1 for future targeting of therapeutics to sensory neurons

Thesis submitted for the degree

of

Master of Science by Research

by

Marie O'Connell, B.Sc(Ed), M.Sc.

Supervised by

Prof. J. Oliver Dolly

International Centre for Neurotherapeutics

School of Biotechnology

Dublin City University

Ireland

January 2014

Declaration

I hereby certify that this material, which I now submit for assessment in the programme of study leading to the award of Master of Science by research is entirely my own work, and that I have exercised reasonable care to ensure that the work is original, and does not to the best of my knowledge breach any law of copyright, and has not been taken from the work of others save and to the extent that such work has been cited and acknowledged within the text of my work.

Signed: marie o'connell (Marie O'Connell) **ID No.:** 58116702

Date: 27th January 2014

Dedication

I would like to dedicate this work to my mother Doreen. You are the best fighter I know, you have been through so much but you continue to push through without complaints. I am so grateful to have such a strong, positive, selfless and inspirational mother like you; you are the greatest!

Table of Contents

Abstract

Chronic pain affects ~3 % of the world population. Interestingly, relief can be achieved with botulinum neurotoxin type A (BoNT/A), which blocks neurotransmitter release. An *in vivo* model of neuropathic pain, established in rat, revealed attenuation by BoNTs of chronic pain symptoms including heat hyperalgesia, weight bearing, mechanical and cold allodynia.

With the long-term aim of developing a more selective therapy, a means was sought for producing antibodies to target Zn^{2+}-dependent proteases of BoNT exclusively into sensory neurons in order to cleave and inactivate SNAREs [soluble NSF (N-ethylmaleimide sensitive factor) attachment protein receptors] - proteins essential for exocytosis. Thus, single chain variable fragment (scFv) and polyclonal antibodies were generated against transient receptor potential vanilloid 1 (TRPV1). scFvs obtained bound the TRPV1-A antigen but were unable to detect TRPV1 in transfected mammalian cells. Rabbit polyclonal antibodies specific for human TRPV1 were produced, characterised and purified. Encouragingly, these antibodies bound saturatably to TRPV1-expressing cells (but not control) and got internalised, as illustrated by vesicular staining following stimulation with capsaicin.

This data supports the ability of BoNT to relieve chronic pain, and the specific TRPV1-A antibodies produced may be applicable for future targeting of SNARE proteases to sensory neurons.

Acknowledgements

I would like to acknowledge the following people for their support throughout this work:

I would firstly like to thank the PRTLI funded Targeted Therapeutics and Theranostics programme for giving me the opportunity to pursue this research. I am extremely grateful for this generous support.

I would like to thank Prof. J. Oliver Dolly for supervising me throughout my time at ICNT. Your door was always open if I wanted advice. I also would like to offer my gratitude for giving me the opportunity to co-write the review with you, it was a valuable experience.

I offer my special thanks to Ms. Sharon Whyte; you bring such positivity everywhere you go. You are a breath of fresh air.

I offer my gratitude to Mr. Sanjay Boddul who provided me with support in the lab and company for tea and lunch.

Thank you to ICNT members, both past and present. I offer my particular gratitude to Drs. Matthew A. King, Om Prakash, Tom Zurawski, Laura Casals-Díaz, Liam O'Hara, Marie Le Berre, Bandita Bagchi and Ms. Catherine Hagedorn. I am also extremely grateful to Ms. Carolyn Wilson, Ms. Gillian O'Meara, Dr. Rachel Gurrell and Prof. Richard O'Kennedy for your support and contribution to this research.

I would like to acknowledge Prof. John McCafferety, colleagues at Cambridge University and Dr. Arman Rahman for their contribution to the recombinant antibody aspect of the project.

Throughout this research, I have become more involved in sports; running, football and boxing. This has introduced me to many new friends, inspirational athletes and coaches (including Clare Grace, Billy Roche and John, Rivie and Jimmy McCormack) who see life with such positivity and who are not afraid to work hard to achieve their goals. I am forever grateful for this opportunity.

I offer my appreciation to friends who have been there for me throughout including; Krystal Cronin, Bernadette O'Donovan, Shona McCarrick, Jun Wang, Claire Leonard, Suzanne Walsh, Joanna Walsh, Fiona Martin, Ailsa Byrne and Orla Brennan.

I am forever grateful to Mr. Brian Kirby for your continuous support throughout; you have given me ongoing encouragement, you listened to me talk endlessly about experiments and provided me with sound advice. I feel very lucky to have such a wonderful person as you as part of my life.

And lastly, I would like to especially thank my parents Donal and Doreen and my brother Pat for your support throughout my education. You both worked hard to give everything to Pat and me. I am extremely proud to have such a great family, it is now time that I give something back to you.

List of abbreviations

/A, Serotype A

ANOVA, Analysis of variance

Ara-C, Cytosine-ß-D-arabinofuranoside

BoNT/A, B, C1, D, E, F and G, Botulinum neurotoxin serotype A, B, C1, D, E, F and G

BOTOX®, Botulinum toxin A-haemagglutinin complex

BSA, Bovine serum albumin

CGRP, Calcitonin gene-related peptide

CNS, Central nervous system

C-terminal, Carboxyl-terminal

DAPI, 4', 6'-diamino-2-phenylindole

DC, Di-chain

DMEM, Dulbecco's modified Eagle's medium

DRG, Dorsal root ganglion

DTT, Dithiothreitol

ECL, Enhanced chemiluminescence

EDTA, Ethylenediamintetracetic acid

ELISA, Enzyme linked immunosorbent assay

Fc, Constant fragment

FLAG® tag, an 8-amino acid peptide (Asp-Tyr-Lys-Asp-Asp-Asp-Asp-Lys)

HBSS, Hanks buffered salt solution

Hc, Binding domain

HC, Heavy chain

HEK, Human embryonic kidney 293 cells

HEPES, N-2-hydroxyethylpiperazine-N'-2-ethanesulfonic acid

H_N, Translocation domain

hTRPV1, Transient receptor potential vanilloid subfamily, member 1 from human

IHC, Immunohistochemistry

IMAC, Immobilized metal ion affinity chromatography

IPTG, Isopropyl β-D-1-thiogalactopyranoside

K, Kilo

KLH, Keyhole limpet hemocyanin

LC, Light chain

LCH_N, Light chain and translocation domain

$LC.H_N.H_{CN}$/A, Comprised of the light chain, translocation domain and N-terminal heavy chain of BoNT/A, but lacking the binding domain

N, Sample size

NGF, Nerve growth factor

NO, Nitric oxide

NPY, Neuropeptide Y

O.D., Optical density

P, Probability

P5, Postnatal day 5

PBS, Phosphate buffered saline

PBST, Phosphate buffered saline with Tween 20

PCR, Polymerase chain reaction

PFA, Paraformaldehyde

PMSF, Phenylmethylsulfonyl fluoride

PNS, Peripheral nervous system

PVDF, Polyvinyllidene Fluoride

rTRPV1, Transient receptor potential vanilloid subfamily, member 1 from rat

SC, Single chain

scFv, Single-chain variable fragment

SDS, Sodium dodecyl sulphate

SDS-PAGE, Sodium dodecyl sulfate polyacrylamide gel electrophoresis

SEM, Standard error of the mean

SNAP-23, Synaptosomal-associated protein of Mr = 23 K

SNAP-25, Synaptosomal-associated protein of Mr = 25 K

SNARE, Soluble N-ethylmaleimide-sensitive factor attachment protein receptor

SNL, Spinal nerve ligation

SP, Substance P

SV2, Synaptic vesicle protein 2

TBS, Tris-buffered saline

TBST, TBS with Tween-20

TM, Transmembrane

TMB, 3,3’,5,5’-tetramethylbenzidine

VAMP, Vesicle-associated membrane protein

WB, Western blot

List of key definitions

Pain- an unpleasant subjective sensory experience initiated by noxious stimuli, inflammation or damage to the nervous system.

Nociceptive pain- this is a short acting response to a noxious stimulus.

Nociceptors- these are sensory receptors in the peripheral nervous system.

Congenital analgesia- an inability to sense pain due to a nerve growth factor tyrosine kinase A mutation that results in a loss of high-threshold sensory neurons.

Inflammatory pain- an acute pain produced by tissue damage resulting in the release of peripheral inflammatory mediators to the affected inflamed area to promote healing.

Allodynia- a normally non-painful stimulus is perceived as painful.

Hyperalgesia- responses to noxious stimuli are enhanced.

Neuropathic pain- pain produced from lesions to the peripheral or central nervous systems.

Secondary hyperalgesia- the transfer of sensitivity from injured to the non-injured regions.

Dysfunctional pain- this is pain that occurs in the absence of inflammation, lesion to the nervous system or noxious stimulus.

Peripheral sensitisation- this term is used to describe the release of neuropeptides and inflammatory mediators that leads to a decrease in the threshold of nociceptive afferents and enhanced responsiveness of the peripheral terminals of nociceptors.

Central sensitisation- Release of neuropeptides and inflammatory mediators during the process of peripheral sensitisation, leads to amplification of the

impulses transferred to cell bodies of either the dorsal root or trigeminal ganglia, producing central sensitisation.

List of figures

List of tables

Posters, presentations and publications

Posters:

Marie O'Connell, Sanjay Boddul, Jiafu Wang, Jianghui Meng and J. Oliver Dolly. **A pain laboratory to screen therapeutics *in vivo***: presented to the (Bio) pharmaceuticals and Pharmacological Sciences meeting (2011) at Dublin City University, Glasnevin, Dublin 9.

Presentations:

Marie O'Connell*, Jiafu Wang*, and J. Oliver Dolly* (In collaboration with Weredeselam M. Olango† and David Finn†). **Novel long-acting anti-nociceptives evaluated in an animal pain model:** presentation to the (Bio) pharmaceuticals and Pharmacological Sciences meeting (2011) at Dublin City University, Glasnevin, Dublin 9.

*International Centre for Neurotherapeutics, Dublin City University, Glasnevin, Dublin 9.

†National University of Ireland, Galway, Ireland.

Publications:

J. Oliver Dolly and **Marie Ann O'Connell** (2012). **Neurotherapeutics to inhibit exocytosis from sensory neurons for the control of chronic pain**. Curr Opin Pharmacol **12**(1): 100-108.

1. GENERAL INTRODUCTION

1.1. History of pain

In the past, limited knowledge of anatomy and bodily functions meant that pain was not understood. Aristotle (384-322 BC) considered the heart to be essential for life and the centre for feelings; however, he regarded the brain as unimportant. He displayed a keen interest in sensation and believed that touch was linked to pain and that animals would not survive if they did not possess the ability to sense touch. He considered pain to be an emotion. An anatomical investigation could not be explored at the time as vivisection and dissection of the dead were not allowed (Perl, 2011). Galen (130-201 AD), a physician-philosopher of Alexandria, was able to use vivisection to oppose Aristotle's views. He believed that the brain was responsible for feeling and regarded pain as a sensation (Perl, 2007). This theory was developed, by a Muslim philosopher and physician named Avicenna (980-1037 AD), who proposed pain to be an independent sensation from touch (Dallenbach, 1939).

In the 15th century, Leonardo da Vinci, an exceptional artist, became deeply absorbed in science and incorporated the views of Aristotle, Galen, Avicenna with his own (Figure 1-1). He dissected human corpses and arrived at the viewpoint that pain was a sensation that was relayed by nerves that also transfer information about touch (Perl, 2011).

Many theories of pain grew from these initial findings; however, the scientific tools necessary to test such hypothesises were not fully established at that time. The eighteenth century brought about huge advancement in conventional thinking from Isaac Newton and Thomas Hartley, who postulated that neuronal transmission were vibrations that travelled through nerves. A more detailed account of the evolution of pain theories can be found in the following insightful articles (Perl, 2011, Perl, 2007). Many great people have contributed to our knowledge of pain today and we are fortunate to possess the scientific tools necessary to investigate current views; however, many unanswered questions still remain.

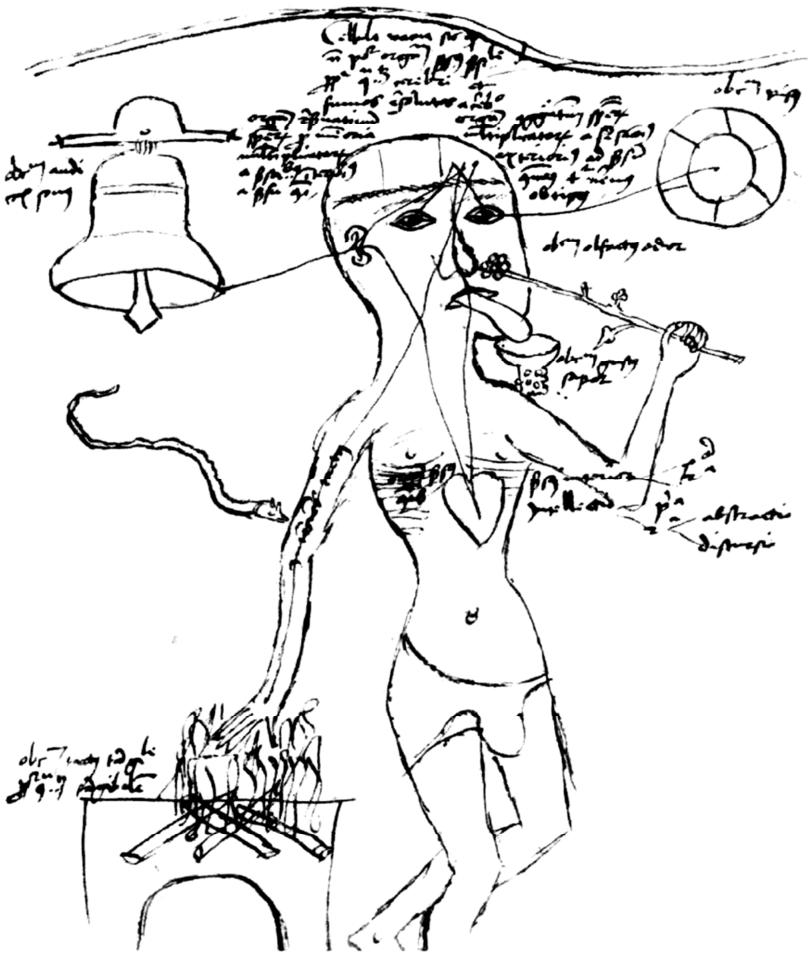

Figure 1-1 A 15th century portrait depicting early Renaissance theories of sensation.

The Aristotelian concept of the heart playing a central role is portrayed along with Galen's and Avicenna's ideas of the involvement of the nervous system. It includes the five senses (vision, taste, hearing, smell and pain). Pain induced by either noxious stimuli or toxin is depicted along with the transmission of pain signals through nerves. Image taken from Perl, 2011.

1.2. Anatomy and physiology of pain

1.2.1. Nociceptors

Pain receptors (nociceptors) are free nerve endings of nerve fibres, located throughout the body, that convert noxious stimuli into electrical impulses and transfer these signals along axons (Julius and Basbaum, 2001). First-order afferent nerve fibres are classified according to their type, i.e. A, B or C and are characterised on the basis of their structure, diameter and conduction velocities

(Figure 1-2). The two types of primary afferent nociceptors include Aδ and C fibres. B fibres are myelinated and transmit autonomic impulses. **Aδ** fibres are small diameter (1-5 µm) lightly myelinated, fast conducting afferents with velocities of 12-30 m/s that make up ~20% of the pain afferents. Activation of these fibres generates a localised 'sharp' immediate pain. ***C fibres*** account for ~ 80% of the nociceptor primary afferents, they are unmyelinated, have low conduction velocities (< 2 m/s), and arise from polymodal nociceptors (nociceptors that respond to a wide range of noxious stimuli). Pain perceived by C fibres is not localised and is described as 'dull or aching', it usually takes longer for these fibres to receive input from noxious stimuli due to their lower conduction velocities. Their cell bodies are positioned in the dorsal root or trigeminal ganglia and axons terminate in the dorsal horn of the spinal cord.

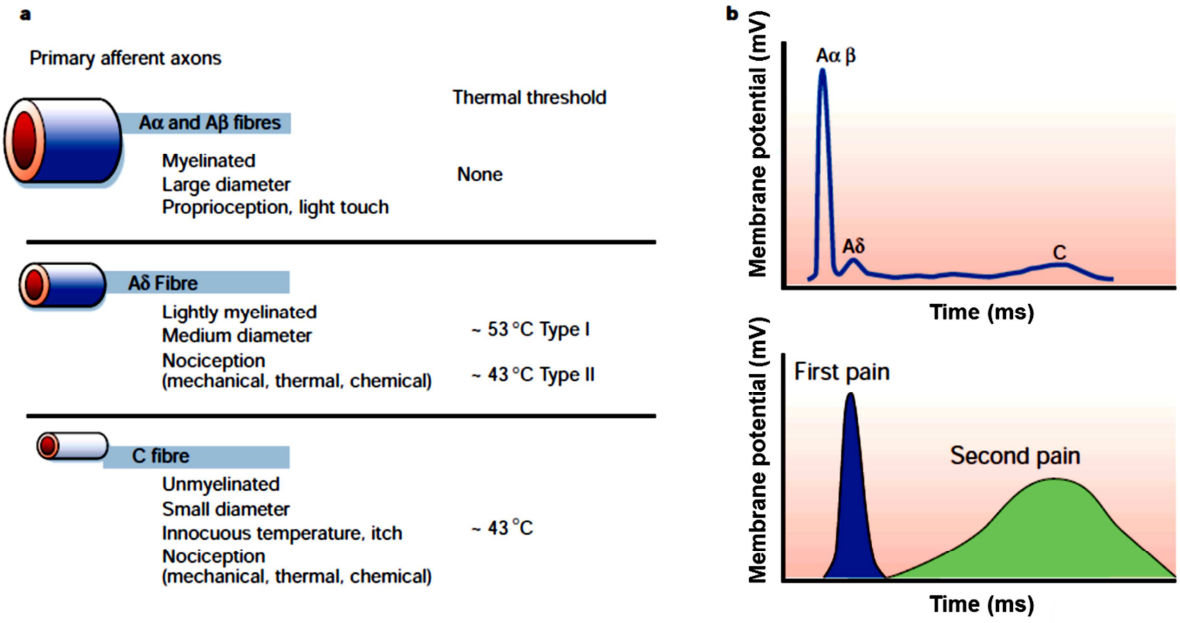

Figure 1-2 Classification of nociceptors.

a) *Small (Aδ) and medium- to large-diameter (Aα, β) myelinated afferent fibres are found in peripheral nerves, as well as small-diameter unmyelinated afferent fibres (C).* ***b)*** *Schematic of the action potential of a peripheral nerve. Aδ or C fibres are most widely expressed in nociceptors, and differ in their conduction velocities (6–25 and ~1.0 m* s^{-1}*, respectively) which represent the first (fast) and second (slow) responses to painful stimuli. Image taken from Julius and Basbaum, 2001.*

1.2.2. Neuroeffector functions

In conditions of chronic pain, peripheral nociceptors are continually activated even in the absence of stimuli, usually indicative of an abnormal chemical processing environment. These nociceptors release, by exocytosis, neuropeptides and inflammatory mediators such as substance P, calcitonin gene-related peptide (CGRP), brain-derived neurotrophic factor, bradykinin, histamine, nerve growth factor, serotonin, noradrenaline, adenosine, interleukins and neuropertide Y; efflux of others (nitric oxide, prostaglandins and H^+) occurs by non-exocytotic means (Dray, 1995). Some of these substances are primary activators of nociceptors, while others act secondarily by sensitising nerve terminals to reduce their activation thresholds.

1.2.3. The spinal cord and transmission of signals

The spinal cord plays a crucial role in the pain pathway as a great deal of information processing takes place here, especially in the dorsal horn of grey matter. The spinal cord is separated incompletely into two symmetrical halves by the dorsal median sulcus and ventral median fissure. A small central canal is located in the centre; surrounding this canal is the spinal grey matter, composed of nerve cell bodies, their dendrites and synaptic connections. The outer region of the spinal cord contains white matter comprising of ascending and descending nerve fibres. The grey matter is H/butterfly shaped; the dorsal horn is usually arranged into six numbered layers/laminae based on their Rexed's light microscopy classification (Figure 1-3). Pain afferents from the dorsal root terminate in both laminae I (marginal zone) and II (substantia gelatinosa). Signals transferred from Aδ fibres are relayed to the lateral spinothalmic tract, travels to the ventrobasal and posterior nuclei or to the thalmic relay nuclei and onwards to the post central somatosensory area of the cerebral cortex. Signals sent by C fibres reach the medial nucleus of the thalamus, and continue to the pre-frontal somatosensory region of the cerebral cortex.

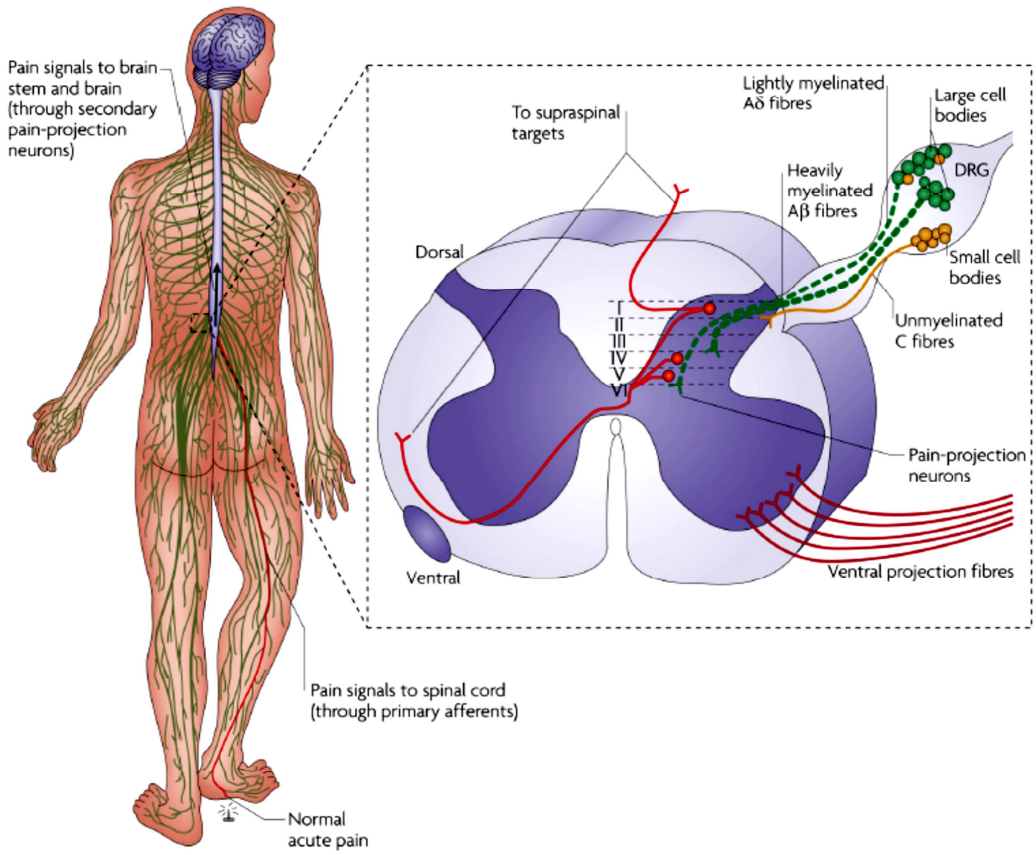

Figure 1-3 Spinal cord and transmission of pain signals.

Pain signals are propagated to the spinal cord dorsal horn via pain receptors/nociceptors. Acute nociceptive pain, stimulates the release of pain mediators from primary afferent terminals that project to laminae I, IV and V in the spinal cord dorsal horn. Aβ, Aδ and C fibres also project to laminae II–VI. Pain signals from the dorsal root ganglia (DRG) are sent to the dorsal spinal cord, brain stem and eventually to the brain, where pain is perceived. Image taken from Milligan and Watkins, 2009.

1.2.4. The pain gate theory

Aβ fibres convey sensations of light touch (normally innocuous stimuli), and those that innervate the same segment of C fibres have the ability to inhibit C fibre mediated pain; this is referred to as the pain ***gate control theory***, proposed by Melzack and Wall in 1965 (Melzack and Wall, 1965). This concept is described as a gating mechanism in the spinal dorsal horn; firing of large C fibres, inhibit interneurons so that input is then transferred to the second order neurone, leading to pain. Aβ fibres can reactivate the interneurone and close

the gate, preventing pain signals from being propagated onwards to relieve pain. (Figure 1-4).

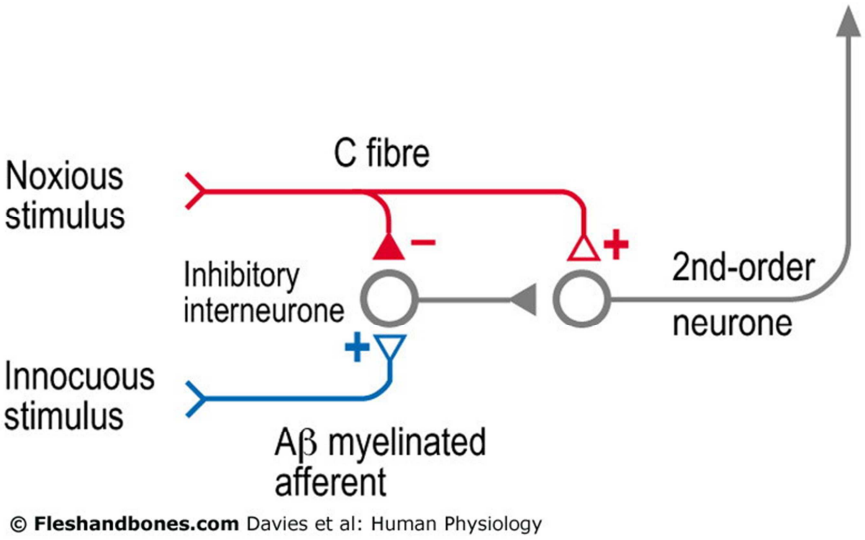

Figure 1-4 Schematic of the pain gate control theory.

The gate control theory is a term used to describe the regulation of activity between Aβ- and C-fibres. When C-fibre input is greater than that of Aβ-fibres, the gate opens, permitting activation of the second order neurone. Aβ fibres can disinhibit the interneurone, closing the gate, resulting in pain control.

1.2.5. Descending inhibitory pathways

Descending pain modulation is controlled by various areas of the brain including the pariaqueuctal grey matter in the midbrain and the region surrounding the nucleus raphe magnus in the medulla. The periaqueductal grey matter receives neuronal messages via a range of CNS sources including the thalamus, hypothalamus, cerebral cortex and spinal cord (Figure 1-5). The periaqueductal grey matter transmits its analgesic effect by activation of the nucleus raphe magnus and the nearby medulla. Pain mediating neurons containing 5-hydroxytryptamine and noradrenaline primarily arise from the nucleus raphe magnus and medulla, respectively, and project from the medulla to the dorsal horn.

1.2.6. Ascending pain pathways

Secondary pain processes project to the contralateral spinothalamic and spinoreticular tracts. The spinothalamic tract comprises of fibres from laminae I and V of the dorsal horn that synapse in the ventrobasal thalamic nuclei. Fibres from these nuclei project within the posterior region of the internal capsule to parts of the cerebral cortex including the somatosensory cortex. The spinorecticular tract includes medial fibres from the spinothalamic tract that project to the nuclei in the midbrain retricular formation, the nucleus raphe magnus, the periaqueductal grey matter, the hypothalamus and the medial nuclei of the thalamus (Figure 1-5). Projections from these regions transfer information to various regions of the brain such as the cortex and limbic system (Basbaum et al., 2009). These two pain pathways are believed to be responsible for the diverse sensory features of pain. The spinoreticular tract pain pathway is thought to contribute to pain intensity feedback control (mediated through the descending pathway), as well as affective and emotional aspects of pain. However, the spinothalamic somatosensory cortex pathway is involved in the appreciation of special and sensory aspects of pain.

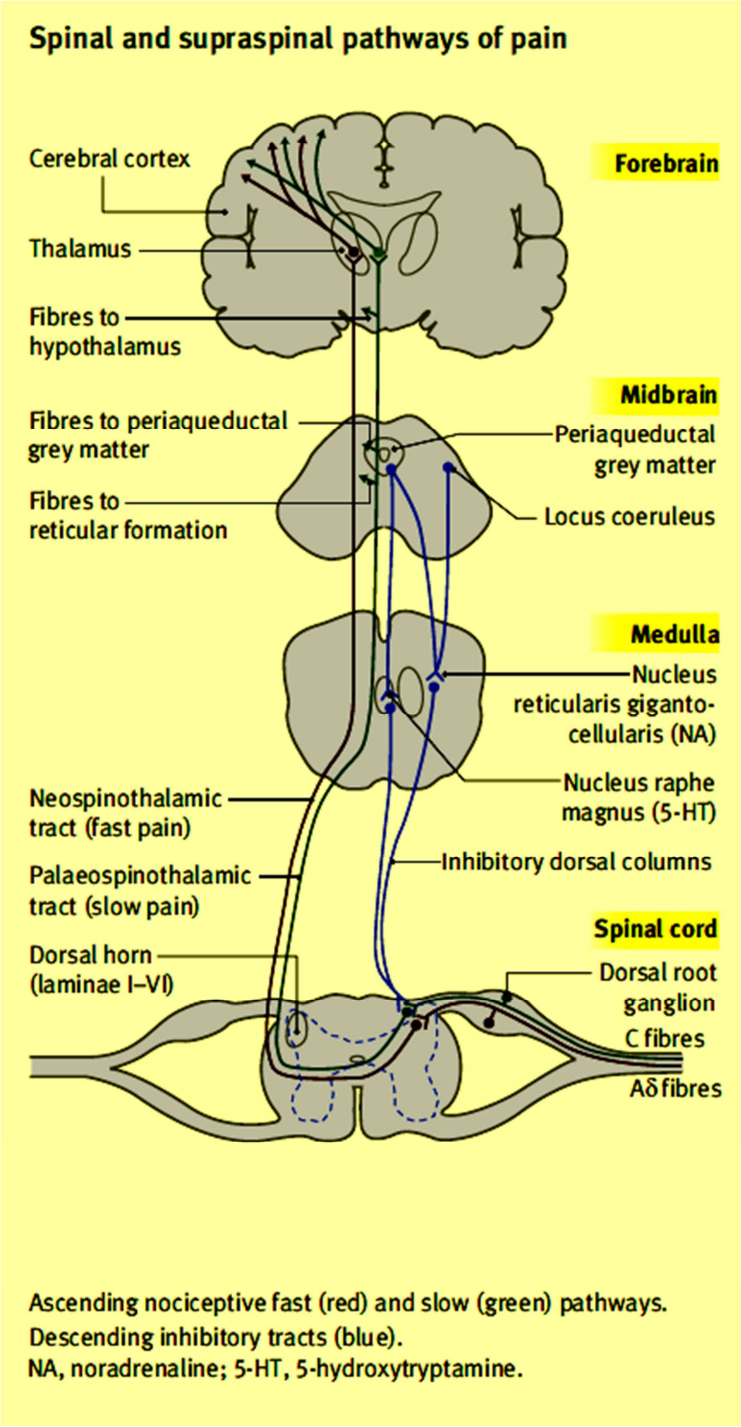

Figure 1-5 Schematic of spinal and supraspinal pathways of pain.

Second-order neurons project to higher centres through the contralateral spinothalamic and spinoreticular tracts, which are found in the anterolateral white matter of the spinal cord. Ascending nociceptive fast and slow pathways are depicted in red and green, respectively. Descending inhibitory tracts are illustrated in blue. Abbreviations; 5-HT, 5-hydroxytryptamine, NA, noradrenaline. Image taken from Steeds, 2009.

1.3. Classification of pain

Pain may be described as an unpleasant subjective sensory experience initiated by noxious stimuli, inflammation or damage to the nervous system. It can be further classified according to its type, with nociceptive pain being the most widely experienced (Figure 1-6). ***Nociceptive pain*** is a short acting sensation to a noxious stimulus. It serves a protective function, whereby high threshold ***nociceptors*** (sensory receptors in the peripheral nervous system) are activated by painful stimuli and signals are propagated from the periphery through the spinal cord, brain stem, and thalamus to their destinations- the cerebral cortex, where the sensation is perceived (Woolf, 2004). Nociceptive pain is an important and essential alarm system that alerts the individual of fore coming danger to prevent the body from damage. Those that have inefficient nociceptive control systems, including patients with ***congenital analgesia*** (resulting from a nerve growth factor tyrosine kinase A mutation that leads to a loss of high-threshold sensory neurons), have reduced life expectancies due to their inability to protect themselves from harmful noxious stimuli (Miranda et al., 2002). Acute, ***inflammatory pain*** is produced by tissue damage resulting in the release of peripheral inflammatory mediators to the affected inflamed area. The purpose of this short-term response is to encourage healing. Following inflammation, the sensory nervous system adapts by lowering the nociceptor activation threshold, so that normally non-painful stimuli produce pain ***(allodynia)*** and responses to noxious stimuli are enhanced ***(hyperalgesia).*** Once the site of injury heals, this pain usually subsides; however, in some cases it may become chronic. Maladaptive pain is unique to acute/adaptive pain (nociceptive and inflammatory), in this case abnormal pain processing continues long after the noxious stimulus is present or the injury has healed. ***Neuropathic pain*** may result from lesions to the peripheral or central nervous systems leading to alterations in plasticity and lowering of nociceptive thresholds to produce allodynia, hyperalgesia and ***secondary hyperalgesia*** (transfer of sensitivity to the non-injured area). In contrast, ***dysfunctional pain*** is quite puzzling as it occurs in the absence of inflammation, lesion to the

nervous system or noxious stimulus, which leads to increased nociceptive signalling.

Chronic (long-term inflammatory, neuropathic and dysfunctional) pain poses serious health implications in a range of conditions including: arthritis, multiple sclerosis, chronic back and shoulder, chronic migraine and myofacial pain. A recent epidemiological study revealed that chronic pain affects ~ 35% of the Irish population, exerting huge pressures on both the economy and patient quality of life with 61% of subjects in one case study being unable to work resulting in a 19% job loss (Raftery et al., 2011). What is even more alarming is the fact that the majority of those affected do not positively respond to non-addictive treatments available on the market; additionally, analgesics prescribed are transient-acting, and produce undesired negative effects which leads to difficulties with long-term use. Thus, there is an urgent clinical unmet need for efficacious, long-acting treatments to meet the requirements of chronic pain sufferers.

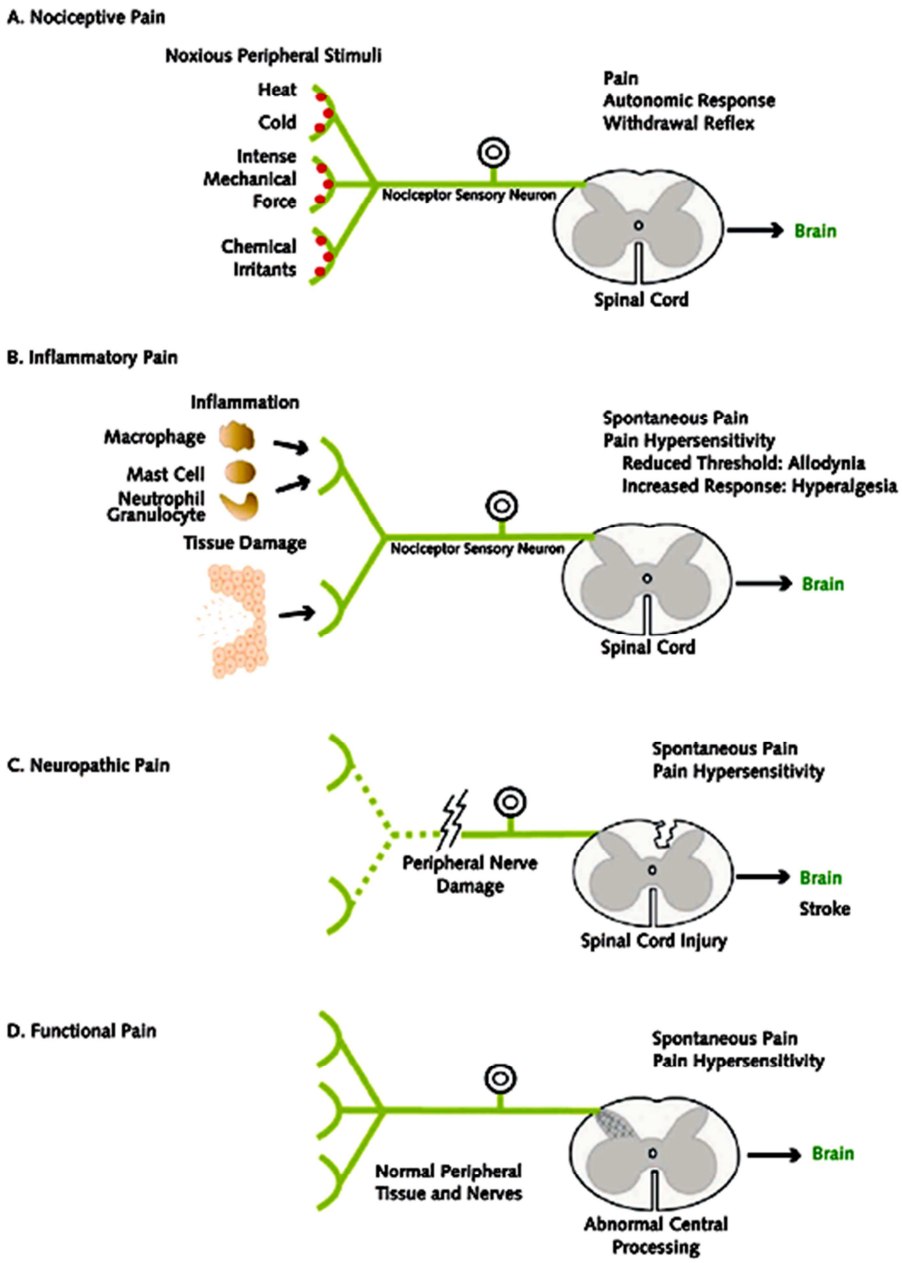

Figure 1-6 Classification of pain.

Pain may be subdivided according to its type (nociceptive, inflammatory, neuropathic or functional/dysfunctional). Nociceptive or inflammatory are pain produced in response to noxious stimuli (nociceptive) or tissue damage (inflammatory). Neuropathic is pain produced following lesion to the peripheral or central nervous systems, while dysfunctional pain is produced by increased nociceptive signalling in the absence of inflammation, lesion to the nervous system or noxious stimuli. Image taken from Woolf, 2004.

1.4. Mechanisms involved in chronic pain

Chronic pain is a complex disease that involves multiple mechanisms (Figure 1-7). Following (peripheral) inflammation, expression of ion channels are altered, e.g. the transient receptor potential vanilloid type (TRPVI) channel increases, thereby, lowering the susceptibility to heat activation. Alterations of K^+ and Na^+ channels increase membrane excitability so that ectopic signals are abnormally triggered, resulting in spontaneous pain sensations.

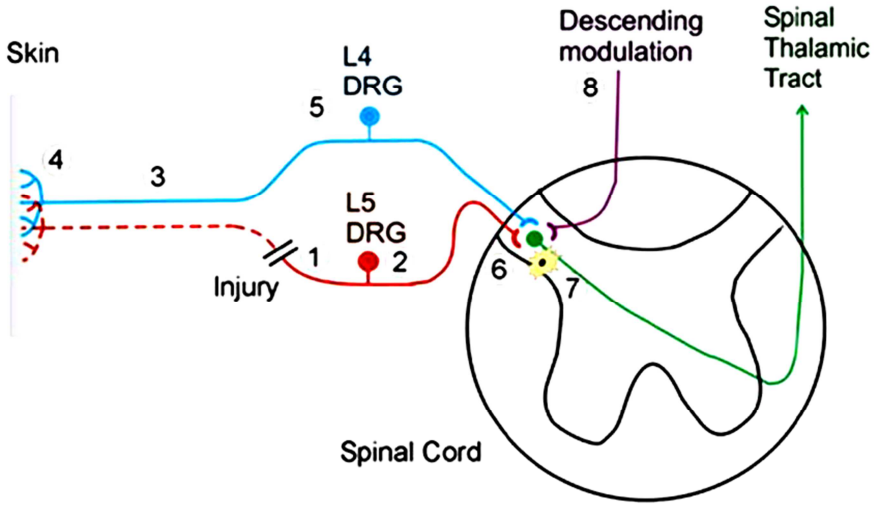

Figure 1-7 Mechanisms involved in chronic pain.

Damage/injury to the spinal nerve leads to changes at many levels. This schematic illustrates eight different sites of pathophysiological changes. (1) At the injury site, spontaneous neural activity and ectopic sensitivity to mechanical stimuli occurs. (2) Expression of molecules in the dorsal root ganglion of the damaged nerve are changed. Spontaneous neural activity initiates in the dorsal root ganglia (DRG). (3) The furthest region of the injured nerve undergoes Wallerian degeneration; this introduces the surviving nerve fibers from uninjured areas of the nerve to an inflammatory soup. (4) Increased trophic factors from the partly denervated tissue may result in sensitisation of primary afferent nociceptors. (5) The expression of various molecules in the dorsal root ganglion of the non-injured nerve is altered. (6) Sensitisation occurs in the postsynaptic dorsal horn, thus, modifying the response to cutaneous stimuli. (7) Activated microglial cells contributes to this sensitisation. (8) Changes that take place in the descending modulation of dorsal horn neurons. Schematic taken from: Campbell and Meyer, 2006.

1.4.1. Peripheral and central sensitisation

In chronic pain, repeated stimuli reduces the threshold of nociceptive afferents leading to enhanced responsiveness of the peripheral terminals of nociceptors, this is referred to as ***peripheral sensitisation***. This results in normally innocuous stimuli being perceived as noxious. This sensitisation is induced by the actions of neuropeptides and inflammatory mediators released by either Ca^{2+} regulated exocytosis such as substance P, CGRP, bradykinin, nerve growth factor, serotonin or neuropeptide Y or by non-exocytotic mechanisms (e.g. nitric oxide, prostaglandins or H^{+}) (Dray, 1995). Release of these above-noted neuropeptides and inflammatory mediators amplifies the impulses transferred to the cell bodies of either dorsal root or trigeminal ganglia, producing ***central sensitisation*** (Latremoliere and Woolf, 2009, Woolf, 2011). These are major processes that both contribute dramatically to the hyper-responsiveness to signalling substances.

1.4.2. Changes in the ectopic activity of afferent neurons and alterations in the expression of molecules

In chronic pain conditions, following peripheral nerve damage, spontaneous ectopic activity occurs in both the injured and nearby uninjured nociceptive afferents resulting in spontaneous pain. Redistribution of Na^{+} channels are thought to be partially responsible for these symptoms. Numerous other proteins, including voltage gated K^{+} channels may also play a contributory role in the changes to membrane excitability of nociceptive neurons. Receptor proteins such as the TRP family of cation channels are also affected by this process. A key member of this family includes TRPV1 which is widely expressed in C and Aδ fibres, TRPV1 is activated by heat and capsaicin (the pungent irritant found in chilli) evoking a burning painful sensation. Following nerve damage, TRPV1 expression is reduced in the injured nerve but up-regulated in the uninjured nerve. This altered TRPV1 expression can generate spontaneous nerve activity in response to natural body temperature if the noxious heat sensor threshold is reduced.

1.4.3. Immune mechanisms

Following injury, mediators are released by nociceptors or non-neuronal cells (e.g. macrophages, platelets, fibroblasts); these infiltrate to the site of injury to promote or speed healing (Figure 1-8). In chronic pain, these substances remain long after the injury has healed and create an abnormal processing environment and may be referred to as “inflammatory soup” which includes a multitude of substances including; neurotransmitters (e.g. serotonin), peptides (e.g. CGRP, SP), lipids (e.g. prostaglandins, endocannabinoids), cytokines and chemokines (Basbaum et al., 2009). This “inflammatory soup” directly contributes to peripheral sensitisation of nociceptors and primary afferents.

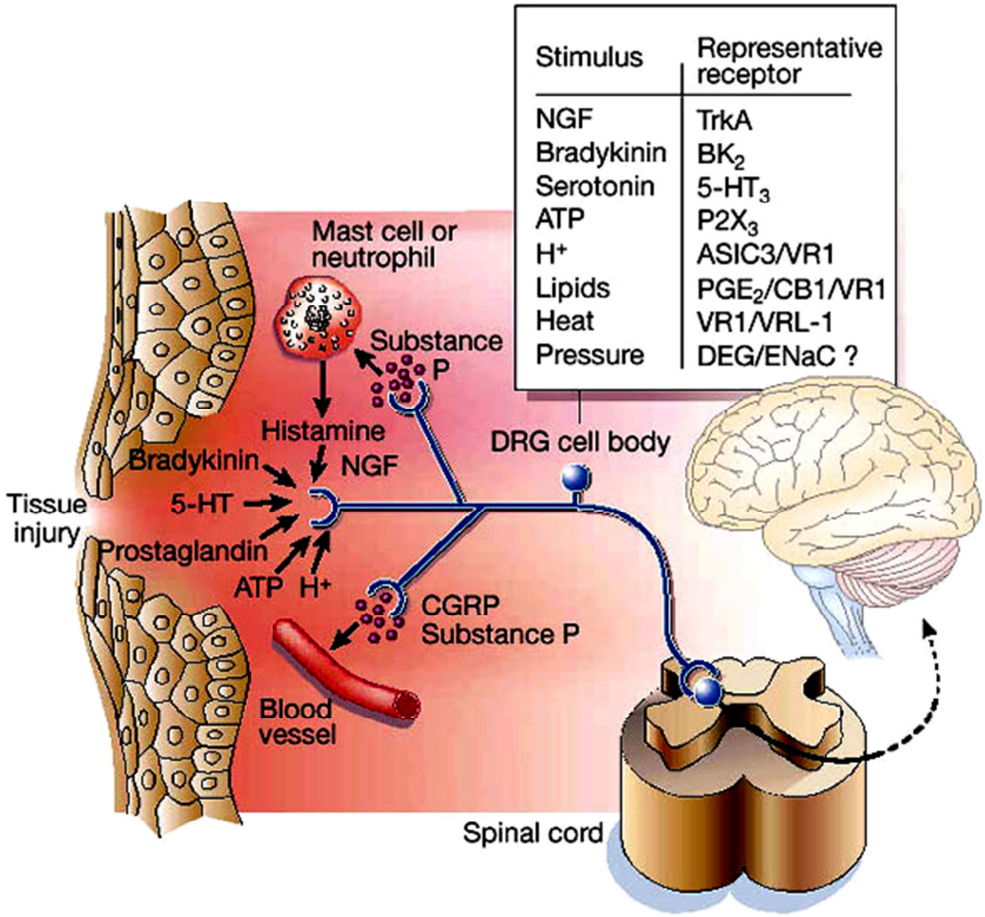

Figure 1-8 Components of the inflammatory soup.

Following injury/damage, mediators are released to promote healing. In neuropathic pain states, alterations of these inflammatory mediators continues long after healing has ceased. These immune cells sensitise primary afferents, pain receptors and second order neurons to create pain hypersensitivity. Abbreviations correspond to the following; 5-HT, 5-hydroxytryptamine, H^+, protons, ATP, adenosine triphosphate, TrkA, tyrosine kinase receptor A, BK_2, bradykinin receptor, 5-HT3, 5-hydroxytryptamine, P2X3, purinergic receptor, ASIC3, acid-sensing ion channel 3, VR1, vanilloid receptor 1, PGE2, prostaglandin E2, CB1, cannabinoid receptor, VRL-1, vanilloid receptor 1-like receptor, DEG, degenerin, ENaC, epithelial sodium channel. Image taken from Julius and Basbaum, 2001.

1.5. Current pharmacological treatments and limitations

Unfortunately, the majority of sufferers do not respond to currently available non-additive medicines; also, commonly-used analgesics are short-acting, cause unwanted adverse effects which are a serious problem for repeated use in chronic pain sufferers. Hence, there is a huge unmet need for more effective long-acting treatments. The current therapeutic strategy for the treatment of neuropathic pain generally involves a stepwise approach to determine which treatment or combinations most efficaciously relieve pain with the least side-effects. Drugs currently available include ion channel blockers, opioids and antidepressants (Figure 1-9). The following articles provide a more compressive understanding of the pharmacological treatment options for neuropathic pain (Baron et al., 2010, Dray, 2008, Davis, 2007, Dworkin et al., 2007, Markenson, 1996).

1.5.1. Ion channel blockers

Gabapentin and pregabalin bind to subunits of the voltage-gated Ca^{2+} channel on primary nociceptor afferents, and reduce neurotransmitter release by inhibiting depolarisation. Both display similar pharmacodynamics (Sills, 2006), but pregabalin is better absorbed than that of its predecessor (Guay, 2005). They are efficacious in treating neuropathic conditions such as diabetic neuropathy (Wiffen et al., 2005, Dworkin and Kirkpatrick, 2005); however, the major limitation with these treatments is that doses need to be carefully adjusted to prevent kidney failure. Lidocaine is a non-specific Na^{+} channel blocker that is generally used topically to relieve pain by inhibiting local excitability.

1.5.2. Opioids

Opioids bind to specific G-protein-coupled receptors with various affinities representative of their potencies. Opioid receptors are divided into three types, μ, δ and κ and may be activated by either endogenous or exogenous opiate peptides which act as receptor agonists. Efficacy has been achieved with

opioid treatment (Dworkin et al., 2007); however, the long-term side effects and abuse potential limit their usefulness in chronic neuropathic pain.

1.5.3. Antidepressants

Tricyclic antidepressants have been used to treat patients suffering from neuropathic pain, independent of their action on depression. Antidepressants can control pain in a variety of ways including blocking; Na^{+} and Ca^{2+} channels, NMDA receptors and the reuptake of neurotransmitters (Sindrup et al., 2005). Efficacy has been found in patients with painful diabetic peripheral neuropathy (Hempenstall et al., 2005). However, a majority of neuropathic pain sufferers do not positively respond to tricyclic antidepressants and lack of efficacy has been found in patients with conditions such neuropathic cancer pain (Mercadante et al., 2002). Typical side effects such as fatigue and dry mouth also limit their usefulness (Dworkin et al., 2007).

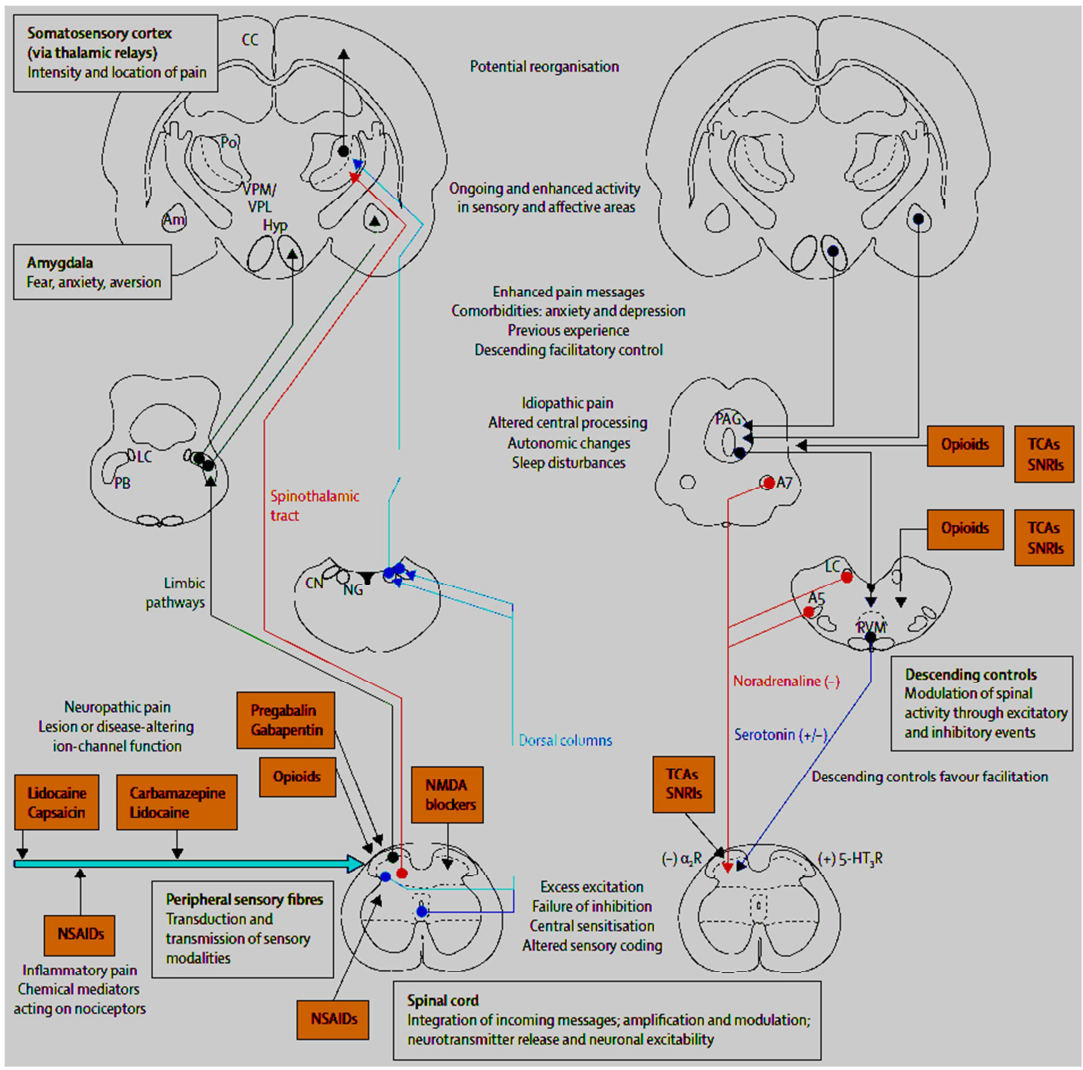

Figure 1-9 Pathways and mechanisms involved in pain, including treatment options.

The ascending and descending pain pathways, are illustrated in the left and right, respectively. The roles of specific regions are described in yellow boxes. Modulation following tissue or nerve damage are listed as well as treatment options located in red boxes corresponding to their action sites. The purple arrow represents peripheral input. Abbreviations correspond to the following; Am, amygdala, A5 and A7, brainstem nuclei containing noradrenergic neurons, CC, cerebral cortex, CN, cuneate nucleus, Hyp, hypothalamus, LC, locus coeruleus, NG, nucleus gracilis, NSAIDs, non-steroidal anti-inflammatory drugs, PAG, periaqueductal grey matter, PB, parabrachial nucleus, Po, posterior nuclei of the thalamus, RVM, rostro-ventral medial medulla, SNRIs, serotonin–noradrenaline reuptake inhibitors, TCAs, tricyclic antidepressants, VPM and VPL, ventrobasal thalamus, medial and lateral components (Gilron et al., 2013).

1.6. Botulinum neurotoxin type A as an emerging treatment

Botox®, Allergan was first approved in 1989 in the United States for the treatment of strabismus, benign essential blepharospasm and conditions of the VIIth nerve; collective data have confirmed the safety margin of this therapeutic and its benefits in a range of indications. Evidence for the potential of BoNTs in pain began to develop as early as the 1980's. A study of rodent nerve-muscle preparations paralysed with BoNT/A and later imaged by fluorescent immuno-microscopy, demonstrated an accumulation of the pain mediator CGRP in the presynapse providing one of the first clues of its potential benefits in pain (Lande et al., 1989). Supportive evidence built up as dystonia patients administered with intra-muscular injections of BOTOX® experienced relief of pain before the onset of muscle relaxation (Brin et al., 1987). More conclusive clinical data was collected when people injected with BOTOX® into the forehead for the treatment of glabellar lines reported an improvement in the severity and number of migraine episodes (Binder et al., 1998). It was initially concluded that BoNTs effect on pain was a secondary effect to muscle spasm. It is now accepted that this interpretation is not accurate because timing and degree of pain relief do not completely correspond to the reduction in muscle spasms (Brin, 2009). Together, these initial exciting findings stimulated a new interest of researchers and clinicians in BoNT as a potential anti-nociceptice.

Clinical data further supported this hypothesis including; a double-blind, randomised placebo-controlled study of 30 migraine sufferers revealed that BOTOX® treatment of any severity was well tolerated and relieved significantly the frequency of migraine attacks at day 90, and the frequency of severe attacks at days 60 and 90 days (Barrientos and Chana, 2003). Another double-blind, placebo-controlled trial was performed to investigate if this bio-therapeutic would be suitable to treat chronic tension-type headache. All sufferers responded positively to local injections of BOTOX® resulting in less headaches and precranial muscle tenderness (Relja and Telarovic, 2004). A further randomised, double-blind, placebo-controlled study of 29 patients with focal painful neuropathies and mechanical allodynia revealed, for the first time, that BOTOX® exerted direct analgesic effects in these subjects independent of its

role on muscle tone (Ranoux et al., 2008). The effectiveness of this treatment for refractory neck pain was also investigated in a randomised, double-blind placebo-controlled investigation of 47 subjects assigned to either BOTOX® or placebo (Miller et al., 2009). A significant decrease in the mean pain intensity was recorded in the treated group; a substantially larger proportion responded to all three outcomes compared to the placebo group. More recently, two multi-center double-blind, randomised, placebo-controlled trials of the PREEMPT (Phase 3 REsearch Evaluating Migraine Prophylaxis Therapy) clinical program were conducted; 1384 chronic migraine suffers were randomly allocated to either onabotulinumtoxinA (BOTOX®) or placebo. The results from this large trial demonstrated BOTOX® to be an effective prophylactic treatment (Dodick et al., 2010) as one dose significantly reduced the occurrence of headache days, a major benefit that lasted six months. Following such encouraging results from these clinical studies, Allergan Inc. was granted approval by the FDA for BOTOX® as a treatment for chronic migraineuers (headaches for 15 days or more per month) in the UK, United States and other countries; status of applications to other countries are pending (Aoki and Francis, 2011).

1.6.1. Botulinum neurotoxins

Botulinum toxin was first discovered in the blood of a patient with botulism by a Belgian scientist named Van Ermengem in 1897, as a product of *Clostridium botulinum* and the agent responsible for botulism food poisoning (Schantz and Johnson, 1997). BoNTs are a class of homologous di-chain proteins (serotypes A-G), possessing unique characteristics, from *Clostridium botulinum* whose active form consists of a Zn^{2+}-dependent proteolytic light chain (LC; Mr ~50k) joined by a disulphide and non-covalent bonds to a heavy chain (HC; Mr ~100k) (Figure 1-10). All toxin serotypes block acetylcholine release at the peripheral cholinergic nerve endings, producing temporary denervation and muscle relaxation. The action of BoNT involves a number of important steps including; 1. **Binding** to neuronal ecto-acceptors via the C-terminal half of the HC (H_C), 2. **Endocytosis** of the toxin mediated by its HC N-terminal moiety (H_N) and 3. **Translocation** of the LC into the cytosol (Figure 1-11). This leads to blockade of Ca^{2+}-regulated exocytosis of transmitters and all mediators by the cleavage

of SNAREs which are responsible for vesicle fusion with the plasmalemma (Meng et al., 2007). Serotypes differ in their target SNAREs; BoNT/A, C1 and BoNT/E cleave SNAP-25 by removing 9, 8 and 26 amino acids residues from the C-terminus of SNAP-25, respectively. The light chains of the remaining BoNT serotypes cleave syntaxin (BoNT-C1) and synaptobrevn (BoNT-B, BoNT-D, BoNT-F and BoNT-G) (Dolly, 2003). SNARE cleavage inactivates the proteins and disturbs the normal functioning of the SNARE complex, inhibiting exocytosis. BoNT/A is the most widely used clinically and the most toxic serotype. BoNT/A has been shown to block acetylcholine release from gamma motor neurons that innervate the intrafusal fibres in muscle spindles; this may change secondary feedback and assist in pain relief (Rosales et al., 1996). However, the direct actions of BoNT on the release of pain mediators is believed to play an important role in its therapeutic effect (Aoki, 2005).

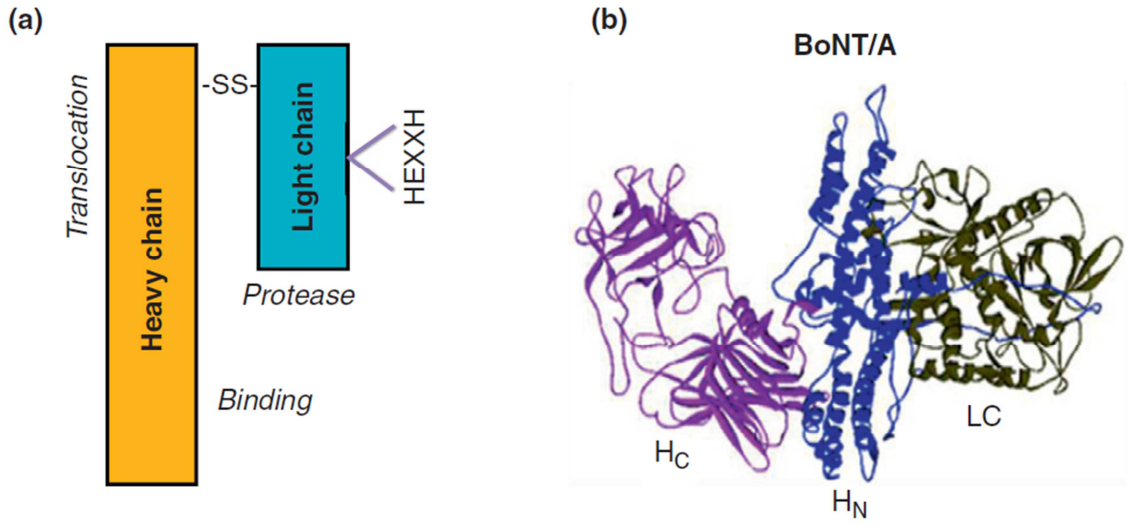

Figure 1-10 Structure of BoNT/A.

BoNTs are cleaved by proteases into their active form composed of a ~50 K light chain and a ~100 K heavy chain linked by a disulphide and non-covalent bonds. The H_C region is responsible for binding, the H_N for translocation and the LC for protease activity. Image taken from Dolly and O'Connell, 2012.

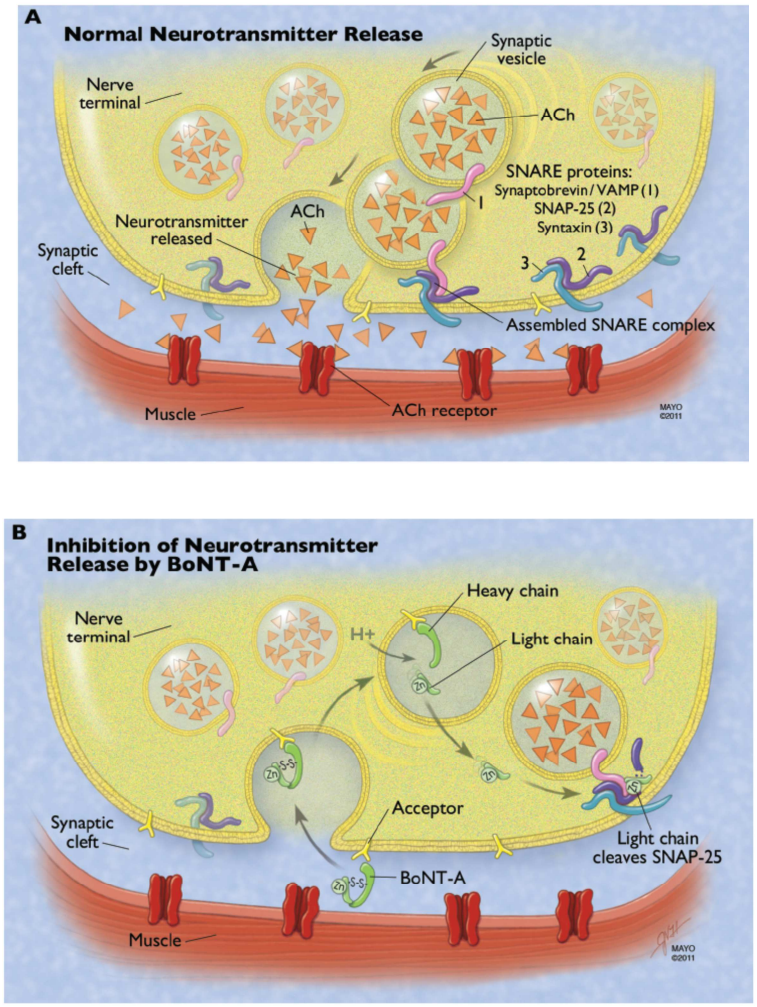

Figure 1-11 Mechanism of action of BoNT/A at the neuromuscular junction.

A) Illustrates normal neurotransmitter release at the neuromuscular junction (NMJ). B) The steps involved in BoNT/A endocytosis at the NMJ, including cell surface binding, vesicle internalisation, translocation of the LC protease into the cytosol, and proteolytic cleavage of the requisite SNARE. This results in inhibition of neurotransmitter release. BoNT/A cleaves SNAP-25. Abbreviations; BoNT-A, botulinum neurotoxin serotype A, H^+, protons, Ach, acetylcholine, SNAP-25, synaptosomal-associated protein 25, VAMP, vesicle-associated membrane protein. Image taken from Robertson and Garza, 2012.

1.6.2. A hypothetical mechanism of action for pain relief by BoNT/A

The hypothesised anti-nociceptic mechanism of action of BoNT/A has been described in the following article (Aoki and Francis, 2011):

1. Administration of BoNT/A directly and acutely blocks the release of pain neurotransmitters at the periphery leading to a reduction in peripheral sensitisation and an alleviation of pain.
2. Reduction of peripheral sensitisation decreases the signals propagated to the central nervous system and, in turn, indirectly reduces central sensitisation.

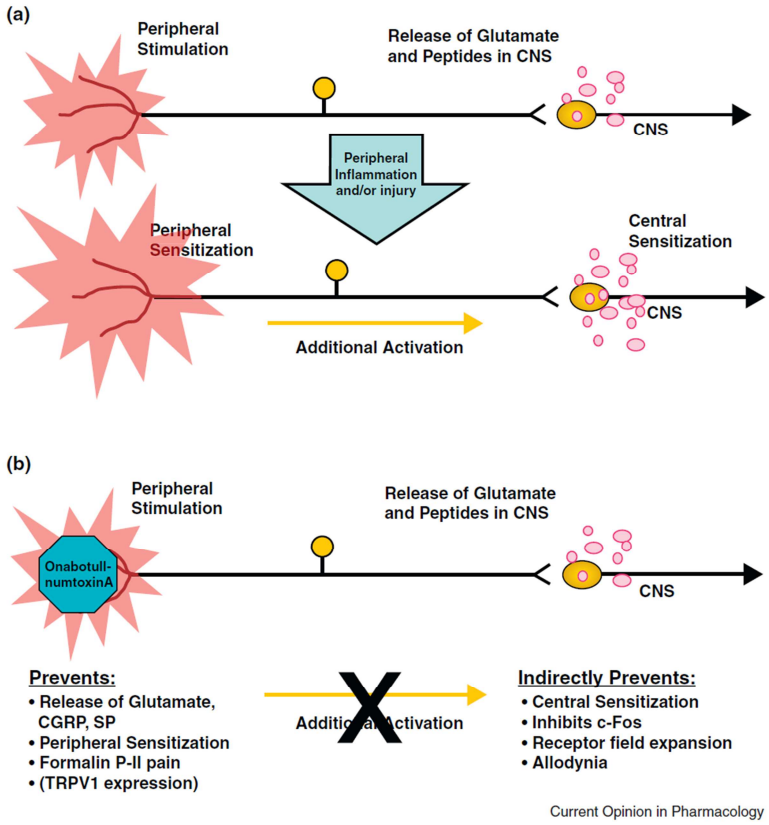

Figure 1-12 Hypothesised mechanism of action of BoNT pain relief by /A.

A) *Neuropeptides and inflammatory mediators are secreted following application of painful stimuli or injury, generating peripheral sensitisation. This increases the signals propagated to cell bodies in both the dorsal root and trigeminal ganglia, producing central nervous system sensitisation. Abbreviations refer to the following; Glu, glutamate; Sp, substance P; CGRP, calcitonin gene related peptide; NGF, nerve growth factor; BDNF, brain derived neurotrophic factor.* ***B****) The actions of BOTOX® on sensitisation. Treatment with the toxin inhibits the exocytotic release of neurotransmitters and pain mediators; as a result, peripheral sensitisation is blocked directly and central sensitisation indirectly. Figure taken from Dolly and O'Connell, 2012.*

1.7. Project aims

- To adopt the spinal nerve ligation model of chronic pain in the rat
    - To optimise and validate the chronic pain model
    - To evaluate the efficacies of BoNT-based therapeutics *in vivo*
- To develop and characterise polyclonal and scFv antibodies to a prime pain target for future targeting of BoNT-based proteases exclusively to sensory neurons

2. MATERIALS AND METHODS

2.1. Materials

2.1.1. Antibodies/markers

Item	$1^O/2^O$ Ab	Catalogue number	Supplier	Species raised in	WB dilution	IHC dilution
Anti-rat TRPV1 (extracellular)-ATTO-488 Synthetic peptide: (C)NSLPMESTPHK*SRGS, corresponding to amino acid residues 605-619 of rat TRPV1 with replacement of cysteine 616 (C_{616}) with serine. 3rd extracellular loop.	1^O	ACC-029-AG	Alomone Labs Ltd.	Rabbit	N/A	**1:50**
Anti-rat TRPV1 (extracellular) polyclonal (C)NSLPMESTPHK*SRGS, corresponding to amino acid residues 605-619 of rat TRPV1 with replacement of cysteine 616 (C_{616}) with serine. 3rd extracellular loop.	1^O	ACC-029	Alomone Labs Ltd.	Rabbit	1:200	**1:100**
Anti-human TRPV1 (extracellular) polyclonal Synthetic	1^O	N/A Produced in-house	N/A Produced in-house	Rabbit	3 µg/mL	**10 µg/mL**

peptide: SLPSESTSHR WRGPAC, corr esponding to amino acid residues 606-621 of human TRPV1.						
Anti-TRPV1 monoclonal Synthetic peptide: YTGSLKPEDAE VFKDSMVPGE K, corresponding to C terminal amino acids 817-838 of Rat Vanilloid Receptor 1.	1^{O}	AB10295	Chemicon	Guinea Pig	1:1000	**N/A**
Anti-FLAG® M2 monoclonal antibody	2^{O}	F3165	Sigma-Aldrich, Ireland	Mouse	0.5–10 µg/mL	**20 µg/mL**
Anti-mouse-Alexa-488	2^{O}	A21121	Bio-Sciences Ireland Ltd.	Goat	1:500	**N/A**
Anti-rabbit-Alexa-568	2^{O}	A11011	Bio-Sciences Ireland Ltd.	Goat	1:500	**N/A**
Anti-rabbit-HRP	2^{O}	711-035-152	Jackson Immuno research Europe Ltd.	Donkey	1:5000-10000	**N/A**
Monoclonal anti-FLAG® M2-CY3	2^{O}	A9594	Sigma-Aldrich, Ireland	Mouse	N/A	**1-10 µg/mL**

Table 2-1 Primary and secondary antibodies.

2.1.2. Reagents

Item	Catalogue number	Supplier
3 M Sodium Acetate, pH 5.5	71196	Sigma Aldrich Ireland Ltd.
3,3'-N-epsilon-Maleimidocaproic acid hydrazide-TFA; solid	22106	Fisher Scientific Ireland
Benzonase Nuclease	E1014	Sigma Aldrich Ireland Ltd.
Capsaicin	M2028	Sigma Aldrich Ireland Ltd.
Chloroform	C2432	Sigma Aldrich Ireland Ltd.
Collagenase type 1a	C9891	Sigma Aldrich Ireland Ltd.
Corning® cell culture 25 cm^2 flasks	CLS3289	Sigma Aldrich Ireland Ltd.
Corning® cell culture 75 cm^2 flasks	CLS3290	Sigma Aldrich Ireland Ltd.
Cytosine-β-D-arabinofuranoside (Ara-C)	C1768	Sigma Aldrich Ireland Ltd.
Dispase type II	D4693	Sigma Aldrich Ireland Ltd.
Gibco® DMEM		GibcoBRL
Ellman's reagent	1008-6113	Fisher Scientific Ireland
Freund's adjuvant complete	F5581	Sigma Aldrich Ireland Ltd.
Freund's adjuvant incomplete	F5506	Sigma Aldrich Ireland Ltd.
Immobilon Western Chemiluminescent HRP Substrate	WBKLS0100	Merck Millipore
Immobilon™ PVDF membrane, 0.45µm	IPVH00010	Merck Millipore
Isopropyl β-D-1-thiogalactopyranoside (IPTG)	I5502	Sigma Aldrich Ireland Ltd.
Laminin	L2020	Sigma Aldrich Ireland Ltd.
Miris TransIT-LTI	MIR 2300	Mirus Bio LLC.
NGF 7S	N0513	Sigma Aldrich Ireland Ltd.

Ni-NTA superflow resin	30410	Qiagen Ltd.
Nunc Maxisorp ELISA plates flat bottom	442404	Bio-Sciences Ltd.
PD10 desalting columns	54805	Sigma Aldrich Ireland Ltd.
Poly-L-lysine	P4832	Sigma Aldrich Ireland Ltd.
Propan-2-ol	I9516	Sigma Aldrich Ireland Ltd.
Protein A-Sepharose® from Staphylococcus aureus	P3391	Sigma Aldrich Ireland Ltd.
RNAase-free water	W4502	Sigma Aldrich Ireland Ltd.
RNAlater®	R0901	Sigma Aldrich Ireland Ltd.
SuperscriptIII RT-PCR (kit)	18080-051	Bio-Sciences Ltd.
Thrombin, restriction grade	69671-3	Merck Chemicals Ltd.
TMB ELISA substrate	2023	Bio-Sciences Ltd.
Traut's reagent 2-iminothiolane hydrochloride	1068-8644	Fisher Scientific Ireland
Trizol	15596-026	Bio-Sciences Ltd.

Table 2-2 Reagents used for immunisation, RNA extraction, cell culture, protein expression and purification and chemical conjugation.

2.2. Methods

2.2.1. Botulinum neurotoxins

Experiments involving recombinant BoNTs were approved by the Irish Environmental Protection Agency and were performed under a strict set of safety guidelines (containment level 2). Recombinant toxins used in these studies were constructed by Dr. Jiafu Wang and expressed, purified and activated, as previously described (Wang et al., 2011).

2.2.2. Antibody production and conjugation

2.2.2.1. Selection of peptides

Two peptides were selected corresponding to either end of the extracellular loops of human TRPV1 (Table 2-3). TRPV1-A or B peptides were synthesised and conjugated to either BSA or KLH commercially by Anachem Ltd., UK. The free peptide was used as a control for blocking and for competition experiments, while the TRPV1-KLH peptide was used for screening.

Peptide	Epitope	Amino acids	Peptide sequence
TRPV1-A	Human TRPV1	606-621	**SLPSESTSHRWRGPA**
TRPV1-B	Human TRPV1	637-649	**ELFKFTIGMGDLE**

Table 2-3 Epitopes chosen from the hTRPV1 protein sequence for immunisation.

2.2.2.2. Immunisation

Rabbits were immunised with ~ 30 µg of TRPV1-A and -B peptides conjugated to BSA, prepared in sterile filtered PBS, with an equal volume of complete Freund's adjuvant added to the final mixture. This was subsequently vortexed until visibly dissolved. Boosts consisted of ~ 8 µg of TRPV1-A and –B BSA, prepared in PBS in the presence of an equal volume of incomplete Freud's adjuvant. Each solution was injected subcutaneously using a 25G needle. A pre-bleed was taken the day before the first immunisation and subsequent bleeds were taken 7 days after each boost. Each test bleed was centrifuged at 680 x g for 20 mins at 4^{O}C and serum extracted were stored at -20^{O}C for analysis.

2.2.2.3. Enzyme-linked immunosorbent assays (ELISA)

Nunc plates were coated overnight with 2 µg/ml of either TRPV1-A or TRPV1-B peptides conjugated to KLH. Plates were blocked with 200 µl of 5 % milk marvel for 1 hr in PBS. Serial serum dilutions were prepared in PBS with 0.1 % tween 20 (PBST) with 5 % milk marvel; 100 µl of each serial dilution was added

to the plate and incubated for 1 hr at room temperature. Following incubation, plates were washed 3 times in both PBST and PBS. Donkey-α-rabbit HRP secondary antibody (1:1000) in PBST with 5% BSA was added to each well and incubated for 1 hr at room temperature. This was followed by 3 washes with PBST and PBS. TMB (3,3',5,5'-tetramethylbenzidine) was added to each well and the reaction monitored. The reaction was stopped with 1M HCL (50 µl)/well and the plate was read on a Tecan plate reader at 595 nm.

2.2.2.4. RNA extraction

The spleen of rabbit was removed and placed in RNAlater solution (Sigma Aldrich, Ireland) in an RNase-free tube. This was centrifuged for 10 mins at 680 x g and RNAlater solution was removed; 10 mL of Trizol was added to the sample on ice and homogenised by sonication with power output of 50 % for 1 min or until the whole spleen was homogenised. The sample was allowed to stand at room temperature for 5 mins before being centrifuged at 595 x g for 10 mins at $4^{O}C$. The supernatant was carefully removed and transferred to a clean RNase-free tube; 3 mL of chloroform was added, mixed briefly for ~ 15 seconds with a vortex and incubated for 15 mins at room temperature. Then, the solution was centrifuged at 12,000 x g for 15 mins. The upper, aqueous layer was carefully removed and transferred to a clean tube; 15 mL of propan-2-ol was added to this, vortexed for 15 seconds and the solution allowed to stand at room temperature for 10 mins. This was centrifuged at 12,000 x g for 15 mins at $4^{O}C$ or until a pellet was visible. The supernatant was carefully removed and 10 mL of 75 % v/v ethanol was added and centrifuged at 12,000 x g for 10 mins at $4^{O}C$. The supernatant was removed and the pellet allowed to air-dry for a few mins; 250 µl of RNAase-free water was added and gently mixed to ensure that the RNA went into solution. The RNA was stored on ice, quantity was determined using the nanodrop, and was aliquoted and stored at – $80^{o}C$.

2.2.2.5. Cloning

Cloning was carried out by Dr. Arman Rahman. Table 2-3 details the list of primers for this work and Figures 2-1 and 2-2 illustrate the vector maps for pSang4 and pSang10.

Location	Name	Sequence
5' end of VH	RABVH1a1Nco	GCCCAGCCGGCCATGGCT CAG TCG GTG GAG GAG TCC GGG GGT CGC CTG
	RABVH1a2Nco	GCCCAGCCGGCCATGGCT CAG TCG GTG GAG GAG TCC GAG GGA GGT CT
	RABVH1a2Nco	GCCCAGCCGGCCATGGCT CAG TCG GTG GAG GAG TCC GGG GGA GAC CTG
	RABVHX32Nco	GCCCAGCCGGCCATGGCT GAG CAG CTG AAG GAG TCC GGG GGA GGC CTG
	RabVH1Sfi	CCT TTG GTT GTT CCT TTC TAT GCG GCC CAG CCG GCC ATG GCT
3' end of VH	RabJHXho	TGGAGCCTTAGGCGCGCCACTCGAGACGGTGACC AGGGTGCCTGGGCC
5' end of V kappa	RABVK1Nhe	CAACCTGCAATG GCTAGC GAT GTC GTG ATG ACC CAG ACT CCA TCC
	RABVK2Nhe	CAACCTGCAATG GCTAGC GAT GTC ATG ATG ACC CAG ACT CCA TCC
	RABVK3Nhe	CAACCTGCAATG GCTAGC GAC CCT RTG CTG ACC CAG ACT GCA TC
	RABVK4Nhe	CAACCTGCAATG GCTAGC GCA GCC GTG CTG ACC CAG ACA CCA TCG
	RABVK5Nhe	CAACCTGCAATG GCTAGC GCC AAG GTG CTG ACC CAG ACT CCA GCC
	RABVK6Nhe	CAACCTGCAATG GCTAGC GCC CTT GTG ATG ACC CAG ACT CCA TCC
	RABVK7Nhe	CAACCTGCAATG GCTAGC GCT CAA GTG CTG ACC CAG ACT GAA TC
3' end of V kappa	rabKJ1Not	TTTGTAGTCCAGTGCGGCCGCTTTGATTTCTACCT TGGTGCCAGCTCCAAA
	rabKJ2Not	TTTGTAGTCCAGTGCGGCCGCTTTGACCACCACCT CGGTCCCTCCGCCGAA
	rabKJ3Not	TTTGTAGTCCAGTGCGGCCGCTTTGATTTCCAGTT TGGTCCCTGGGCCAAG
	rabKJ4Not	TTTGTAGTCCAGTGCGGCCGCTTTGATCTCCACCA TGGTCCCTGAGCCAAA
	rabKJ5Not	

		TTTGTAGTCCAGTGCGGCCGCTTTGATCTCCAGCT TGGTCTCCTCGCCAAA
3' end of V constant	RabKCNot	TTTGTAGTCCAGTGCGGCCGCGTCACCCCTWTTG AAGCTCTGGACGA W = A/T
3' end of V constant incorporating cys constant	CysRabKNot	W = A/T TTTGTAGTCCAGTGCGGCCGCGCAGTCACCCCTW TTGAAGCTCTGGACGA
	RABHKSfi	GTT CCT TTC TAT GC*G GCC* CAG CC*G GCC* ATG GCT G Allows extension of all VH primers to incorporate sfi site

Table 2-4 Primers that were used for amplification of rabbit VH and VLs.

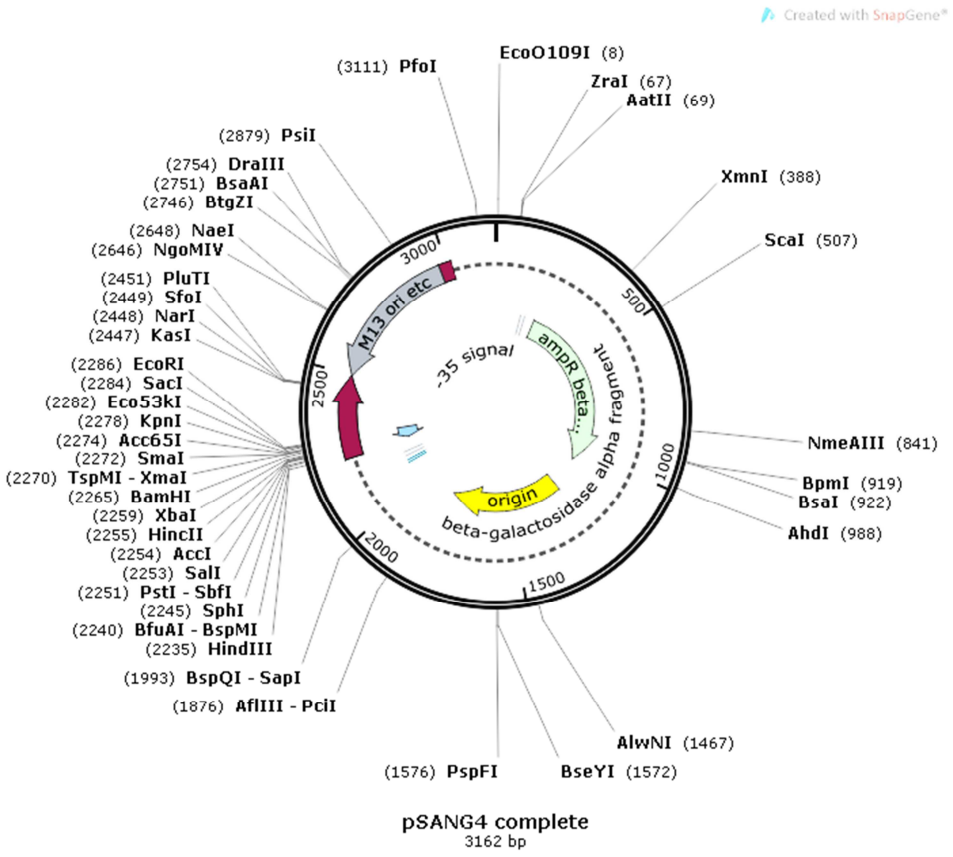

Figure 2-1 pSang4 vector map. Source: John McCafferty Cambridge University.

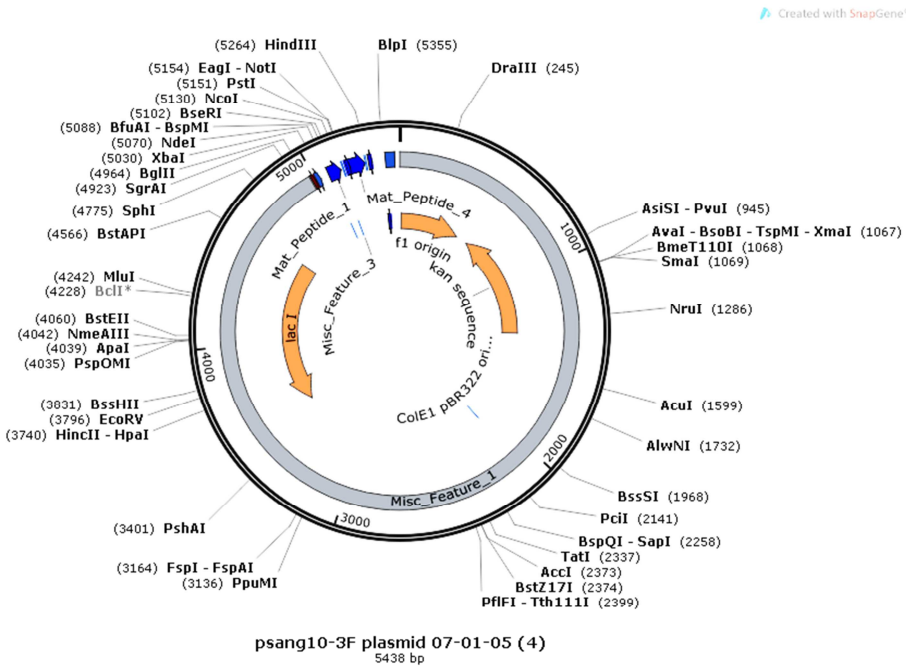

Figure 2-2 pSang10 vector map. Source: John McCafferty Cambridge University.

2.2.2.6. Bio-panning and phage display

Bio-panning and phage display were performed by Dr. Arman Rahman.

2.2.2.7. Expression of scFv clones in *E. coli*

Each scFv clone was seeded onto a 2TY agar plate containing glucose plus kanamycin and grown overnight at 37^{O}C. From each of these plates, a single colony was picked and seeded into a 5 mL starter culture (2TY medium, 2 % glucose, 100 µg/mL kanamycin) and grown overnight at 30^{O}C. A 1:1000 dilution of each of these starter cultures was inoculated into 2TY medium containing 2 % glucose and 100 µg/mL of kanamycin. This was grown until an Abs 600 of 0.6-0.8 was reached; temperature was reduced to 22^{O}C and 1 mM of IPTG was added to induce the culture, which was grown overnight for a further 16-20 hrs.

2.2.2.8. Cell lysis

2.2.2.8.1. Periplasmic cell lysis

Cultures were centrifuged at 12,000 x g for 30 min at 4^{O}C; supernatants were discarded and cell pellets allowed to air dry. To the cell pellets, ice cold TES lysis buffer (30 mM Tris-HCL, 20 % sucrose, pH 8.0) and protease inhibitor (Benzonase 25 U/mL) were added, resuspended and allowed to stand on ice for 10 min. TES 20 % lysis buffer solution was added containing protease inhibitor (Benzonase 25 U/mL) and 1 M $MgSO_4$; and the resuspension was placed on a roller at 4^{O}C for a further 40 min. The solution was transferred to a clean nalgene tube and centrifuged at 40,000 x g in an ultracentrifuge for 40-50 min. A sample of the clarified lysate was collected for analysis on SDS-PAGE and the remaining supernatant was purified as described in 2.2.2.9.1.

2.2.2.8.2. Whole cell lysis

Cultures were centrifuged as described in 2.2.2.8.1 and resuspended thoroughly in the following lysis buffer (150 mM NaCl, 150 mM HEPES, 1 mM PMSF, 2 mg/mL lysosome); the resuspended solution was placed on a roller at 4^{O}C for 40 min. The solution was then freeze/thawed- placed in a - 80^{O}C freezer for 1 hr and thawed in a 20^{O}C waterbath. The solution was then centrifuged at 47,900 x g in an ultracentrifuge for 45 min at 4^{O}C. An aliquot of the clarified supernatant was collected for analysis on SDS-PAGE and the remaining was purified as described in 2.2.2.9.1.

2.2.2.9. Purification

2.2.2.9.1. Purification of scFv antibodies

scFv antibodies were purified by IMAC. Briefly, 2 mL of superflow Ni-NTA resin was added to a commercial 20 mL column and washed with equilibration buffer (20 mM HEPES, 150 mM NaCl, pH 8.0). The clarified supernatant was mixed with equilibration buffer at a 1:1 ratio and incubated with the resin for 1 hr at 4^{O}C on a roller. Following binding, the mixture was placed back into the column and the flow through collected and stored on ice. The resin/bound scFv was washed three times with wash buffer (equilibration buffer plus 5 mM imidazole).

Bound scFv was eluted in 8-10 fractions with one bed volume 2 mL of elution buffer per fraction (20 mM HEPES, 150 mM NaCl, 500 mM imidazole). The eluted fractions were buffer exchanged into PBS using a PD10 column, following standard guidelines. Concentrations of the eluates were determined by Bradford assay as per commercial guidelines using a range of BSA standards to construct a standard curve. Samples from each of the IMAC stages were separated by SDS-PAGE and protein stained as described in 2.5.1 and 2.5.2. Purified and buffer exchanged fractions were stored at - 20^{O}C

2.2.2.9.2. Purification of polyclonal α-hTRPV1 serum

Polyclonal serum was purified by Protein-A-Separose fast flow resin from *Staphylococcus aureus* (Sigma Aldrich, Ireland). To a commercial column, 2 mL of Protein A resin was added and washed with ~ 10 bed volumes of wash buffer (Tris-HCL, pH 8.0). In the meantime, polyclonal serum was allowed to thaw on ice and subsequently centrifuged at 680 x g for 20-30 mins to remove any debris. Polyclonal serum was then diluted 1:1 with 1xTBS, applied to the beads and placed on a roller at 4^{O}C for 1 hr to allow binding. Following binding, the solution was allowed to flow through the column, was collected and stored on ice. The column was washed with 10 bed volumes of wash buffer (100 mM Tris-HCL, pH 8.0). The bound IgG antibodies were eluted with elution buffer (0.1 M of glycine, pH 3.0) into a tube containing one tenth of the bed volume of neutralisation buffer (1 M Tris-HCL, pH 9.0). The pH of the combined elution and neutralisation buffers were first assessed before antibody elution to ensure that the pH was within the desired range ~7.4. Concentrations of eluted samples were determined by standard Bradford assay and fractions containing protein were pooled and buffer exchanged into PBS on PD10 columns. Concentration of the buffer exchanged sample was reassessed as described above and samples from each of the purification steps were separated by SDS-PAGE and protein stained as described in 2.5.1 and 2.5.2. Buffer exchanged purified fractions were stored at - 20^{O}C

2.2.2.10. Conjugation of anti-human TRPV1 IgG antibodies to the LC-H_N-H_{CN}/A

Conjugation of the LC-H_N-H_{CN}/A (comprised of the light chain, translocation domain and N-terminal heavy chain of BoNT/A, but lacking the binding domain) to the Fc portion of the antibody was attempted by oxidation of the carbohydrates present in the Fc region with periodic acid (from sodium *meta*periodate) to form reactive aldehyde groups on the antibody. These groups react with hydrazides at low pH ranges of 5-7 to form hydrazone bonds. Traut's reagent was used to introduce free sulfhydryls into the LC-H_N-H_{CN}/A. A heterobifunctional crosslinker, namely 3,3'-N-[e-maleimidocaproic acid] hydrazide trifluroacetic acid salt (EMCH), containing a reactive sulfhydryl and hydrazide group was reacted with the LC-H_N-H_{CN}/A. The maleimide group reacts with the sulfhydryl group present in the LC-H_N-H_{CN}/A and the hydrazide group reacts with the oxidised antibody, together these reactions should form the antibody-LC-H_N-H_{CN}/A conjugate.

2.2.2.11. Screening of TRPV1 antibodies

Lysates from HEK WT cells and HEK cells over-expressing human TRPV1 were separated by SDS-PAGE (as detailed below in 2.5.1). Following transfer of the proteins onto PVDF membranes, any non-specific binding of the membranes were blocked by BSA; membranes were then incubated with equal volumes of the crude cell lysates in blocking buffer overnight at 4^{O}C. Membranes were then washed thrice in TBST and incubated for 1 hr in secondary antibody (donkey-anti-rabbit-HRP 1:5000). Membranes were subsequently rewashed thrice and developed using a chemilluminance method of detection and visualised in a G-BOX.

2.3. Cell culture

2.3.1. Dorsal root ganglia- neuronal dissection and primary culture

DRGs were dissected from P3-P5 rat pups. Briefly, the spinal cord was removed, opened along the middle and carefully pushed back to allow clear visibility of the ganglia. These were removed using a 45^{o} angled forceps,

dissociated and cultured similarly to the method of Malin et al., 2007 with the following modifications. The ganglia were washed once in ice-cold DMEM and incubated with shaking at 37^{O}C for 30 min with 2.4 U/mL and 1 mg/mL of dispase II and collagenase I. Cells were triturated and plated onto glass coverslips pre-coated with poly-L-lysine and laminin 0.1 mg/mL and 20 µg/mL. Cells were cultured in DMEM containing 10 % (v/v) foetal bovine serum, 100 U/mL penicillin, 100 µg/mL streptomycin plus 50 ng/mL 2.5s NGF, and maintained in a humidified atmosphere at 5% CO_2 and 37^{O}C. Half of the medium per well was replaced with medium containing Ara-C (10 µM) from days 1-5 and complete medium was added every second to third day thereafter.

2.3.2. Culture of human embryonic kidney cells

HEK293 cells were maintained in DMEM (supplemented with 10% fetal bovine serum, streptomycin, penicillin and L-glutamine). The cells were transiently transfected with pcDNA3 encoding either human or rat TRPV1 according to the transfection reagents recommended guidelines using a 3:1 ratio of the Miris TransIT-LTI transfection reagent to DNA.

2.4. Immunocytochemistry and quantification

2.4.1. Immunocytochemistry

2.4.1.1. Permeabilised cell staining

HEK293 cells WT and those transiently transfected with TRPV1 were washed with PBS and fixed for 20 min at room temperature with 3.7% PFA. Non-specific binding sites were blocked with 1% BSA in PBS; 0.25% Triton X-100 was added to allow permeabilisation for 30 min at room temperature. Subsequently, cells were incubated overnight at 4^{O}C with varying concentrations of the purified anti-human TRPV1 rabbit primary antibodies in blocking buffer. This was followed with three washes in PBS, and 1 hr incubation at room temperature with an Alexa-conjugated goat anti-rabbit IgG secondary antibody (1:500) prepared in PBS with 10% goat serum.

2.4.1.2. Staining of intact cells

Staining of non-permeabilised cells was carried out similarly to section 2.4.1.1 with the following modifications. Cells were not fixed prior to incubation and the primary antibody was prepared in blocking buffer without Triton X-100. Following incubation with primary antibody, the cells were fixed, permeabilised and incubated with secondary antibody as above.

2.4.1.3. Basal and stimulated uptake of the TRPV1 antibody

For basal uptake experiments, α-hTRPV1 rabbit antibody 10 µg/mL was applied to HEK cells in complete medium (DMEM supplemented with 10% fetal bovine serum, streptomycin, penicillin and L-glutamine) for various times in a humidified atmosphere at 5% CO_2 and 37^{O}C. Following incubation with the primary antibody, cells were washed, fixed, permeabilised and incubated in secondary antibody prepared in blocking buffer as described above. For stimulated uptake antibody experiments, 1 µM of capsaicin was applied.

2.4.1.4. Internalisation of the anti-human TRPV1 antibody

For assay of internalisation, staining was carried out similarly as for basal uptake. Concentrations used include: 1 µM of capsaicin, 6 µg of filipin, 100 nM of bafilomycin A1.

2.5. Protein assays

2.5.1. SDS-PAGE

Sodium dodecyl sulphate polyacrylamide gel electrophoresis (SDS-PAGE) was used to separate proteins on the basis of size with SDS detergent being added to remove any secondary or tertiary structures. Proteins were loaded onto manually prepared acrylamide gels and run with 1 x electrophoresis buffer (1 litre: 25 mM Tris, 129 mM glycine, 0.1% SDS) at 120 volts (stacking) and 170 volts (resolving gel) until proteins were separated according to their sizes, corresponding to the pre-stained protein marker.

2.5.2. Coomassie Blue staining

Gels were prepared as per 2.5.1 and placed in heated 0.25% Coomassie brilliant blue G 250 (made up with 10% acetic acid and 45% methanol) for 1 hr on a shaker. Gels were then washed once with distilled H_20 and placed in destain (10 % acetic acid plus 30% methanol) until the bands were clearly visible.

2.5.3. Western blotting

Following SDS-PAGE as per 2.5.1, a piece of PVDF membrane with a 0.45 µm pore size (Millipore) was soaked briefly in methanol (30 sec), rinsed once with deionised water and placed in transfer buffer (1 Litre: 25 mM Tris-base, 190 mM glycine, 10% methanol in dH_2O). The sponge and filter paper were also soaked in transfer buffer and assembled as follows: sponge, filter paper, PVDF membrane, protein gel, filter paper and sponge. This cassette was tightly sealed with the membrane side facing towards the positive electrode and carefully placed in a transfer tank for 3-4 hrs at 45 volts at 4^OC (TE62, Hoefer. Inc.). Following transfer, the membrane was blocked for 1 hr at room temperature in either 5% BSA/milk marvel in TBST (0.1% Tween 20 in TBS). The membrane was then incubated with primary antibody in blocking buffer for 1 hr at room temperature. Membranes were then washed with 3 x 10 min washes in TBST and incubated for 1 hr in a horseradish peroxidise conjugated anti-species secondary antibody again in blocking buffer. The membrane was washed as described above, proteins were visualised by ECL reagent, images grabbed with a G-BOX and quantified by densitometric analysis using Image J software.

2.5.4. Determination of protein concentration by Bradford assay

Concentrations of proteins were determined by Bradford assay, as per commercial guidelines, using a standard curve of BSA.

3. ESTABLISHMENT OF AN *IN VIVO* MODEL OF CHRONIC PAIN TO EVALUATE THE EFFICACIES OF RECOMBINANT BoNTs

3.1. Background

3.1.1. Evidence for the efficacy of BoNTs in the treatment of pain *in vivo*

Strong evidence supports the ability of Botox® to attenuate signalling in animal models of inflammatory pain induced by formalin ((Luvisetto et al., 2006, Aoki, 2003, Cui et al., 2004) or capsaicin ((Wang et al., 2011, Bach-Rojecky and Lackovic, 2005) and neuropathic pain ((Park et al., 2006, Bach-Rojecky et al., 2005, Bach-Rojecky et al., 2010, Marinelli et al., 2010). However, further pre-clinical studies are required to fully elucidate the anti-nociceptive mechanism of BoNTs and, particularly, to assess the therapeutic potential of newly engineered variants. Neuropathic pain studies of BoNT/A are summarised in Table 3-1.

Ref.	Park et el., 2006	Bach-Rojecky et al., 2005	Luvisetto et al., 2007
Species	Rat	Rat	Mouse
Strain	SD	Wistar	CD1
Pain model	SNL- L5 & L6 Neuropathic Pain	Partial sciatic nerve transaction Neuropathic Pain	Chronic constriction injury (CCI) Neuropathic pain
Treatment	BoNT/A	BoNT/A	BoNT/A
Vehicle	Saline	Saline	Saline
Day of drug administration	7 days recovery after surgery	Two weeks following surgery	3 days before CCI and 5 or 12 days after CCI
Route of administration	Intra plantar (40 µl)	Peripheral injection	Intra plantar
Units.	10, 20, 30 or 40 $U.kg^{-1}$	7 $U.kg^{-1}$	(20 µl of 0.005 nM, in 0.9% NaCl; corresponding to 15 pgtox /mouse per paw)
Time of testing post treatment	24 hrs	24 hrs	24 hrs
Behaviour tests selected	Mechanical, cold allodynia (100% Acetone) & rotarod)	Hot plate test, Randall and Selitto	Mechanical allodynia
Days of testing	0, 1, 3, 5, 7, 15	0, 1, 5, 15, 30	-
Study duration	21 days	50 days	90 days

Table 3-1 Literature survey of the efficacy of BoNT/A in neuropathic preclinical pain models.

3.1.2. Inflammatory pain models

3.1.2.1. Formalin-induced pain model

The formalin-induced inflammatory pain model was initially created to screen the anti-nociceptive efficacies of analgesics (Dubuisson and Dennis, 1977). It involves intraplantar injection of formaldehyde (formalin) into the rat paw, which subsequently elicits pain related-behaviour, such as licking/biting and shaking/flinching (Wheeler-Aceto et al., 1990). Pain responses of this model occurs in two phases, namely phase I and phase II; the former is an acute stage which lasts approximately 10 mins, followed by a short rest period and, finally, an extended phase. Pre-treatment with BoNT/A complex dose-dependently abolished the symptoms of formalin-induced behaviour during phase II, but not phase I (Cui et al., 2004). Each stage reflects different physiological mechanisms; stage I is triggered by nociceptor activation by peripheral stimuli, whereas II is dependent on inflammation and spinal cord sensitization (Puig and Sorkin, 1996). This suggests that BoNT/A does not exert a localised analgesic effect but probably reduces central sensitization (Dolly and Aoki, 2006). When different BoNT serotypes, BoNT/A and BoNT/B were injected in this model both peripherally and centrally, BoNT/A did not affect phase I but partially affected phase II. Peripheral administration of BoNT/B on the other hand attenuated the licking response during phase I but not II; however, central administration had a hyperalgesic effect on the interphase (Luvisetto et al., 2006).

3.1.2.2. Capsaicin model

Capsaicin, the main component in chilli peppers, is another irritant widely used to generate an additional model of inflammatory pain. After binding to the TRPV1 ligand-gated cation channel located on C-fibres (Rang et al., 2007), it excites sensory neurons causing intense pain following the release of neuropeptides such as substance P and CGRP. After subcutaneous injection into the paw, capsaicin reduces the threshold to a range of stimuli including mechanical and heat. Pre-treatment with BoNT/A was found to either significantly reduce or completely eliminate the increased response to mechanical or thermal stimuli, when applied 6 days prior to induction of the

model, but was ineffective when applied 24 hrs before induction (Bach-Rojecky and Lackovic, 2005). Heat hyperalgesia involves excitation and sensitization of C-fibres (Field et al., 1999), while mechanical hyperalgesia seems to be facilitated by central sensitization (Gilchrist et al., 1996). Furthermore, a recombinant BoNT chimera (LC/E-BoTIM/A) generated by genetically fusing LC/E to a BoNT/A enzymically-inactive mutant (BoTIM/A) alleviated capsaicin-evoked nociceptive behaviour in this model; this effect was long-acting (Wang et al., 2011). SNARE-dependent exocytosis contributes to the transfer of TRPV1 to the plasma membrane which BoNT/A treatment inhibits. This blockade of exocytosis by BoNT/A may contribute to the positive effects seen in these pre-clinical studies.

3.1.3. Neuropathic pain models

3.1.3.1. Peripheral nerve lesion models

Investigations on this versatile toxin using rodent models of neuropathic pain have likewise yielded beneficial effects (Marinelli et al., 2010, Luvisetto et al., 2007, Park et al., 2006, Bach-Rojecky et al., 2005). Several models of peripheral nerve lesion have been developed (Figure 3-1) to generate neuropathic pain including; the chronic constriction injury model (CCI), partial sciatic nerve ligation model (PSL) and L5/L5 spinal nerve ligation (SNL). The CCI model involves loose ties placed over the sciatic nerve with four chromic gut ligatures at the mid-thigh level (Bennett and Xie, 1988). Partial ligation of the ipsilateral nerve at the upper-thigh level, compressing approximately 1/3-1/2 of the sciatic nerve has been employed to generate a model of causalgia (Seltzer et al., 1990). Another model of causalgia involves tight unilateral ligation of the L5 and L6 spinal nerves located distal to the dorsal root ganglia (Kim and Chung, 1992). Recently, it was found that a single dose of intraplantar or intrathecal BoNT/A significantly attenuated mechanical allodynia in both rats and mice, and thermal hyperalgesia in rats, in a CCI model of neuropathic pain (Marinelli et al., 2010). As soon as 24 hrs following application, the positive effects were observed and, encouragingly, these were long-lasting with a duration of 81 or 25 days following intraplantar injection of the higher dose in mice and rats, and 35 days after intrathecal injection in rats.

This neurotoxin was also applied to another mouse CCI model and a single dose was capable of attenuating chronic pain symptoms for at least 3 weeks (Luvisetto et al., 2007). BoNT/A was applied to an SNL model and it reduced both mechanical and cold allodynia for up to 7 days (Park et al., 2006). Administration of BoNT/A to a PSL model significantly attenuated both thermal and mechanical hyperalgesia in rats at a low dose of 7U/kg (Bach-Rojecky et al., 2005).

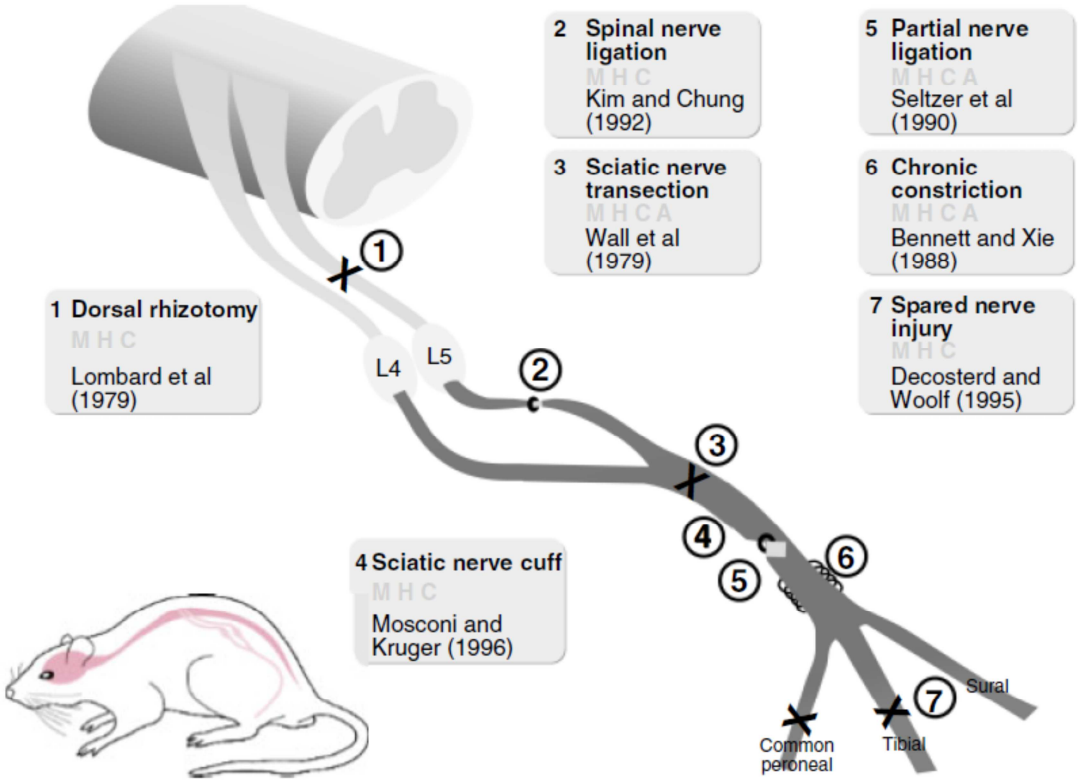

Figure 3-1 Animal models of neuropathic pain.

Schematic of the different approaches used to generate a pre-clinical model of neuropathic pain by nerve ligation or transection. The type of neuropathic pain symptoms produced by each model is listed in the boxes under each of the model names. Abbreviations; M, mechanical allodynia; H, thermal hyperalgesia; C, cold allodynia; A, autotomy. Image taken from Beggs and Salter, 2006.

3.1.4. Environmental factors influencing the development of pre-clinical pain models

Environmental factors play a crucial role in the development of a robust and reproducible pre-clinical pain model. Care must be taken in choosing the most suitable parameters that match the experimental hypothesis which you are evaluating. Please refer to the following insightful article for an overview of the internal and external factors that influence the development of neuropathic pain (Vissers et al., 2003). A study investigating the choice of age on the development of pain in a rat spinal ligation model revealed that younger rats display much more robust symptoms of chronic pain compared to older animals (Chung et al., 1995). A variety of differences were observed with Sprague Dawley rats obtained from different vendors, Charles River rats were fatter and displayed higher adrenocorticotropic hormone output than Harlan rats (Pecoraro et al., 2006). The group who developed the partial nerve injury model of neuropathic pain by tight ligation of 1/3-1/2 of the sciatic nerve (Seltzer et al., 1990), found difficulty in reproducing results even though all the variables were the same for each study. After further investigation they found that rats that were fed a soy diet perioperatively displayed significantly reduced chronic pain behaviour when compared to those on a soy-free diet (Shir et al., 1998). These are just a few examples to illustrate the importance of internal and external factors that may affect the development of a robust, reproducible, chronic pain *in vivo* model for evaluating potential therapeutics.

3.1.5. Recombinantly-engineered BoNTs

The individual structural domains of BoNTs infer unique functions (e.g. acceptor binding, translocation and protease activity). Protein engineering provides an opportunity to combine characteristics of different serotypes to create a therapeutic with the most desirable features. BoNT/A, /E and others have been successfully recombinantly expressed, purified and characterised (Wang et al., 2011, Lawrence et al., 2007, Dolly et al., 2011). Encouragingly, the biological activities of these recombinant products were equal or greater than that or their corresponding native serotypes. BoNT/E (Lawrence et al., 2007) acts faster

than BoNT/A (Wang et al., 2008) in blocking neurotransmitter release; its LC cleaves 17 additional SNAP-25 residues than that of /A (Meng et al., 2009, Dolly et al., 2009). Although rBoNT/E retained full biological activity, its duration of action is short lived (Dolly et al., 2011). Interestingly, site-directed mutagenesis of rBoNT/A revealed that the longevity of /A is linked to a di-leucine motif near the C-terminus of its LC (Dolly et al., 2011, Wang et al., 2011). A novel recombinant composite toxin was created by attaching LC/E to the N-terminus of a protease inactive mutant of BoNT/A. This innovative therapeutic, LC/E-BoTIM/A, bound to sensory neurons, internalised/translocated and cleaved SNAP-25, giving a LC_E-truncated product (Wang et al., 2011). Another composite toxin was engineered by joining LC/E with BoNT/A, providing a double-active therapeutic. The following pre-clinical study aims to investigate the therapeutic efficacies of rBoNT/A, LC/E-BoTIM/A and LC/E-BoNT/A (Figure 3-2), in a rodent spinal nerve ligation model of neuropathic pain.

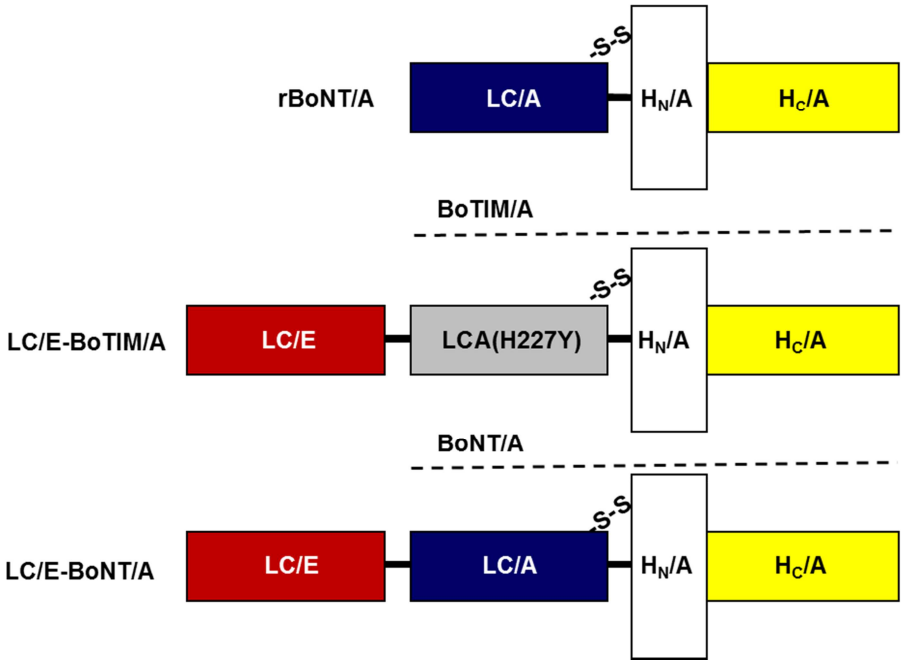

Figure 3-2 Recombinantly engineered BoNTs for evaluation *in vivo*.

rBoNT/A (removes nine residues from the C terminus of SNAP-25), LC/E-BoTIM/A (an enzymatically-inactive mutant of A, delivers a LC/E protease cleaving 17 more C-terminal residues from SNAP-25 than BoNT/A) and LC/E-BoNT/A (contains the combined protease activity of A and E, cleaving 26 SNAP-25 residues).

3.2. Aims and objectives

- To establish a model of chronic pain in the rat by tight ligation of the L5 and L6 spinal nerves
- To investigate the efficacies of BoNT-based therapeutics in this *in vivo* model

3.3. Materials and Methods

3.3.1. Materials

Item	Catalogue number	Supplier
Adson tissue forceps	14226	World Precision Instruments
Agricola Retractor	17005-04	InterFocus Ltd.
Applying instrument	12028-12	InterFocus Ltd.
Base assembly for plantar simulation	37450-278	Ugo Basile
Bead instrument steriliser	34-0575	Harvard apparatus Ltd.
Bone cutter	16101-10	InterFocus Ltd.
Curved rongeur 14 cm	16021-14	InterFocus Ltd.
Dumont # 5 45^{o} angled forceps	14101	World Precision Instruments
Dumont # 5 curved forceps	500232	World Precision Instruments
Dumont # 7 curved forceps	11297-10	InterFocus Ltd.
Ear tag applicator	52-4717	Harvard apparatus Ltd.
Ethicon Perma Hand Silk Suture, Non-Absorbable	W593	Pan Veterinary Ltd.
Ethicon Suture Absorbable	VCP3040H	Pan Veterinary Ltd.
Hot/Cold Plate	35100	Ugo Basile
Incapacitance Tester	IN101R	Linton Instrumentation
Ligation hook	10062-12	InterFocus Ltd.
Michel suture clips	12040-02	InterFocus Ltd.
Noyes scissors curved	501236	World Precision Instruments
Plantar Test- Hargreaves	37370	Ugo Basile
Rotarod	76-0239	Harvard apparatus Ltd.
Touch Test Sensory Evaluator, Kit of 20	1277	Ugo Basile

Table 3-2 Materials used in pre-clinical studies.

3.3.2. Pre-clinical methods

3.3.2.1. Animal husbandry

Male Sprague Dawley rats (Harlan, UK- for SNL studies 001 and 003; Charles River, UK- for SNL study 002), weighing between 200-300g at the start of the study, were housed in groups of four. Subjects were maintained under standard laboratory conditions with a 12 hr light/dark cycle (lights on at 08.00h) with food and water available *ad libitum*. The experimental procedures were performed in accordance with the guidelines of the Research Ethics Committee, Dublin City University, Dublin, Ireland and were carried out under licences granted by the Minister for Health and Children under the Cruelty to Animals Act, 1876 as amended by European Communities Regulations 2002 and 2005 (licence number: 100/3609).

3.3.2.2. Experimental design

For all studies, rats were allowed to acclimatise for at least one week before baseline testing for heat hyperalgesia, weight bearing, mechanical and cold allodynia. Male Sprague Dawley rats were used for all studies; N = 40 (Harlan, UK) - 001, N = 51 (Charles River, UK) - 002 and N = 36 (Harlan, UK) for the final study 003. Surgery was performed over one week and post-surgery data collected for all four tests for two weeks for SNL study 001 and for one week for SNL studies 002 and 003.

3.3.2.3. Drug administration

Drugs were injected by a colleague (to ensure that the tester remained blinded to the study) under brief isoflorane gaseous anaesthesia, induced with 5% isoflurane in 0.8% O_2 and reduced to 2% isoflurane in 0.8% O_2 (less than a min exposure). The chosen treatments (rBoNT/A, LC/E-BoTIM/A, LC/E-BoNT/A or vehicle) were diluted into a 0.9% saline solution with 0.5% BSA before storage on ice until administered. All treatments were given as a 20 µl volume by intra plantar injection into the subcutaneous space beside the third and fourth metatarsal bones of the hindpaw (Figure 3-3); following injection, the needle was carefully withdrawn to prevent release of the drug upon removal.

Figure 3-3 Intraplantar administration of drugs.

Treatments or vehicle were delivered by intraplantar injection between the 3rd and 4th metatarsal of the ipsilateral hindpaw as a 20 µl dose under brief gaseous anaesthesia as described above.

3.3.2.4. Spinal nerve ligation (SNL)

Surgery was conducted under gaseous anaesthesia, (3-5% isoflurane for induction and 2 % for maintenance in 0.8-1% O_2). The L5 and L6 spinal nerve ligation model was performed as outlined by (Kim and Chung, 1992). Briefly, the paraspinal muscles were removed to expose the spinal process and sacrum (Figure 3-4 A). Careful removal of L6 spinal process allows clear visibility of the L4 and L5 nerves lying beneath (Figure 3-4 B). The L6 nerve is located just beneath the sacrum. A 6-0 non-absorbable silk thread was placed around each nerve and tightly ligated to damage the axons in the nerve. Sham operated animals were prepared in the same manner expect the spinal nerves were not ligated.

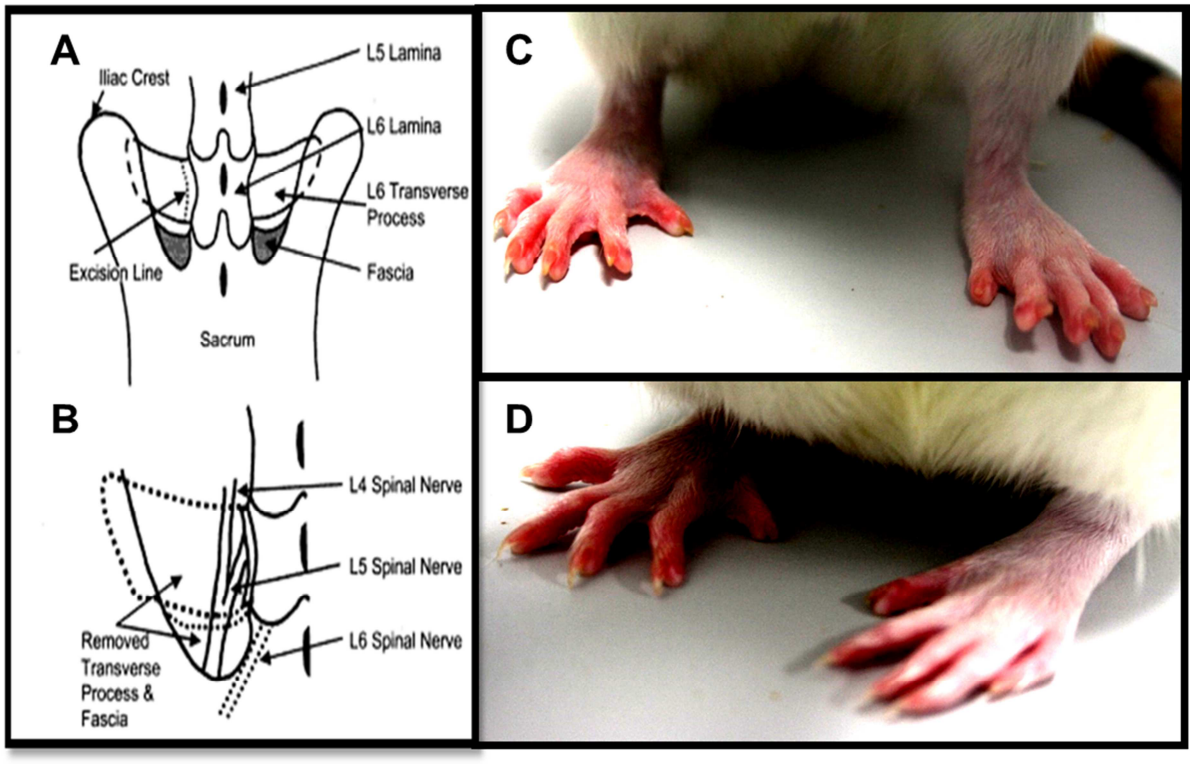

Figure 3-4 Dorsal image of the bony structures at the lower lumber and sacral levels.

A. *lower structural magnification after dissection of the paraspinal muscles.* ***B.*** *higher structural magnification after removal of the L6 spinal process on the left side. Figures* ***A*** *and* ***B*** *taken from Luo, 2004.* ***C****. A sham-operated animal, showing normal flexing of the toes.* ***D.*** *A SNL rat, displaying normal toe flexing of the contralateral limb, while toes of the ipsilateral side are held closely together with accompanied swelling.*

3.3.3. Behaviour parameters

3.3.3.1. Locomotor dysfunction

Locomotor dysfunction in rats injected with the selected treatment doses were investigated by the rotarod test. Animals were first acclimatised to both the tester and the rotating drums to eliminate stress. Training involved placing the animals onto the rotarod with their heads facing in the direction of the rotation at both constant and acceleration speeds of 15 RPM and 5-15 RPM, until the animal remained on the drum for the duration of the trial and for a minimum of three trials (Figure 3-5). Only those that fulfilled the test criteria were selected for the experiment.

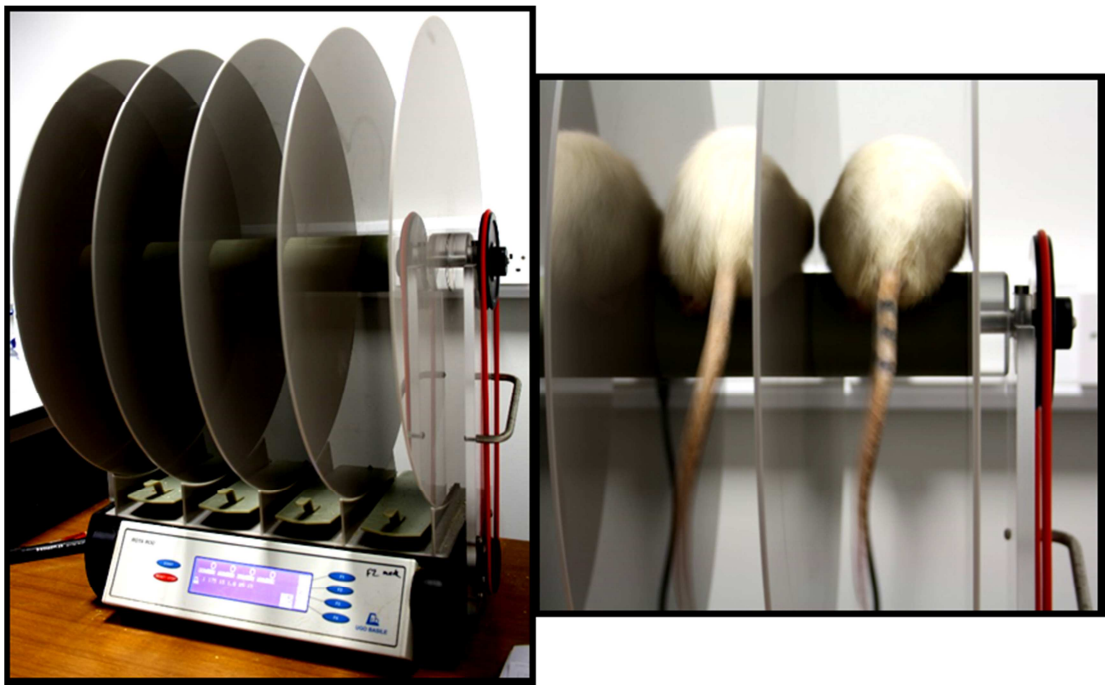

Figure 3-5 The rotarod.

This revolving drum is used to assess locomotor dysfunction in the rat (Method described above).

3.3.3.2. Mechanical allodynia

Mechanical allodynia was assessed by measuring the paw withdrawal threshold in response to a range of innocuous hairs as per a published method (Chaplan et al., 1994). Calibrated hairs (Table 3-2) were applied perpendicularly to the mid plantar surface of the ipsilateral and contralateral hindpaws. A positive response was recorded if the animal responded with a sudden removal of the paw; this was often accompanied with behaviour such as licking, biting or flinching of the paw. No response to the application of the hair was considered negative. As per the Chaplan method, the 15.10g hair was considered the cut-off point. Paw withdrawal threshold was determined using the Dixon up-down method (Dixon, 1980). With this, the 2 g hair is initially applied and depending on the response (positive or negative), consecutive hairs are applied in either a descending or ascending fashion.

3.3.3.3. Cold allodynia

This was assessed following application of a cold plate (Table 3-2) set to 5^{O}C to the plantar surface of rat paws (Figure 3-6). The initial paw withdrawal response latency, the total number of withdrawals and the time spent with the paw raised over 180 seconds were recorded for both the ipsilateral and contralateral hindpaws. Three measurements were taken for each paw with a three to five min rest between recordings to prevent sensitisation of the paw. A cut-off time of 180 seconds was assigned to prevent tissue damage.

Figure 3-6 Measurement of cold allodynia.

Control and neuropathic animals are placed on a test apparatus cooled to 5^{o}C. Control animals very rarely respond by lifting the paw; however, neuropathic rats respond by lifting the injured paw. Both the number of lifts and the time spent lifting significantly increase when compared to the controls. This image illustrates a neuropathic animal positively responding to cold allodynia.

3.3.3.4. Heat hyperalgesia

This parameter was assessed by the Hargreaves method (Hargreaves et al., 1988). Animals were allowed to acclimatise to a plastic enclosure (Table 3-2, Figure 3-7). A radiant heat source was then applied to the mid plantar region of the ipsilateral and contralateral hindpaws. Intensity was adjusted to achieve a response in normal un-operated animals of 12-14 seconds. Paw withdrawal led to an automatic cut-off of the heat source, a maximum cut-off time of 20

seconds was assigned to prevent tissue damage. A minimum of three readings were recorded per paw with a 3 min break between readings to prevent sensitisation of the paw.

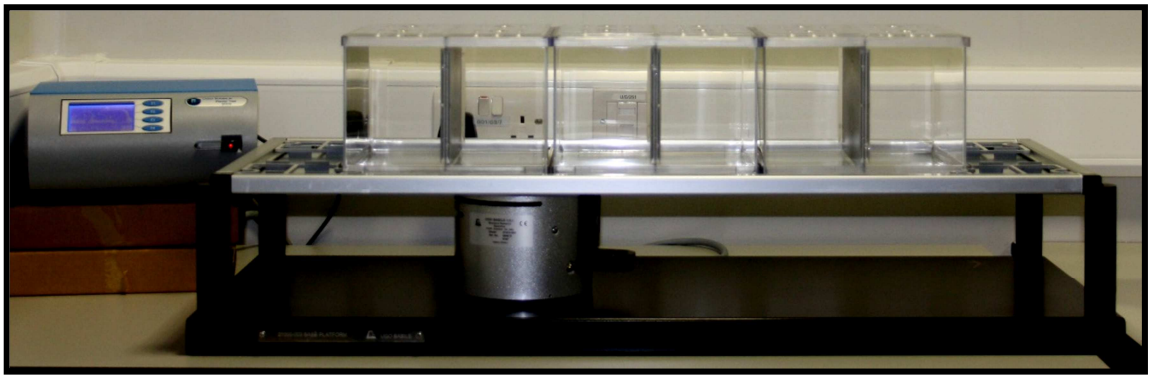

Figure 3-7 The Hargreave's test.

Once animals are habituated to the plastic enclosure, an infrared heat source is placed under the ipsilateral and contralateral hindpaws. The responses recorded reflects heat hyperalgesia.

3.3.3.5. Weight bearing

Changes in weight distribution between the injured and control hind limbs were assessed by an Incapacitance tester (Table 3-2) following a published method (Bove et al., 2003). Briefly, animals were placed facing forward on a sloped plexiglass chamber, with each hindpaw positioned over the designated force plate (Figure 3-8). Over a period of 5 seconds the force applied by each hind limb was averaged to give a number in grams. Four readings were collected for each paw and averaged to get the mean value. The percentage weight distribution of the ipsilateral paw was determined by the following calculation:

Percentage weight distribution of the ipsilateral hind limb = [((Weight bearing of the mean ipsilateral paw)/ (weight bearing of the mean ipsilateral + contralateral hindpaws) x 100].

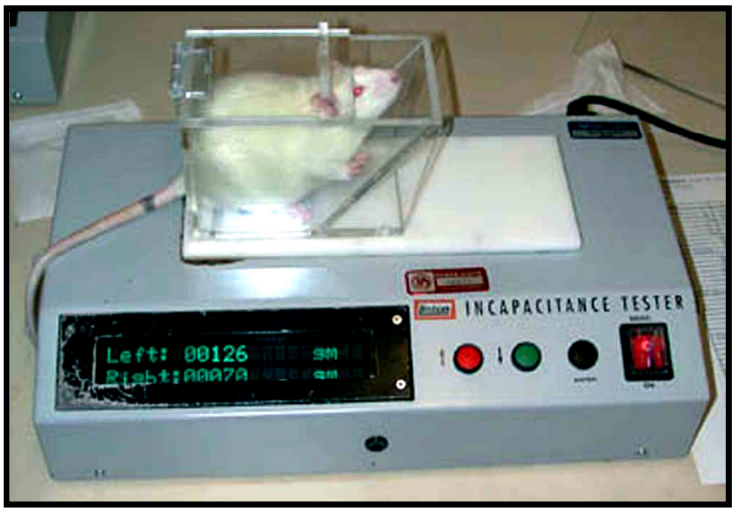

Figure 3-8 Incapacitance tester.

This instrument is used to measure weight distribution of the ipsilateral and contralateral hindpaws. Animals are placed on a sloped surface and force transducers measure the weight placed on each hind limb in grams. The average of all readings per paw are used to calculate the percentage weight distribution on the injured paw as described above. Image taken from Bove et al., 2003.

3.3.4. Statistical analysis for pre-clinical studies

Data was analysed with a repeated measures two way analysis of variance (ANOVA) with time and drug treatment as factors, using a software package Graphpad Prism. A Dunnet's post-hoc test was chosen to determine the significance between groups. Data was considered as significant with $P < 0.05$ and all results were expressed as means ± standard error of the mean (± SEM).

3.4. Results

3.4.1. No significant difference in animal weights was observed between treatment groups.

Administration of treatments had no significant effect on rats' body weights (Figure 3-9) relative to the SNL vehicle treatment group: **(A)** (Group, F (3, 34) = 1.22, P = 0.3166), **(B)** (Group, F (4, 46) = 1.381, P = 0.2552). Overall, rats gained weight during the duration of the studies: **(A)** (Time, F (19, 646) = 28.71, $P < 0.0001$), **(B)** (Time, F (12, 552) = 284.0, $P < 0.0001$). Weight loss was

observed in the rBoNT/A-treated group **(A)**, which suggests that the dose was too high; however, this did not reach significance.

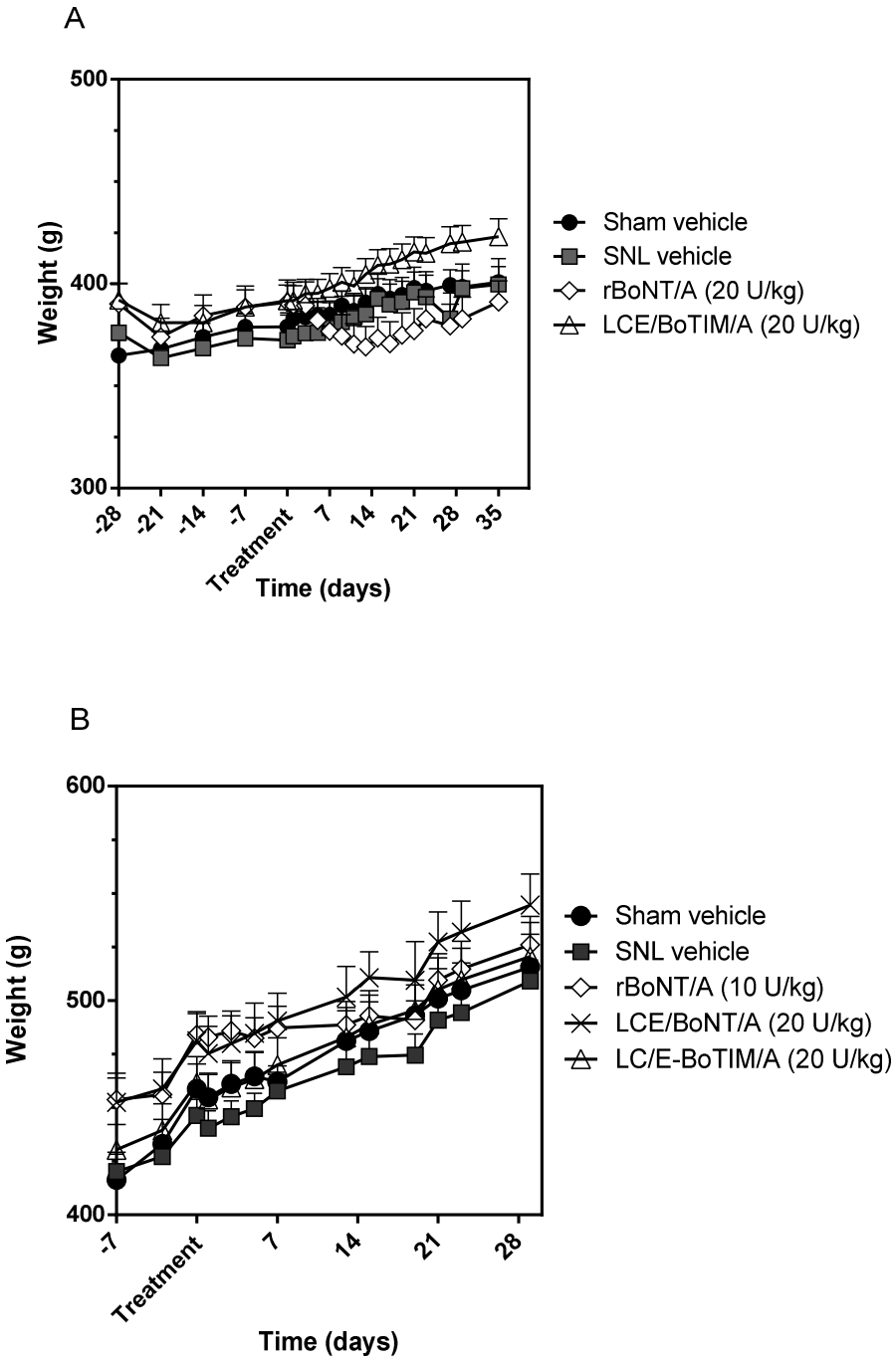

Figure 3-9 Changes in body weights following treatment with BoNTs or vehicle in SNL studies 001 (A) or 002 (B).

There was no significant effect found on body weights when compared to the control (SNL- vehicle) group. See text for details of statistical analyses.

3.4.2. A dose-range study revealed that a high (unacceptable) dose of rBoNT/A (20 U/kg) resulted in a drop in body weight that was matched with severe loco-motor dysfunction.

Administration of BoNT-based therapeutics resulted in a slight plateau/drop in weight, lasting ~ one day post-treatment in all BoNT-treated groups apart from the rBoNT/A group (20 U/kg), which did not begin to gain weight until ~ 5 days post-treatment (3-10 A). Subsequently, animals began to steadily gain weight for the duration of the study. The changes in body weight could not be statistically analysed as the N numbers are too low (N = 1-2, per group) for cost reasons.

Treatment with rBoNT/A (20 U/kg) resulted in severe locomotor deficits (Figure 3-10 B), lasting from the day of treatment until day 5 (corresponding to the drop in weight) where it slowly began to recover. At day 15, one of the group had already completely recovered, while the second animal did not completely return to baseline (N = 2). Loco-motor dysfunction was also observed in the rBoNT/A (15 U/kg), N = 2, LC/E-BoNT/A (30 U/kg), N = 1 and the LC/E-BoTIM/A (30 U/kg), N = 1 groups. N numbers of these groups would need to be increased to fully evaluate if these effects are statistically significant.

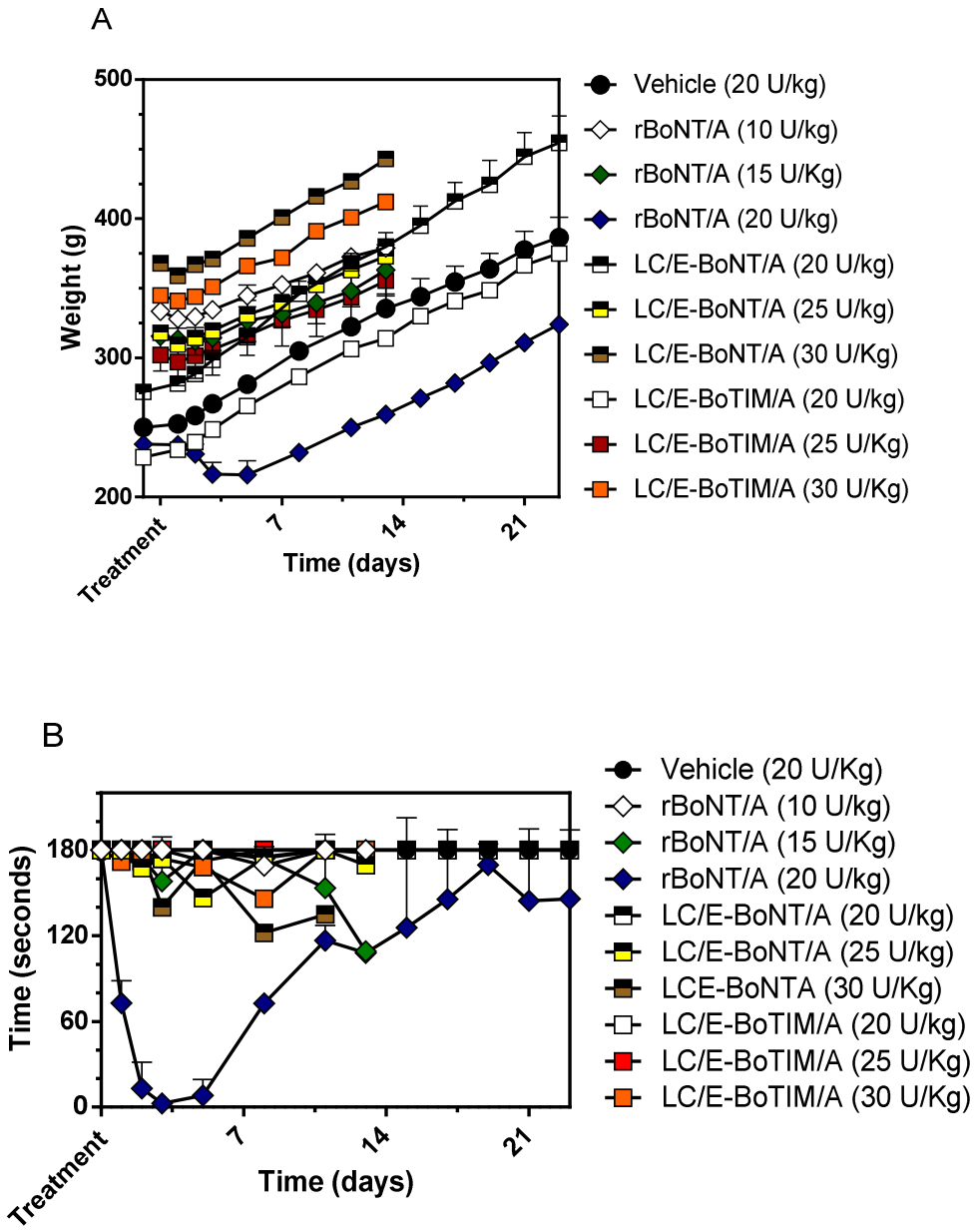

Figure 3-10 Changes in body weights and loco-motor dysfunction following treatment with BoNTs or vehicle.

A) *Body weights* ***B)*** *loco-motor dysfunction in acceleration mode. All groups apart from the rBoNT/A-treated animals gained weight throughout the dose-range study. The following treatments led to locomotor dysfunction: rBoNT/A (20U/kg), LCE/BoNT/A (30 U/kg) and rBoNT/A (15 U/kg). N = 1-2 per group. See section 3.3.3.1 for method details.*

3.4.3. LC/E/BoNT/A attenuated mechanical allodynia at days 7 and 19 post-treatment

Ligation of the spinal L5 and L6 nerves induced mechanical allodynia in both studies (Figure 3-11), **(A)**, (Group, F (4, 39) = 21.85, P < 0.0001), (Time, F (7, 273) = 21.64, P < 0.0001), **(B)**, (Group, F (4, 20) = 35.67, P < 0.0001), (Time, F (7, 140) = 9.105, P < 0.0001). Post hoc Dunnet's test revealed that the significance between the SNL vehicle and the BoNT-treated groups lie in the LCE/BoNT/A (20 U/kg) at days 19 **(A)** and 7 post treatment **(B)**.

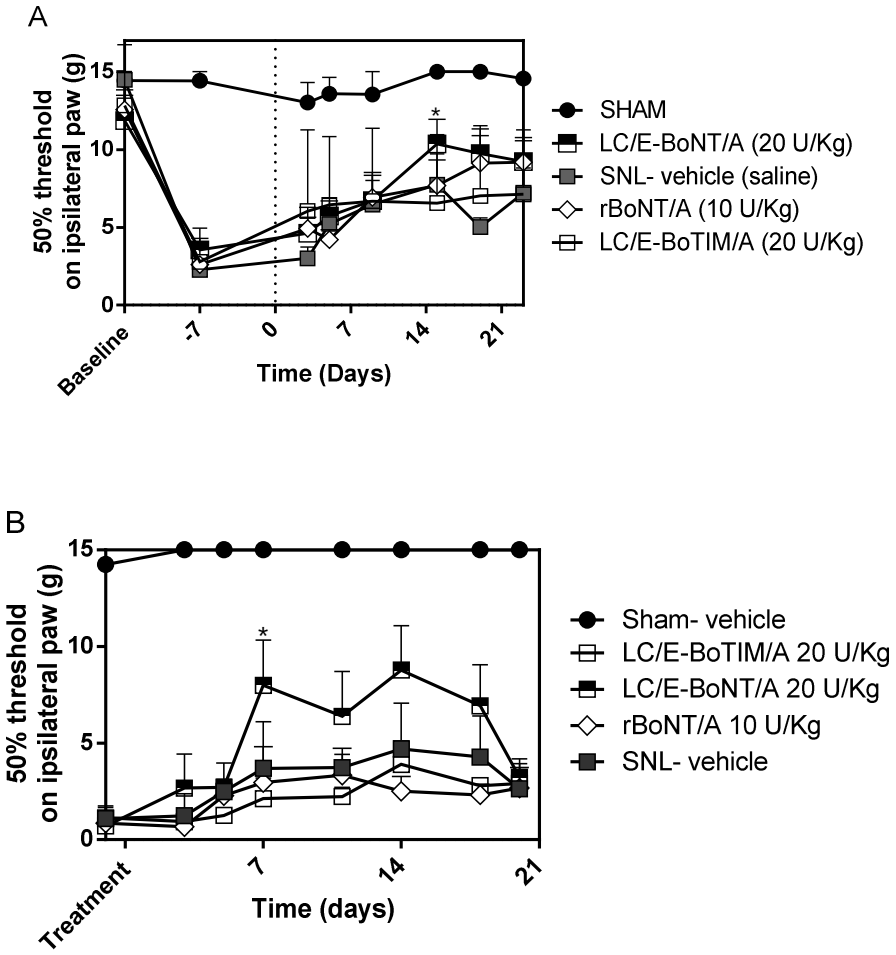

Figure 3-11 Efficacy of BoNT-based therapeutics at relieving mechanical allodynia.

A) *SNL study 002,* ***B)*** *SNL study 003. LC/E-BoNT/A significantly improved mechanical allodynia at days 7 (B) and 19 (A) post treatment. Refer to text for statistical analyses. See section 3.3.3.2 for method details.*

3.4.4. LC/E-BoTIM/A and LC/E-BoNT/A significantly increased the latency of the first paw withdrawal in response to cold allodynia at days 15 and 9, respectively

SNL surgery successfully developed cold allodynia, a desired feature of neuropathic pain in all three studies (Figure 3-12) **A)**, **B)** and **C)**. The latency of the first paw withdrawal decreased significantly in all SNL groups and this feature remained significant for the duration of all three studies. **(A)**, (Group, F (3, 30) = 120.9, P < 0.0001, (Time, F (12, 360) = 33.31, P < 0.0001, **(B)**, (Group, F (4, 38) = 16.47, P < 0.0001), (Time, F (8, 304) = 24.54, P < 0.0001, **(C)**, (Group, F (4, 38) = 85.52, P < 0.0001), (Time, F (11, 418) = 93.02, P < 0.0001). A Dunnet's post hoc between the vehicle and all other groups, revealed a significant increase in paw withdrawal latency at day 15 post treatment in the LC/E-BoTIM/A (20U/kg) treated group, $P \leq 0.05$ **(A)** and at day 9 post treatment in the LC/E-BoNT/A group **(C)**. The SNL vehicle control group remained significant when compared to the sham control group for all time-points post-surgery, indicating that this neuropathic pain feature is long lasting.

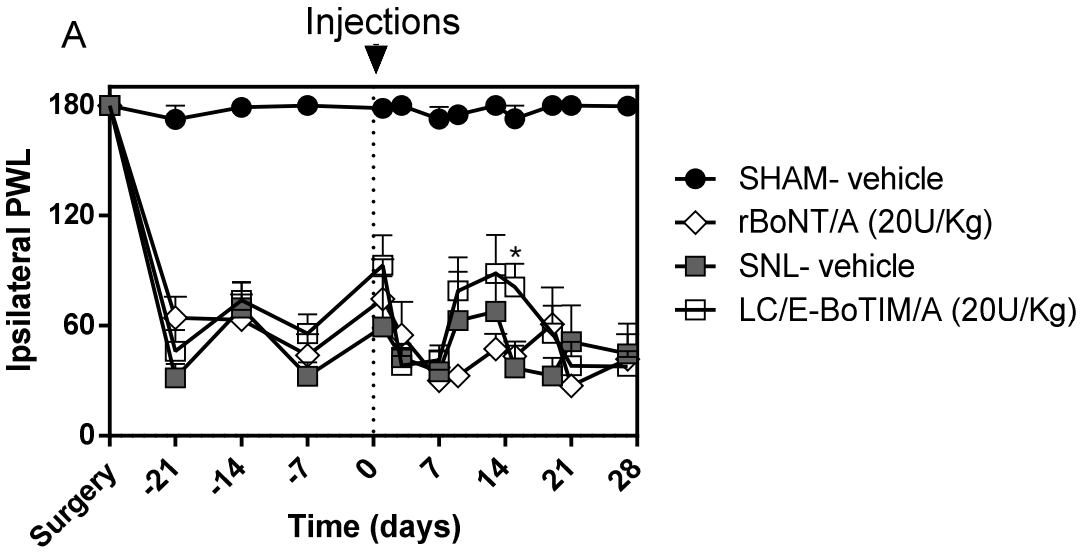

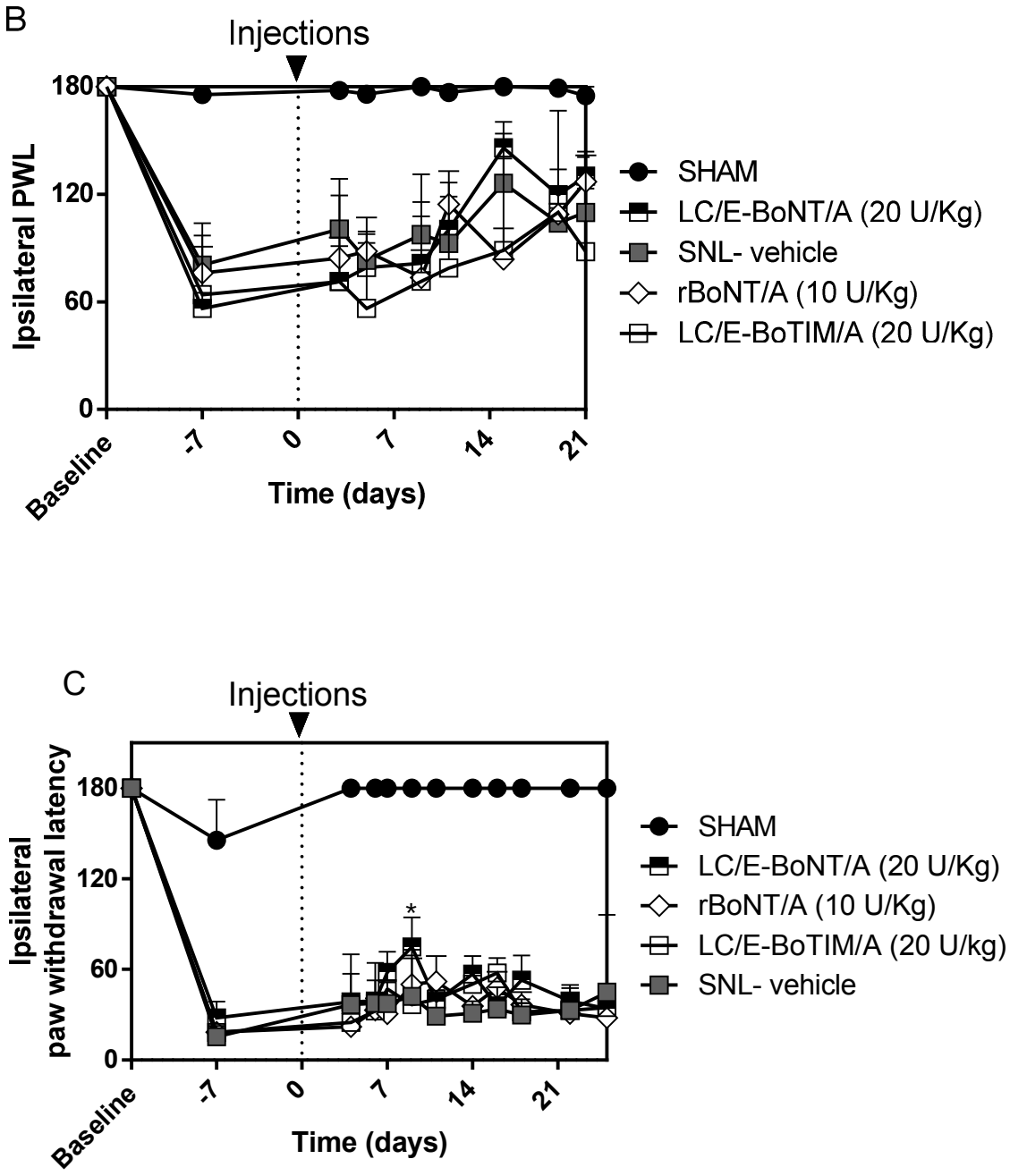

Figure 3-12 Changes in cold allodynia paw withdrawal latencies, following administration of drug treatments.

Ligation of spinal nerves significantly reduced paw withdrawal latencies to cold stimuli. Treatment with either LC/E-BoTIM/A ***(A)*** *or LC/E-BoNT/A* ***(C)*** *significantly attenuated this allodynia at days 15 and 9, respectively. Refer to text for statistical analyses.* ***A)*** *SNL study 001,* ***B)*** *SNL study 002 and* ***C)*** *SNL study 003. See section 3.3.3.3 for method details.*

3.4.5. SNL surgery significantly increased the total paw withdrawal latency to cold allodynia; no significant increase in latencies was found between the SNL vehicle and BoNT-treated groups

Following SNL surgery, the total paw withdrawal latencies significantly increased within groups (Group, F (4, 37) = 7.244, P = 0.0002), this significance lasted from day 7 post-surgery until the end of the study (Time, F (8, 296) = 18.64, P < 0.0001). Post hoc Dunnet's test revealed that when the vehicle SNL group was compared to all other groups at any given time point; no significance was found between the SNL vehicle and SNL BoNT-treated groups, significance was found only between the sham and SNL vehicle groups (Figure 3-13).

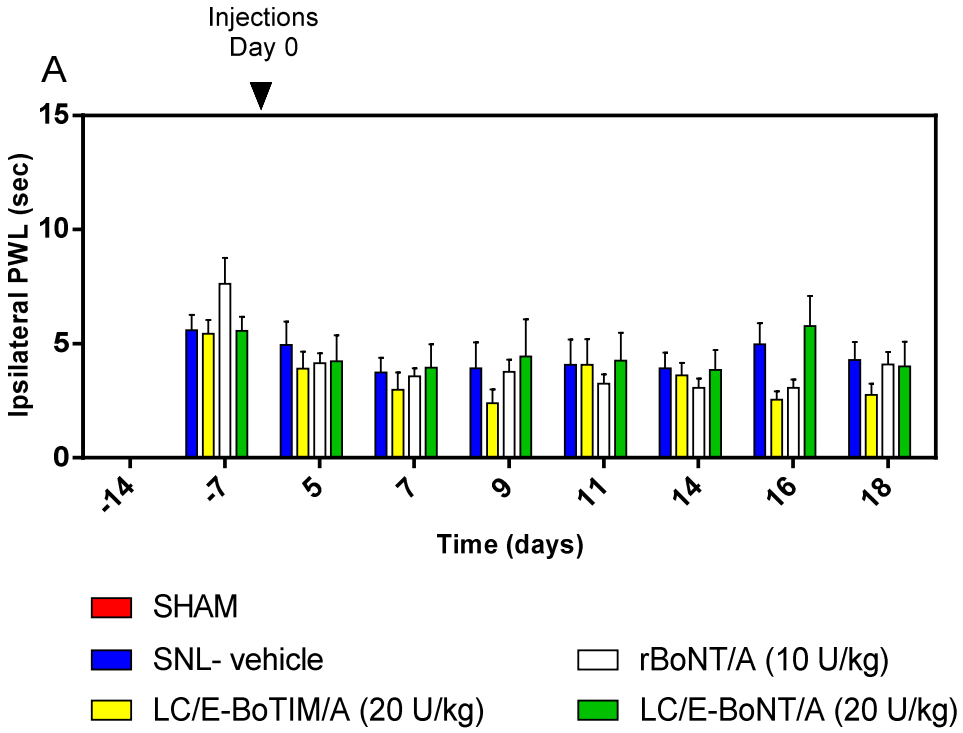

Figure 3-13 Total ipsilateral paw withdrawal latency to cold allodynia.

The total time spent lifting, significantly increased post-surgery. However, no effect was observed in the drug treated groups. Refer to text for details of statistical analyses. See section 3.3.3.3 for method details.

3.4.6. Treatment with BoNTs revealed a significant decrease in the cumulative number of ipsilateral cold paw withdrawal lifts post-treatment when compared to the SNL vehicle treated group at days 7, 13 and 15 for LC/E-BoTIM/A and at day 15 for rBoNT/A

SNL surgery produced a model of chronic pain with statistical significance in the total number of ipsilateral hind paw lifts between groups and over time (Figure 3-14), **A)** (Group, F (3, 30) = 18.26, P < 0.0001), (Time, F (12, 360) = 21.96, P < 0.0001), **B)** (Group, F (4, 38) = 9.271, P < 0.0001), (Time, F (11, 418) = 12.79, P < 0.0001). **C)**, (Group, F (4, 39) = 16.19, P < 0.0001), (Time, F (11, 429) = 32.45, P < 0.0001). Dunnet's post hoc analysis revealed, **A)** a statistical effect between the SNL vehicle group and the LCE-BoTIM/A group at days 7, 13 and 15 post treatment and at day 15 in the rBoNT/A treatment group. For **B)** and **C)**, Post hoc analysis revealed that significance lies between the SNL and sham operated groups.

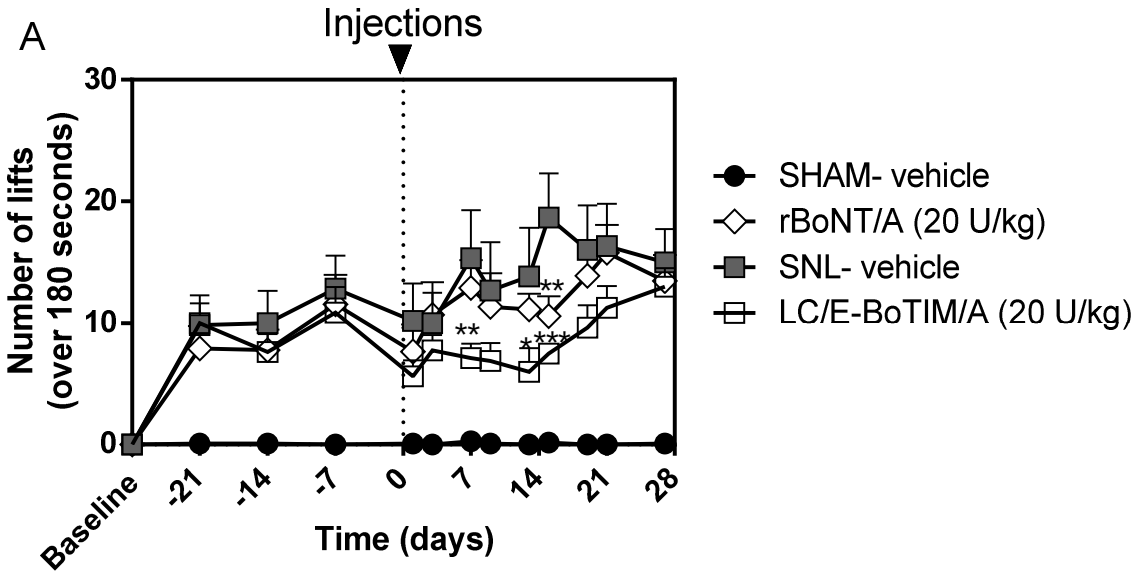

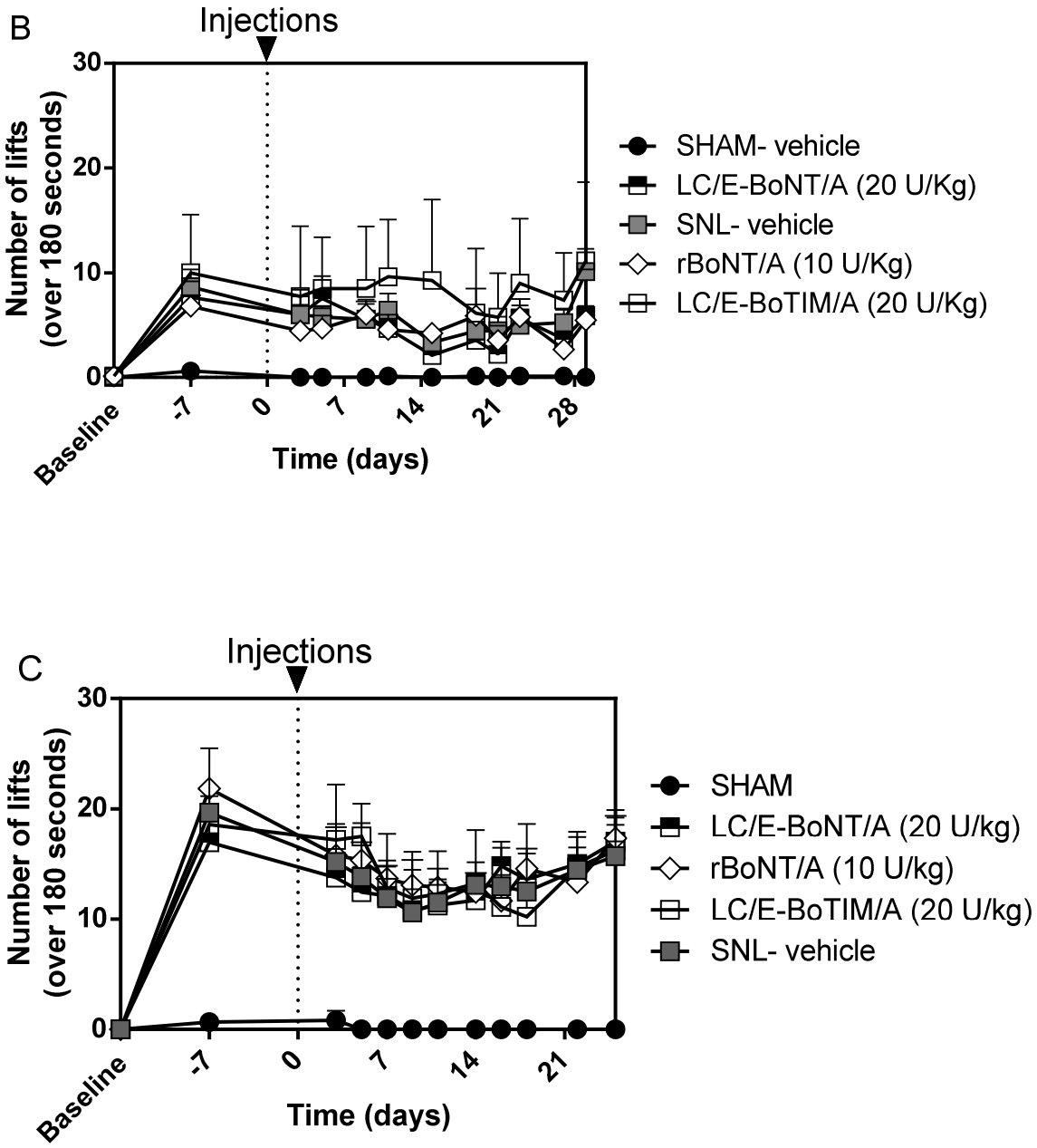

Figure 3-14 Cumulative number of ipsilateral paw withdrawal lifts.

A) *SNL study 001,* ***B)*** *SNL study 002,* ***C)*** *SNL study 003. SNL surgery significantly increased the total number of paw withdrawals in response to cold allodynia in all SNL groups compared to the sham un-operated group. Treatment with BoNTs decreased the cumulative paw withdrawals to this cold stimuli in both the LC/E-BoTIM/A and LC/E-BoNT/A groups at (7, 13 and 15) and (15) days post treatment* ***A)****. No significance was found between the BoNT and SNL vehicle treated groups* ***B)*** *and* ***C)****. Please refer to text for statistical analyses. See section 3.3.3.3 for method details.*

3.4.7. BoNTs significantly attenuated heat hyperalgesia in the LC/E-BoTIM/A group at day 10 and in the LC/E-BoNT/A group at days 19 and 25 post treatment

Analysis of the Hargreaves data from SNL studies 001, 002 and 003 revealed that SNL surgery successfully induced heat hyperalgesia which was significant when compared to the sham control group and this effect lasted through time (Figure 3-15), **A)** (Group, F (3, 31) = 9.540 P = 0.0001), (Time, F (6, 186) = 27.63 P < 0.0001), **B)** (Group, F (4, 42) = 6.716, P = 0.0003), (Time, F (6, 252) = 13.27, P < 0.0001), **C)** (Group, F (4, 39) = 25.43, P < 0.0001), (Time, F (9, 351) = 22.28, P < 0.0001).

However, closer examination with a Dunnet's Post-hoc test, comparing the SNL vehicle group to all other groups, revealed significance only between the SNL vehicle and sham groups, **A)**, P ≤ 0.01, **B)**, P ≤ 0.001, **C)**, P ≤ 0.0001. In **A)** this significance lasted from days -14 until day 0, no significance was found between treated groups and the SNL vehicle group at days 5, 11 and 17 post-treatment. In **B)** this significance was found only at days 0 and 7, no significant difference was found between the SNL vehicle and other groups at any other time-points. In **C)** this significance was the most robust and lasted from days 0 to 25. When the SNL vehicle group was compared to the BoNT-treated groups, a significant increase in paw withdrawal latency to heat hyperalgesia was found in the LC/E-BoTIM/A (20 U/kg) group at day 10 post treatment, P ≤ 0.05, and at days 19 and 25 in the rBoNT/A group (10 U/kg), P ≤ 0.05.

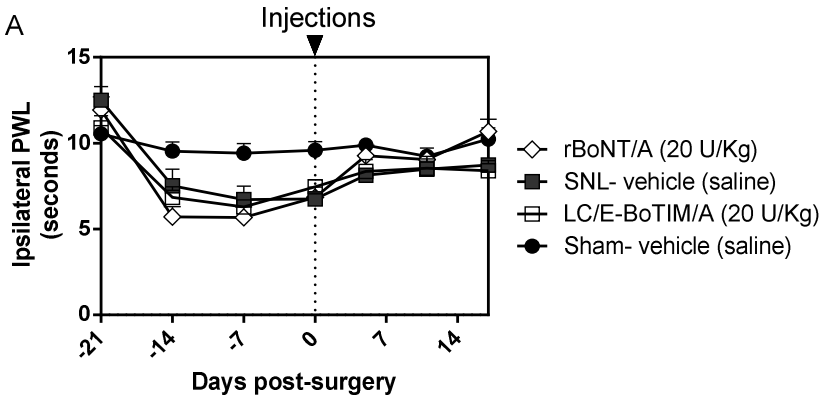

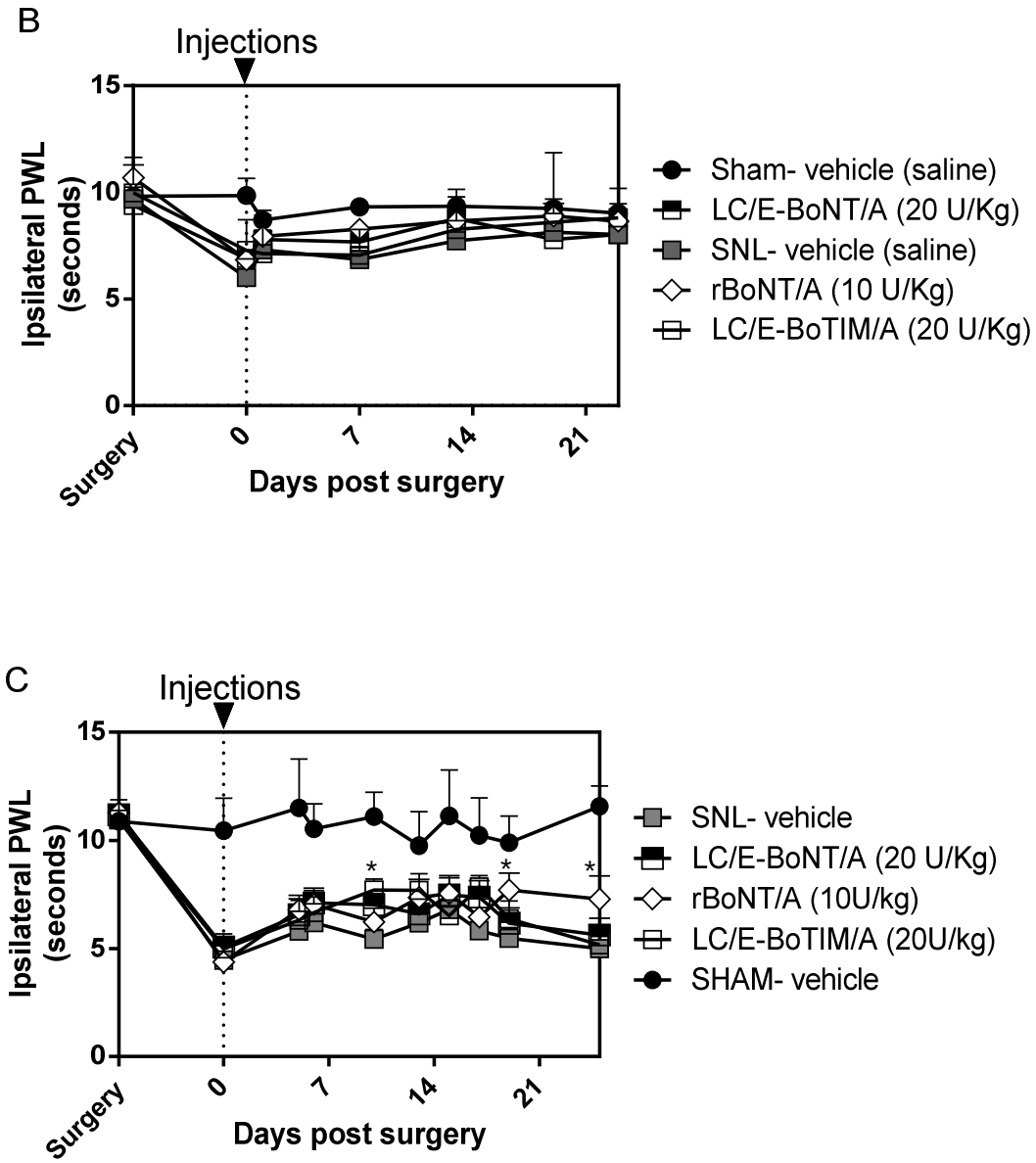

Figure 3-15 Efficacy of BoNTs on heat hyperalgesia.

A) *SNL study 001,* ***B)*** *002 and* ***C)*** *003. Spinal nerve ligation significantly reduced paw withdrawal latencies when compared to the sham group. However, no significant effect was found between the SNL vehicle and BoNT-treated groups in* ***A)*** *or* ***B)****. In* ***C)*** *treatment with LC/E-BoTIM/A or LC/E-BoNT/A significantly improved paw withdrawal latencies to heat hyperalgesia at day 10 and days 19 and 25, respectively. See text for statistical analyses. See section 3.3.3.4 for method details.*

3.4.8. SNL surgery significantly decreased the weight placed on ipsilateral hindpaws post-operatively

Ligation of L5 and L6 spinal nerves, significantly decreased the weight placed on the ipsilateral-lateral hindpaws (Figure 3-16) **A)**, (Group, F (3, 34) = 31.60, P < 0.0001), (Time, F (9, 306) = 23.72, P < 0.0001). **B)**, (Group, F (4, 46) = 13.60, P < 0.0001), (Time, F (6, 276) = 13.75, P < 0.0001). **C)**, (Group, F (4, 39) = 26.38, P < 0.0001), (Time, F (8, 312) = 58.66, P < 0.0001. **A)**, significance was found between the sham and the SNL vehicle group at all time-points post-surgery until day 17; there was no significance found between the SNL vehicle and sham groups at day 23. In **B)**, Significance was only found between the SNL vehicle group and the sham group from days -7 to 13; no significance was found between these groups at days 19 and 23 post treatment. In **C)** weight bearing in all SNL groups remained statistically significant to the sham control group for the duration of the study.

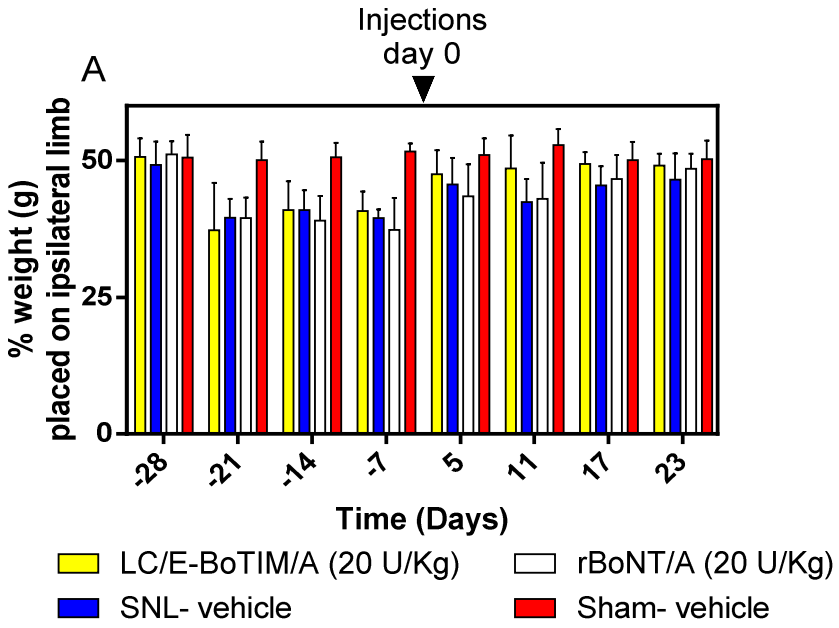

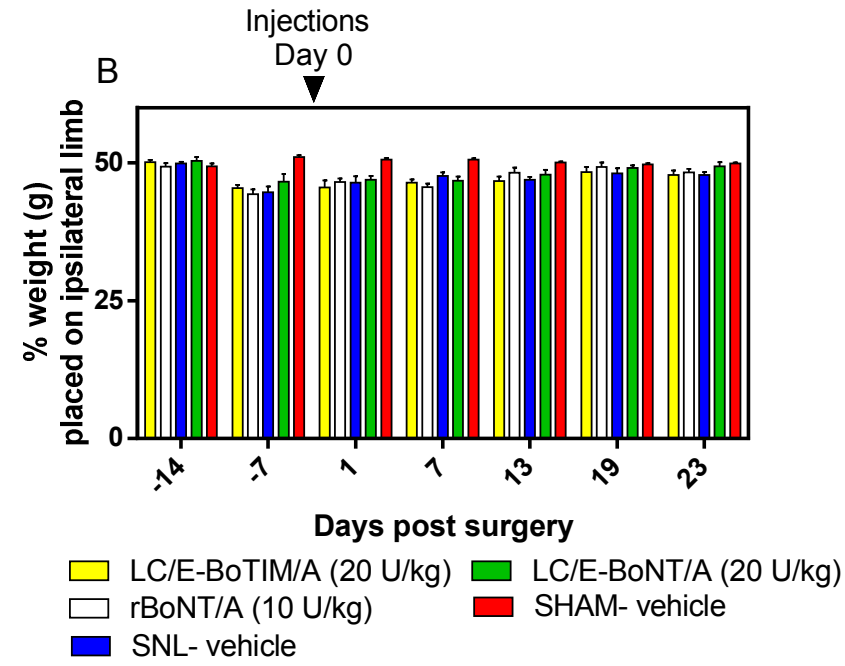

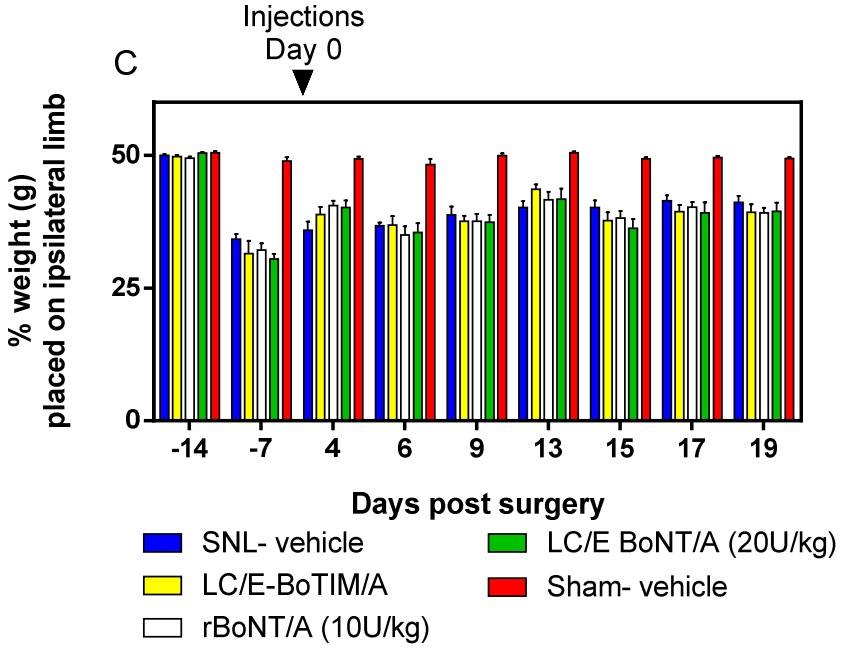

Figure 3-16 Changes in ipsilateral weight bearing following sham or SNL surgery.

SNL surgery significantly decreased weight placed on the ipsilateral hindpaws in all three studies. No significant effect in weight bearing was observed between treatments. See section 3.3.3.5 for method details.

3.5. Discussion and conclusions

A pre-clinical rat model of chronic neuropathic pain involving tight ligation of the L5 and L6 spinal nerves was established in-house to examine the efficacies of BoNT-based anti-nociceptives. No significant difference in animal weights was found between treatment groups, however, in the first study, a drop in body weight that did not reach significance was observed in the rBoNT/A (20 U/kg). It was suspected that this dose was too high and was causing loco-motor deficits. A rota-rod was purchased to evaluate this hypothesis, treatment with rBoNT/A (20 U/kg) did indeed produce severe loco-motor dysfunction lasting from days 2-5 and gradually improving to ~ day 18 where the recovery reached a plateau. This pattern of recovery could reflect the duration of action of the toxin. Although no difference between body weights was observed between treatment groups, there were clear differences observed between suppliers. For the first and third study, animals were purchased from Harlan, UK, whereas for the second study the vendor was changed to Charles Rivers UK because there was a promotion at the time. Charles River rats grew much more rapidly than Harlan animals; while rats supplied from the latter vendor appeared calmer, were easier to train and habituated quicker to tests. LC/E-BoNT/A significantly attenuated mechanical allodynia at days 7 and 19 post-treatment when compared to the vehicle control group. LC/E-BoTIM/A and LC/E-BoNT/A significantly increased the latency of first paw withdrawal in response to cold allodynia at days 15 and 9, respectively. The cumulative number of ipsilateral lifts also significantly decreased at days 7, 13 and 15 for LC/E-BoTIM/A and at day 15 for rBoNT/A. LC/E-BoTIM/A and LC/E-BoNT/A attenuated heat hyperalgesia at days 10 (LC/E-BoTIM/A) and 19 and 25 (LC/E-BoNT/A). Treatment with BoNTs appeared most efficacious at relieving mechanical and cold allodynia. Heat hyperalgesia and weight bearing appear less responsive to treatment. Together these preliminary findings support the use of BoNTs in treating chronic pain conditions.

For the third study, rats were fed a soybean-free diet, as evidence suggests that partial nerve ligation animals on a soy diet perioperatively displayed significantly reduced chronic pain behaviour when compared to those on a soy-free diet

(Shir et al., 1998). For the final study, L5 and L6 nerves were double ligated to prevent natural recovery in the model. Encouragingly, this third study revealed the most robust neuropathic pain features when compared to the other two studies.

3.6. Future work

These *in vivo* results provide some evidence for the ability of BoNT to relieve pain. Behavioural parameters most affected by treatment with BoNTs (mechanical and cold allodynia) were dissected out, along with the most accurate readouts for each test. These preliminary investigations lay the foundation for more sophisticated experiments. Currently, a colleague is using the spared nerve injury model of neuropathic pain, has obtained exciting data with 15 U/kg of rBoNT/A and 75 U/kg of LC/E-BoNT/A. This established robust model could be used to screen novel targeted BoNTs in the future.

4. DEVELOPMENT OF ANTIBODIES TO A PRIME PAIN TARGET

4.1. Background

4.1.1. Antibodies

Antibodies (immunoglobulins) are proteins that are recruited by the immune system to fight again infections. They are highly specific and recognise unique antigens that are located within foreign organisms. They are categorised into five classes (IgG, IgM, IgA, IgD, IgE) depending on their structure. IgG and IgM have two and ten binding sites, respectively; this enhances their avidity. IgG is a Y shaped antibody, containing two antigen binding Fab heavy chains (50 K) and two light chains (25 K) Fc domains joined together by disulphide bonds. Single chain variable fragment scFv antibodies (~ 30 K) are composed of the VH and VL domains joined together by a flexible polypeptide linker. Their smaller size allows better target penetration. Antibodies may be used as innovative tools to target potential anti-nociceptives.

4.1.2. Structure of transient receptor potential vanilliod 1 (TRPV1)

The TRPV1 polymodal receptor was first cloned in 1997 (Caterina et al., 1997); it is a membrane protein cation channel of 838 amino acids and may be activated by a variety of stimuli including: capsaicin, heat (> 43^{o}C), low pH (5.2) and various lipids. It has a tetrameric structure with six transmembrane domains, a pore/gate hydrophobic region located between the fifth and sixth domains and C- and N- termini positioned internally (Figure 4-1). TRPV1 has structural similarity to the voltage gated K^{+} channel. Activation and opening of TRP channels depolarises excitable cells and regulates Ca^{2+} and K^{+} channels.

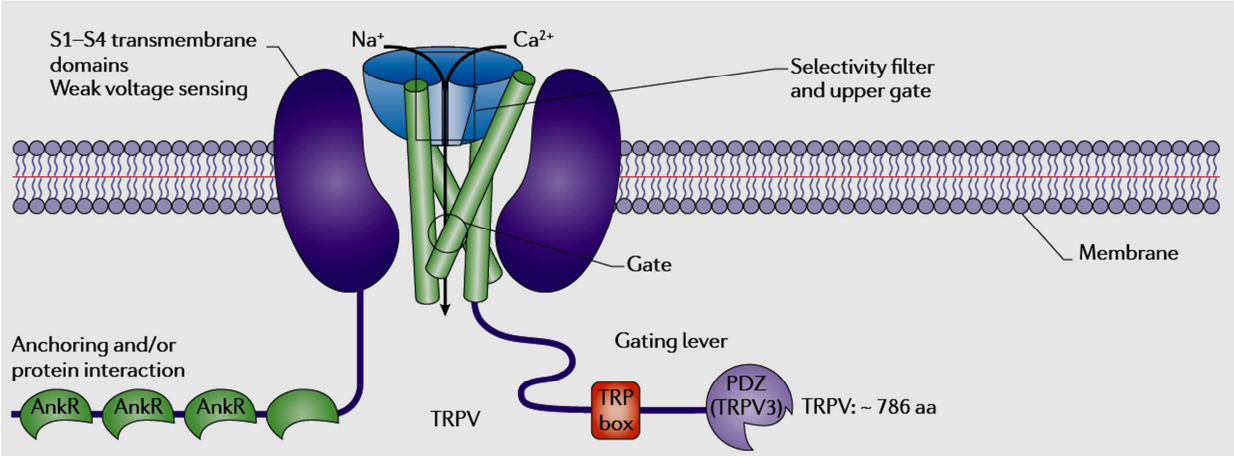

Figure 4-1 Structure of TRPV1.

TRPV1 has six transmembrane spanning domains and a pore/gate forming region located between the fifth and sixth subunits. It is activated by a range of activators including; capsaicin, heat and protons. Ankyrin repeats (AnkR) are present in TRPV channels and are believed to facilitate anchoring. The TRP box is an amino acid sequence that is involved in gating of the channel, opening of the channel/gate allows entry of Na^{2+} and Ca^{2+}. Abbreviations; aa, amino acids, AnkR, ankyrin repeats, PDZ, postsynaptic density protein 95. Image taken from Moran et al., 2011.

4.1.3. TRPV1 as a prime pain target

TRPV1 is located in the peripheral and central nervous systems, being expressed in sensory ganglia and C and Aδ fibres. Following injury or inflammation, pain mediators are released that activate TRPV1 receptors (Figure 4-2). TRPV1 is co-expressed along with TRPA1 in the peripheral nociceptor (Figure 4-3 A). Following activation, action potentials are generated and propagated to the central nervous system stimulating the release of neurotransmitters. Substances released at the peripheral nociceptor can initiate signal transduction pathways that contribute to the trafficking of TRPV1 (Figure 4-3 B).

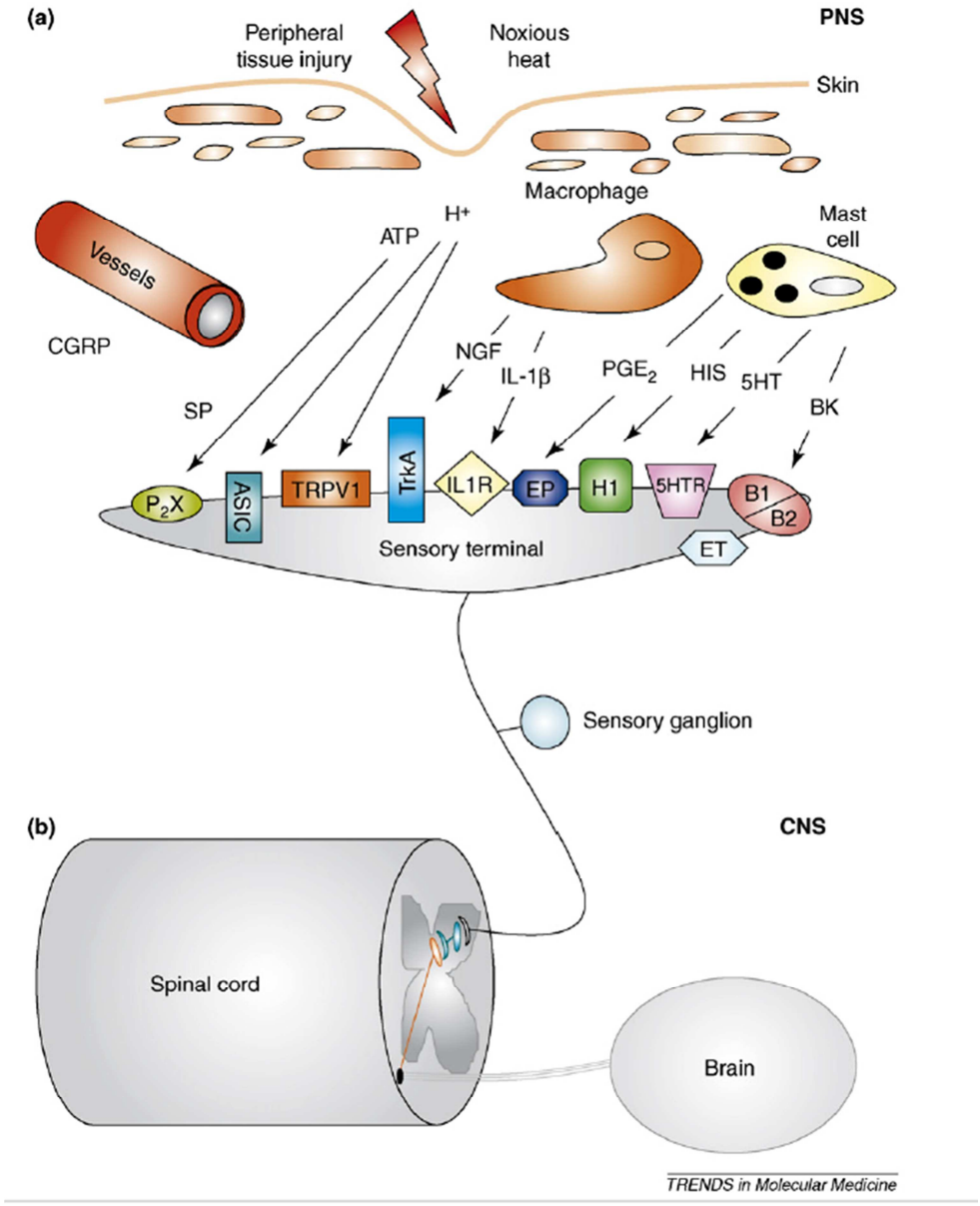

Figure 4-2 Expression and activation of TRPV1.

*TRPV1 is primarily expressed in sensory afferents of the peripheral nervous system and may be activated by a variety of mediators such as heat and protons **(a)**. TRPV1 is expressed along with Trk A, bradykinin, purine and other receptors. In response to activation, sensory neurons release pain mediators such as CGRP and substance P. In turn, signals propagated to the CNS are amplified and painful sensations are perceived by the brain. Abbreviations: 5HTR, serotonin receptor; BK, bradykinin; EP, prostaglandin E2 receptor; ET, endothelin receptor; H1, histamine receptor 1; HIS, histamine; IL1R, interleukin 1 receptor; PGE2, prostaglandin E2; SP, substance P. Image taken from Szallasi et al., 2006.*

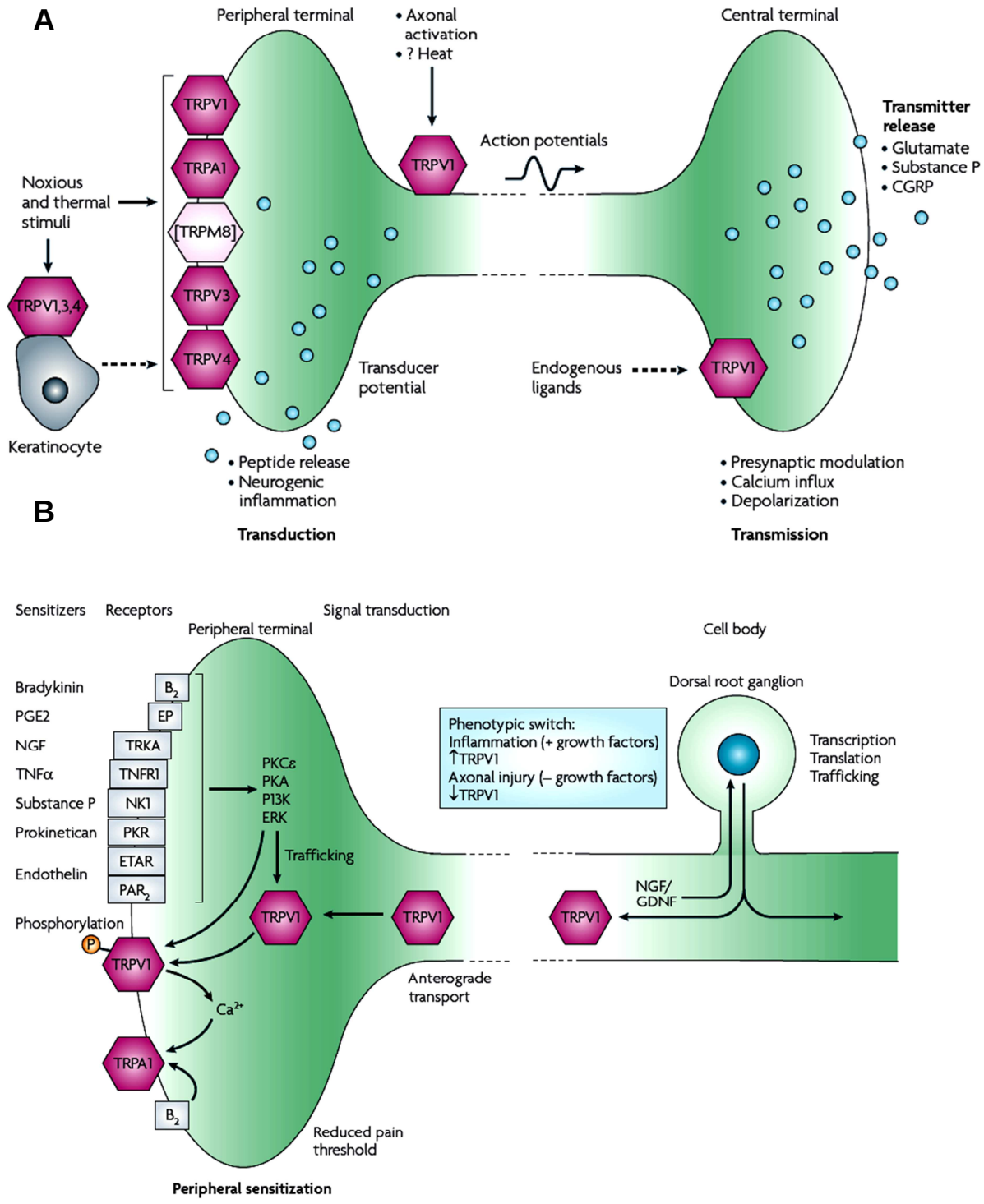

Figure 4-3 Expression of TRP channels in nociceptors (A) and changes produced by inflammation (B).

*TRPV1 is co-expressed along with TRPA1 in peripheral nociceptors **(A)**. Painful stimuli directly activate these pain receptors in the peripheral nervous system, converting these stimuli into electrical impulses and conveying these impulses to the central*

nervous system; this is accompanied by the release of peptides/inflammatory mediators producing neurogenic inflammation and activation of signal transduction pathways. ***(B)*** *These pathways may phosphorylate TRPV1 and other TRP channels and affect their trafficking to the plasma membrane. Growth factors released in response to pain, increase the expression of TRPV1 in the peripheral terminals. Together these changes create an altered processing environment lowering the activation threshold of nociceptors. Abbreviations; CGRP, calcitonin gene-related peptide; B2, bradykinin receptor B2; ERK, extracellular signal-regulated kinase; ETAR, endothelin receptor type A; GDNF, glial-cell-derived neurotrophic factor; NK1, neurokinin receptor 1; PAR2, protease-activated receptor 2; PGE2, prostaglandin E2; PI3K, phosphoinositide 3-kinase; PK, protein kinase; PKR, prokineticin receptor; TNFα, tumour necrosis factor α; TNFR1, TNF receptor 1; TRKA, tyrosine kinase receptor A. Images taken from Patapoutian et al., 2009.*

4.1.4. Intracellular trafficking of TRPV1

Regulated exocytosis is believed to be responsible for TRPV1 receptor surface translocation during nociceptor sensitisation. A yeast two hybrid system was used to identify proteins that interact with the N terminus of TRPV1. This platform identified two proteins-Snapin and Synaptotagmin IX that interact both *in vitro* and *in vivo* with TRPV1. Both of these proteins block protein kinase C (PKC) signalling of TRPV1 while PKC activation leads to fast TRPV1 trafficking to the plasma membrane; the latter is inhibited by BoNT/A. This study concluded that PKC signalling contributes to SNARE-dependent exocytosis of TRPV1 to the plasma membrane (Morenilla-Palao et al., 2004).

To further investigate this hypothesis, an additional inhibitor of exocytosis was used to evaluate SNARE regulated exocytosis of TRPV1. It was found that TRPV1 induced sensitisation stimulated by NGF, ATP and IGF-1; this was accompanied by increased plasma membrane expression that was successfully blocked by application of a 6-mer peptide. On the other hand, TRPV1 sensitisation induced by IL-1β, bradykinin and artemin were not blocked. This data concluded that TRPV1 is involved in the mechanism by which some proinflammatory agents sensitise nociceptors while other proinflammatory agents act independently of TRPV1 (Camprubi-Robles et al., 2009).

The mechanisms involved in TRPV1 desensitisation were evaluated in a recent study whereby both sensory neurons and HEK transfected TRPV1 cells were exposed to capsaicin-an agonist of TRPV1. This induced TRPV1 receptor endocytosis followed by lysosomal degradation in both systems. TRPV1 internalisation as a result of agonist stimulation and Ca^{2+} flux was mediated by a clathrin and dynamin independent endocytic pathway controlled by PKA-dependent phosphorylation. These findings concluded that long term exposure to agonists of TRPV1 led to receptor down regulation by endocytosis followed by lysosomal degradation (Sanz-Salvador et al., 2012).

Experiments in this chapter, were conducted to determine if the α-TRPV1 antibodies generated are internalised and trafficked in a similar fashion to that of TRPV1. Capsaisin was applied to stimulate uptake of the antibody and bafilomycin A1 to increase visibility of vesicular structures (Figure 4-4).

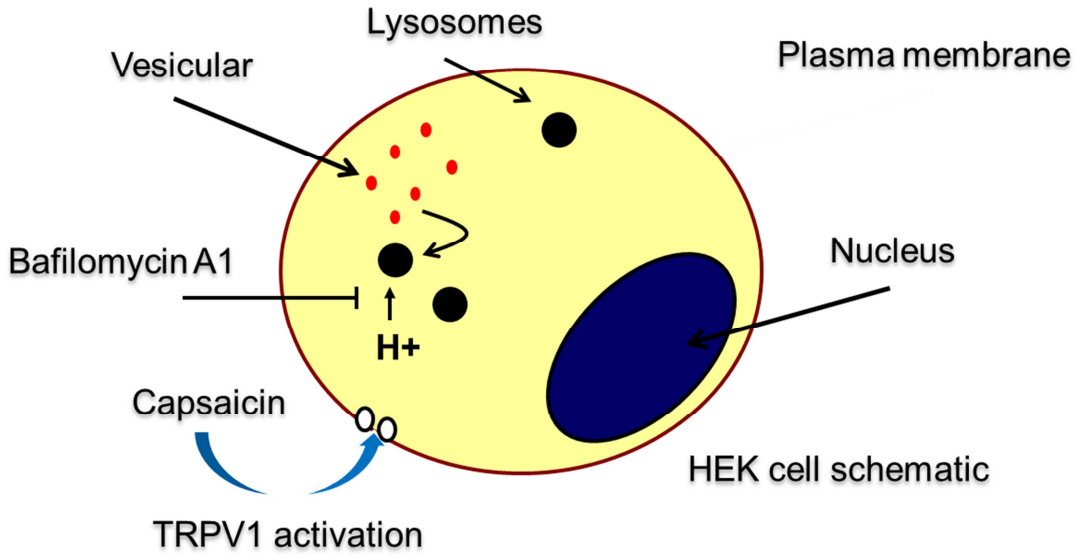

Figure 4-4 Schematic to illustrate the hypothesised intracellular trafficking of TRPV1 in HEK cells.

Capsaicin is an agonist of TRPV1 which activates the TRPV1 channel and stimulates TRPV1 internalisation. Bafilomycin A1 is a specific inhibitor of vacuolar-type H(+)-ATPase and blocks acidification; this should lead to accumulation of the antibody and increased visibility of vesicular staining by preventing the passage of TRPV1 through acidified compartments. Abbreviations; H^+, protons.

4.1.5. Alterations in the expression of TRPV1 following treatment with BoNT

The expression of TRPV1 on the plasma membrane is regulated by exocytosis and increased levels are present in painful states (Camprubi-Robles et al., 2009, Akbar et al., 2008, Gopinath et al., 2005). Application of BoNT/A, a potent inhibitor of exocytosis, is believed to disrupt TRPV1 trafficking to the plasma membrane and, in turn; attenuate pain. A number of studies support this theory; reduced TRPV1 was found in human bladder samples from patients that had BoNT/A locally administered (Apostolidis et al., 2005). A recent study (Shimizu et al., 2012) where BoNT/A was injected into rat trigeminal ganglion neurons revealed reduced TRPV1 immunoreactivity in both the trigeminal ganglion and the fibre terminals. Cleavage of its substrate SNAP-25, was observed two days post-treatment and remained for a minimum of two weeks. A surface biotinylation assay confirmed that BoNT/A blocked TRPV1 trafficking to the plasma membrane. It was concluded from this study that BoNT/A reduces TRPV1 expression by inhibiting its trafficking to the plasma membrane and proteasome degradation (Figure 4-5). A ventral root transection rodent pain model was used to investigate the actions of BoNT/A on pain thresholds and TRPV1 expression in the DRG. Immunohistochemistry and Western blotting data revealed that treatment with BoNT/A significantly decreased TRPV1 expression which was accompanied with a partial attenuation of pain thresholds (Xiao et al., 2013).

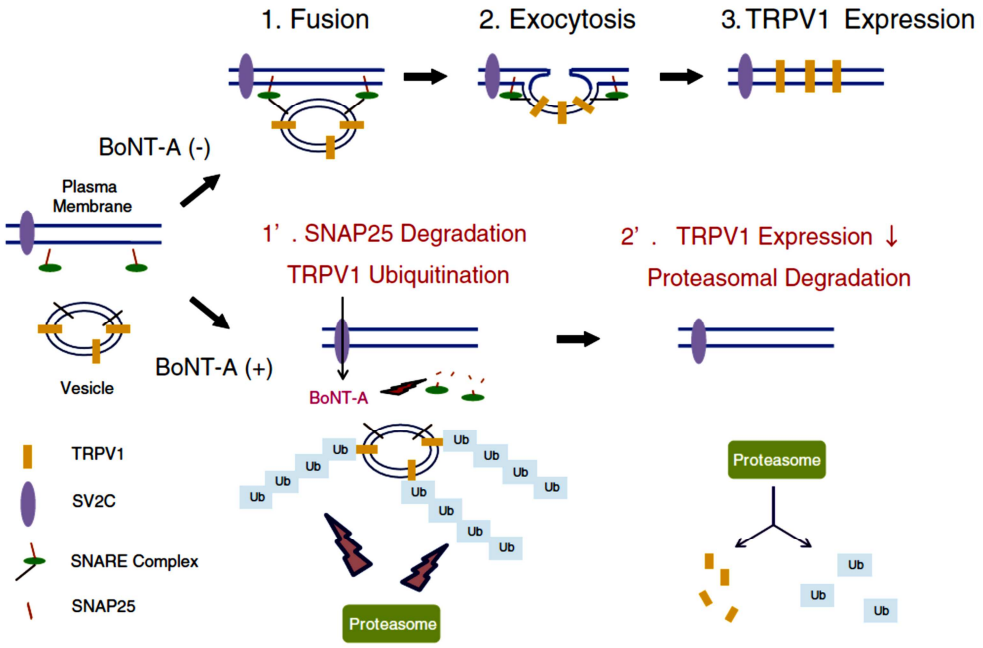

Figure 4-5 Changes in TRPV1 expression following treatment with BoNT/A

The expression of TRPV1 on the plasma membrane is regulated by exocytosis. Fusion of TRPV1 containing vesicles (1) with the plasma membrane under desired conditions leads to exocytosis (2) and expression of TRPV1 on the plasma membrane (3). Application of BoNT/A, binds to its acceptor SV2C, cleaves its substrate SNAP-25 and disrupts exocytosis. This prevents the translocation of TRPV1 to the plasma membrane, inducing ubiquitination (Ub) and proteasomal degradation of (1') leading to reduction of TRPV1 expression (2'). Image taken from Shimizu et al., 2012.

4.2. Aims and objectives:

- To develop and characterise antibodies to human TRPV1.
- To investigate the internalisation and trafficking of α-TRPV1 antibodies.

4.3. Results

4.3.1. Target selection-peptides chosen and rationale

Two epitopes were selected, corresponding to different regions of the human TRPV1 protein sequence (Figure 4-6). The first corresponds to amino acids 606-621 and shares 69% identity to rat, and 63% identity to mouse. This peptide is referred to as TRPV1-A. The second epitope (TRPV1-B)

corresponds to amino acids 637-649 and shares 100% identity to rat and was, therefore, expected to bind both rat and human TRPV1.

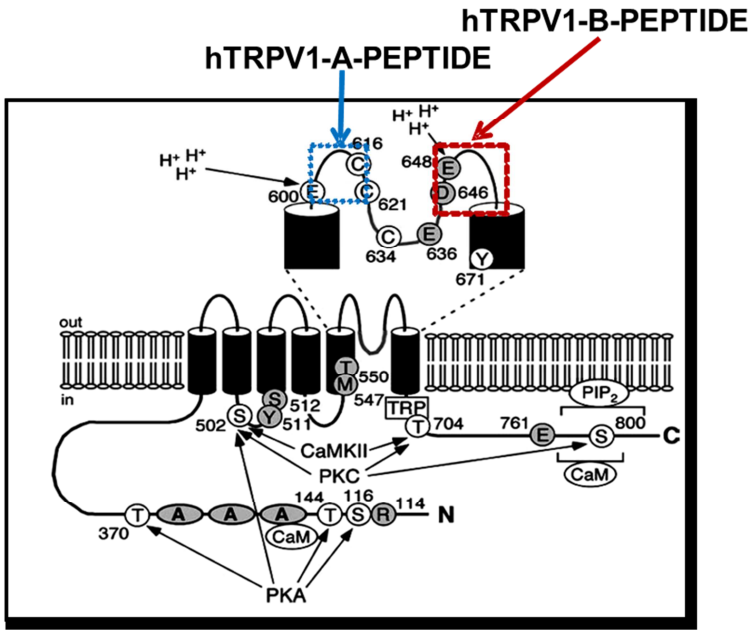

Figure 4-6 Epitopes selected from the human TRPV1 protein sequence for antibody generation.

*hTRPV1-A and hTRPV1-B external epitopes were selected, corresponding to the following amino acids: H-S-L-P-S-E-S-T-S-H-R-W-R-G-P-A-C-OH (amino acids 606-621 of the hTRPV1 sequence for –A (**blue square**)) and ELFKFTIGMGDLE-Cys (amino acids 637-649 of the hTRPV1 sequence for –B (**red square**)). Abbreviations include; PIP2, phosphatidylinositol (4,5)-bisphosphate; CaM, calmodulin; CaMKII, calmodulin kinase II; PKA, protein kinase A; PKC, protein kinase C; S, serine; T, threonine. Image modified from Tominaga and Tominaga, 2005.*

4.3.2. A commercial α-TRPV1 antibody to the same epitope but in rat successfully stained TRPV1 in sensory neurons of rat dorsal root ganglia

Review of the literature revealed that an antibody to a similar region to that of the TRPV1-A peptide was available commercially but had been generated to rat TRPV1. Sensory dorsal root ganglia neurons P5 were cultured and stained; specific staining of TRPV1 was achieved with this commercial antibody (Figure 4-7).

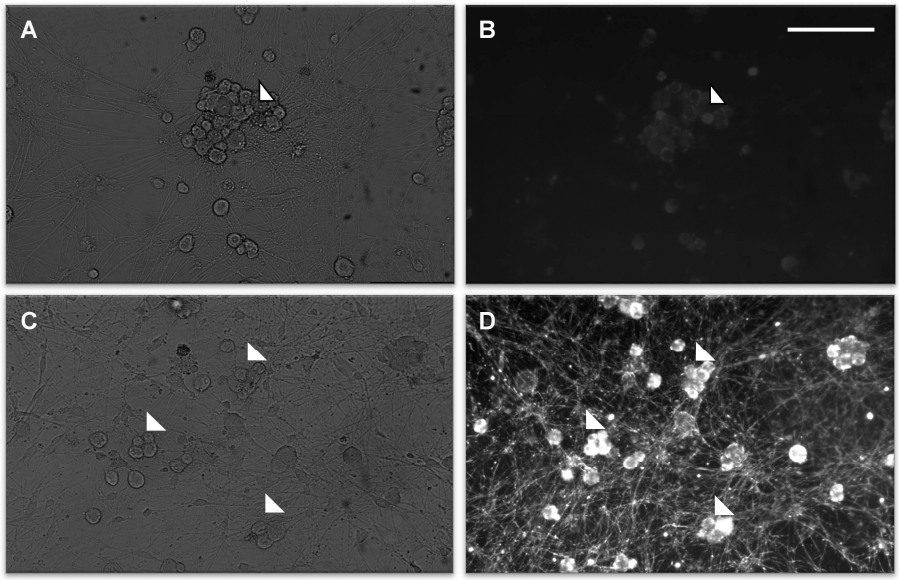

Figure 4-7 Staining of sensory dorsal root ganglia neurons with the commercial α-rTRPV1 antibody.

***A**- Brightfield image for **B**. **B**- No staining was observed with the goat-α-rabbit-Alexa 568 secondary only control antibody (1:1500 dilution). **C**- Brightfield image for **D**. **D**- Positive α- rTRPV1 staining was observed after overnight incubation with the commercial rTRPV1 extracellular antibody 1:50 dilution (Alomone); 2^{o} antibody- goat-α-rabbit-Alexa 568 1:1500 dilution. X 10 magnification, bar represents 100 µm. Arrowheads represent cell bodies. Staining of intact sensory neurons was carried out as described in section 2.4.1.2 of the Materials and Methods chapter.*

4.3.3. Serum from a rabbit immunised with TRPV1-A and TRPV1-B peptides revealed pronounced immunogenicity towards the α-TRPV1-A peptide

The rabbit (named DAKA for identification purposes) immunised with a combination of TRPV1-A and TRPV1-B produced pronounced immunogenicity towards the α-TRPV1-A peptide with a direct ELISA titre of ~ 1/100000 against α-TRPV1-A-KLH coated plates (Figure 4-8). However, the resultant polyclonal antibodies were unreactive to rat TRPV1 (Figure 4.9), suggestive of an issue with the TRPV1-B peptide synthesis. Closer examination of the TRPV1-B-BSA peptide, confirmed this, as no protein of 66 K was visualised after separation on SDS-PAGE (not shown).

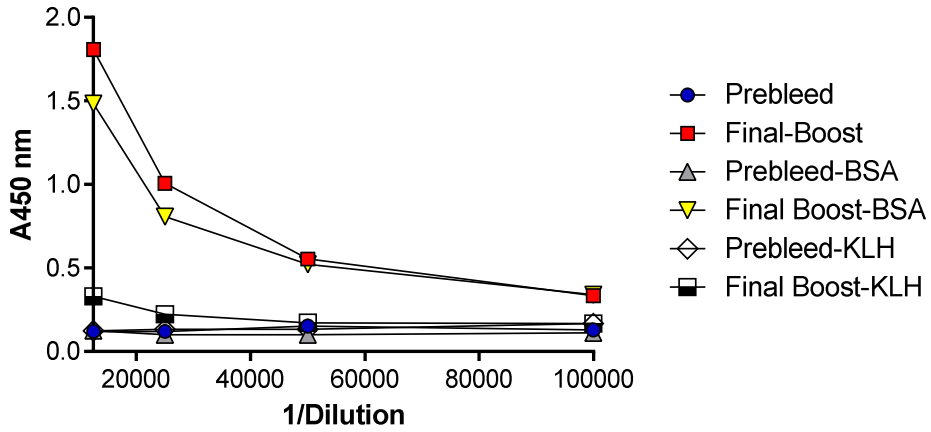

Figure 4-8 Direct ELISA from DAKA.

Nunc plates were coated overnight with 2 µg/mL of TRPV1-A-KLH. Plates were blocked with 200 µl of 5% milk marvel for 1 hr in PBS. Serial dilutions of the serum were prepared in PBST with 5 % milk marvel; 100 µl of each serial dilution was added for 1 hr at room temperature. Plates were then washed 3 times in both PBST and PBS. Donkey-α-rabbit HRP secondary antibody (1:1000) was added to each well in PBST with 5% BSA and incubated for 1 hr at room temperature. This was followed by 3 washes with PBST and PBS. TMB (100 µl) was added to each well and the reaction monitored. The reaction was stopped with 1M HCL (50 µl) and the plate read on a Tecan plate reader. PB- prebleed, FB- final bleed. Absorbance values were read at 450 nm. Direct ELISA was carried out as described in section 2.2.2.3 of the Materials and Methods chapter.

4.3.4. α-hTRPV1-A polyclonal antibodies from the DAKA crude serum detected human but not rat TRPV1

HEK cells were transiently transfected with pcDNA3 encoding either human or rat TRPV1 or left untreated for 24 or 48 hrs prior to lysis in SDS sample buffer. Each sample (10 µl) was separated by SDS-PAGE and subjected to Western blotting. Membranes were sequentially probed with the following antibodies, i) Serum from DAKA immunised with α-hTRPV1-A (external loop) ii) Commercial α-rTRPV1 (external loop Alomone). α-TRPV1-A polyclonal serum detected human but not rat TRPV1 (Figure 4-9 A). Commercial α-rTRPV1 antibodies detected rat but not human TRPV1 (Figure 4-9 B). When the membrane of A was washed with NaN3 and incubated with commercial α-rTRPV1 antibodies, it

detected rTRPV1 (Figure 4-9 C). When the membrane of B was incubated with the polyclonal α-hTRPV1-A antibodies, it also detected hTRPV1 (Figure 4-9 D). In conclusion, Western blot analysis revealed that the polyclonal serum from DAKA detected human but not rat TRPV1 (Figure 4-9). HEK-WT untransfected cells were used as an experimental control, TRPV1 was not detected in this lane, however, a protein band of a higher molecular weight was detected in this lane and in all other HEK cell lanes, this band appears to be specific to a protein in HEK cells.

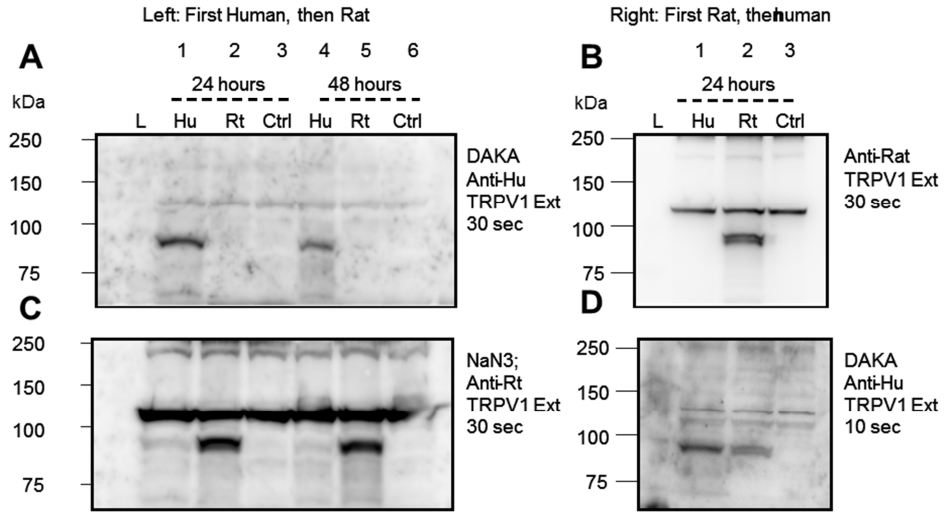

Figure 4-9 Detection of either human or rat TRPV1 by Western blotting of transiently-transfected HEK cell lysates probed with polyclonal TRPV1-A DAKA serum or commercial α-rat TRPV1 external antibody.

HEK cells were transiently transfected with pcDNA3 encoding human (lanes 1, 4) or rat (lanes 2, 5) TRPV1 or left untransfected (lanes 3, 6) for 24 (lanes 1, 2, 3) or 48 hrs (lanes 4, 5, 6). Samples were subsequently lysed and separated by SDS-PAGE and Western blotted. ***A.*** *The membrane was probed with α-hTRPV1-A polyclonal serum and detected human TRPV1, no signal was detected for rat TRPV1 or for the non-transfected control cells.* ***B.*** *The commercial α-rTRPV1 antibody detected rat but not human TRPV1, again no signal was detected in the negative control lane.* ***C.*** *When the membrane of A was washed with NaN3 and developed with the commercial α-rTRPV1 antibody, it detected rat TRPV1.* ***D.*** *The membrane of B was incubated with the α-hTRPV1-A polyclonal serum and subsequently detected human TRPV1, some signal from the previous incubation remained as it was not washed out. Further method details can be found in section 2.2.2.11 of the Materials and Methods chapter.*

4.3.5. α-hTRPV1-A antibodies were purified by protein A-Sepharose

Polyclonal antibodies from the hTRPV1-A immunized DAKA rabbit serum were purified by protein A-Sepharose. Protein stained gel revealed the anticipated antibody heavy and light chains of ~ 50 and 25 K, respectively (Figure 4-10).

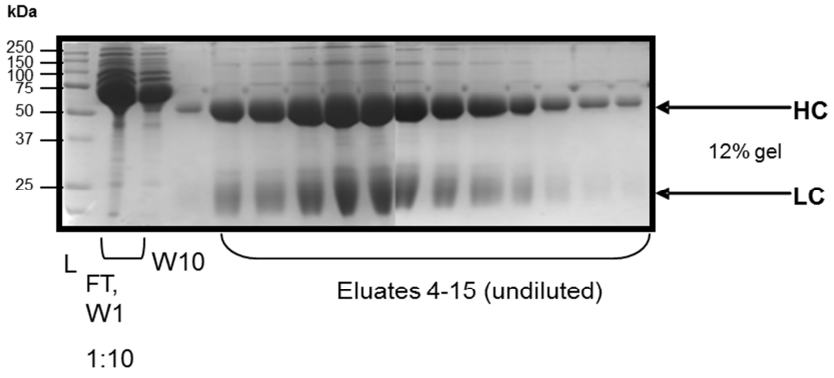

Figure 4-10 Purification of α-hTRPV1 polyclonal antibodies.

IgGs from α-hTRPV1 polyclonal serum were purified by protein A-sepharose and characterised by Coomassie stained 12 % gel. In the presence of reducing agent DTT, proteins separated into their expected heavy and light chains of 50 and 25 K, respectively. Method details can be found in section 2.2.2.9.2.

4.3.6. α-hTRPV1-A purified IgGs bind specifically to hTRPV1 in a dose-dependent manner and are internalised by hTRPV1 transiently-transfected HEK cells

Key immunocytochemistry experiments were performed to determine if α-hTRPV1-A antibodies bind to and are internalized by hTRPV1-expressing cells. To evaluate this, HEK cells transiently over-expressing hTRPV1 were stained with purified polyclonal α-hTRPV1 antibodies. Encouragingly, TRPV1-positive staining was observed in both permeabilised and non-permeabilised conditions, indicative of hTRPV1 antibodies binding to TRPV1; the specificity of this binding was further confirmed by an absence of staining in untransfected HEK-WT cells (Figure 4-11). Immunocytochemistry (Figure 4-12) and Western blotting (Figure 4-13) of transiently-transfected hTRPV1 HEK cells, with increasing concentrations α-hTRPV1-A antibodies revealed that antibody binding is dose-

dependent and specific to TRPV1 (as it was completely blocked by addition of a 100 fold molar excess of the hTRPV1-A blocking peptide).

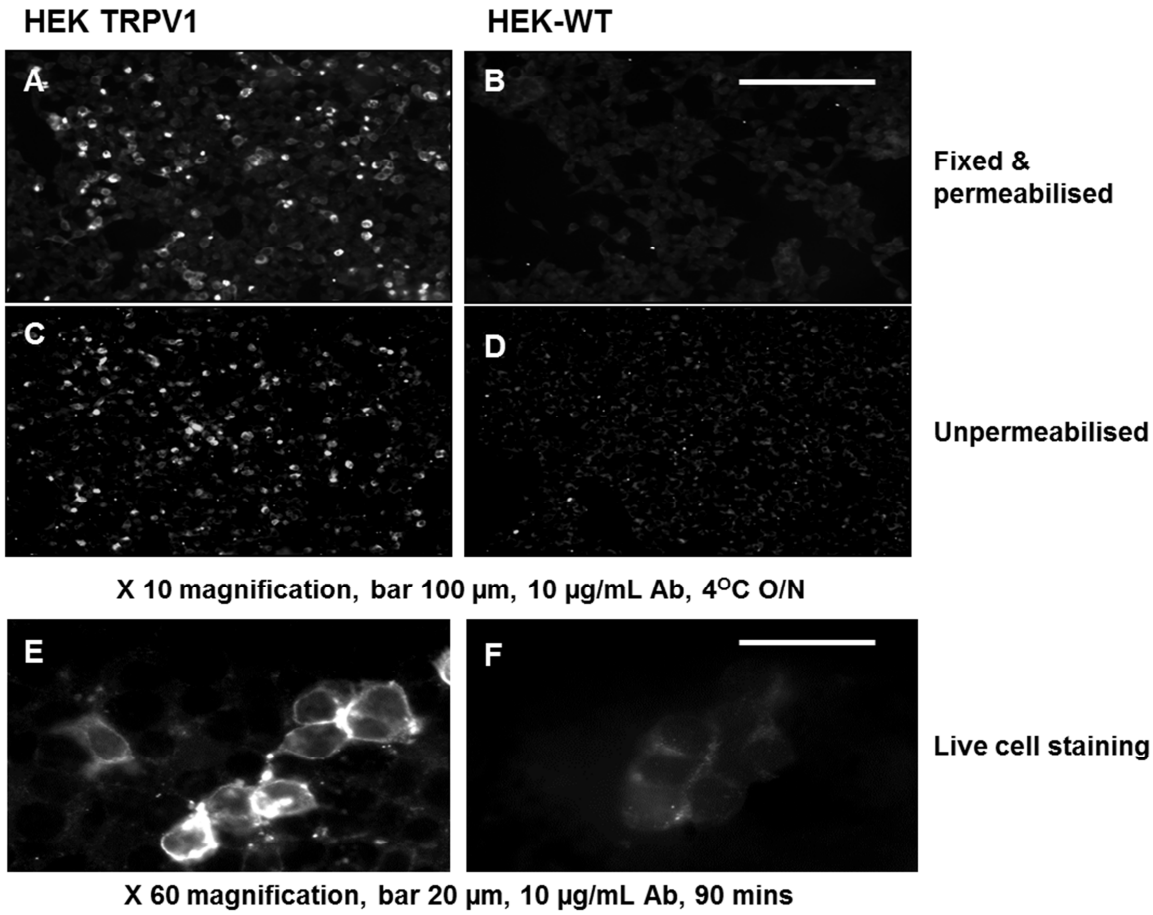

Figure 4-11 α-hTRPV1 antibody staining of permeabilised, unpermeabilised and live HEK cells transiently transfected with pcDNA3 encoding hTRPV1.

*HEK cells were transiently transfected with pcDNA3 encoding either hTRPV1 or left untreated for 24 hrs. α–hTRPV1-IgGs were applied to either permeabilised **(A, B)**, unpermeabilised **(C, D)** or to live cells **(E)**. Positive staining specific to hTRPV1 was achieved and lack of signal in the HEK-WT cells **(B, D and F)**. HEK-TRPV1 live cell staining was predominately located around the plasma membrane **(E)**. Further details regarding methods can be found in sections 2.4.1.1, 2.4.1.2 and 2.4.1.3 of the Materials and Methods chapter.*

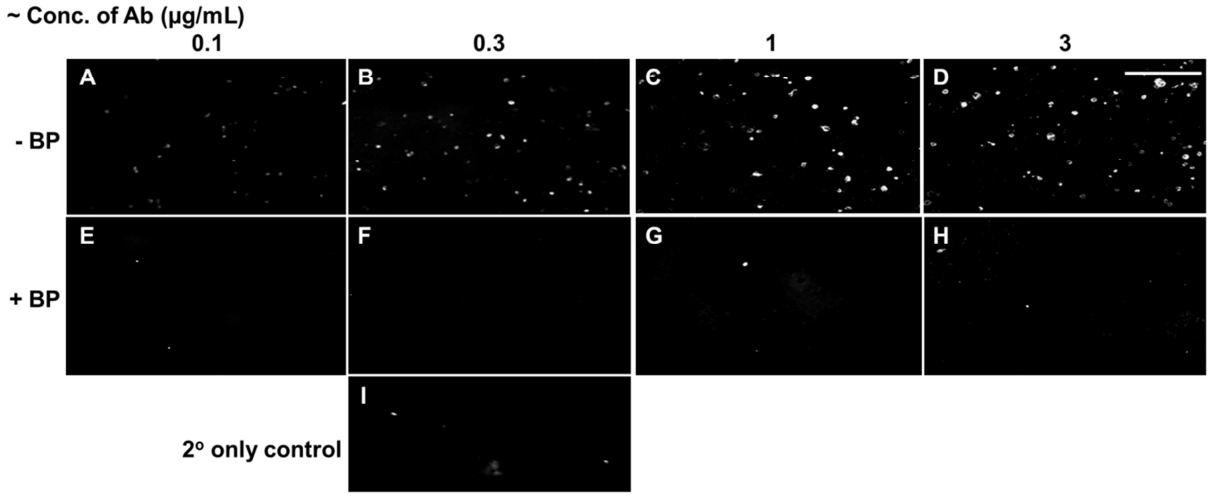

Figure 4-12 α-hTRPV1-IgGs dose-dependently-detect hTRPV1.

*HEK cells were transiently transfected with pcDNA3 encoding either human or rat TRPV1 or left untreated for 24 hrs. Subsequently, cells were blocked, fixed and incubated overnight with increasing concentrations of α-hTRPV1 antibodies with or without a 100-fold molar excess of the free TRPV1-A peptide. Panels **A-H**- HEK cells transiently transfected with hTRPV1 were subsequently incubated with increasing concentrations of α-TRPV1 IgGs (µg/mL)- **A** and **E**- 0.1, **B** and **F**- 0.3, **C** and **G**- 1 and **D** and **H**- 3 µg/mL. Panels **A-D** were incubated without inclusion of the blocking TRPV1-A free peptide – (BP), while panels **E-H** were incubated with addition of a 100-fold molar excess of the free TRPV1-A peptide. Panel **I** – HEK hTRPV1 transfected cells incubated only with the Alexa-conjugated goat anti-rabbit IgG secondary antibody (1:500). Method details can be found in section 2.4.1.2.*

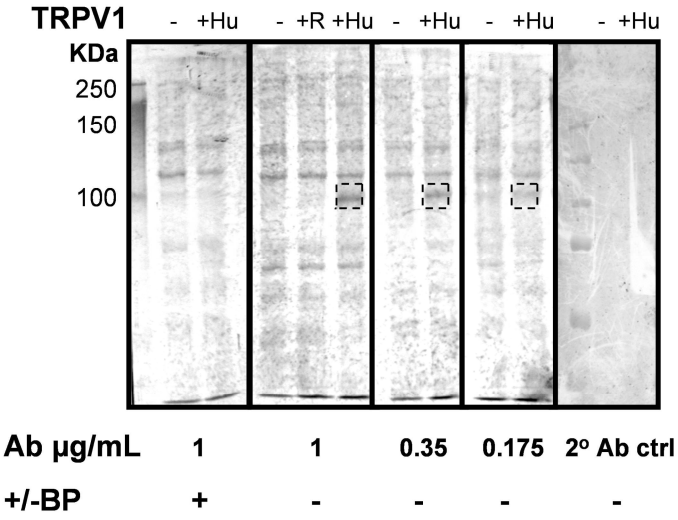

Figure 4-13 Western blot of the reactivities of increasing concentrations of purified α-hTRPV1 antibodies with hTRPV1 HEK cell lysates, in the presence or absence of blocking peptide.

HEK cells were transiently transfected with human or rat TRPV1 or left untreated for 24 hrs prior to lysis in SDS sample buffer. Each sample (10 µl) was separated by SDS-PAGE and Western blotted. Membranes were incubated with the α-hTRPV1-IgG in increasing concentrations, with or without the control free TRPV1-A blocking peptide (100-fold molar excess); the control peptide successfully blocked α-hTRPV1-A-antibody binding sites, thus, no TRPV1 was detected (~ 95 K). TRPV1 was also absent in the 2^{O} antibody only control treated hTRPV1 transfected HEK cells (donkey α rabbit HRP IgG). TRPV1 was only present in hTRPV1 transfected cells and absent from rTRPV1 or WT cells. Method details can be found in section 2.2.2.11 of the Materials and Methods chapter.

4.3.7. α-hTRPV1-A antibody binds to HEK-hTRPV1 transfected cells

Staining of HEK cells transfected with or without hTRPV1 revealed that antibody binding increases with time. This staining is specific to hTRPV1 as no definite staining was observed in non-transfected control cells (Figure 4-14).

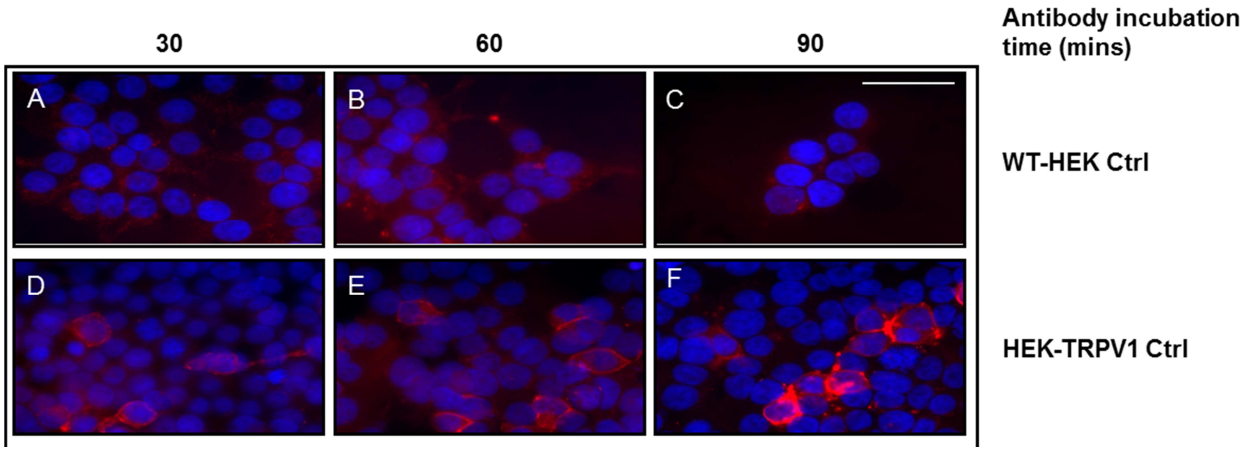

Figure 4-14 Time required for binding of hTRPV1-A antibodies to HEK-TRPV1 transfected cells.

IgG- red, DAPI- blue. α-hTRPV1-A antibodies (10 µg/mL) did not bind to HEK-WT control cells. hTRPV1-A antibodies bound to HEK-TRPV1 transiently-transfected cells. Scale bar represents 100 µm, objective- X 60. Further details can be found in section 2.4.1.3 of the Materials and Methods chapter.

4.3.8. Live cell staining with washout after antibody binding illustrates vesicular staining

Antibody staining of live cells with washout illustrates the transition of the antibody over time. Treatment with bafilomycin A1 (a specific inhibitor of vacuolar-type H(+)-ATPase) lead to an accumulation and increased visibility of vesicular antibody staining, suggestive that the antibody undergoes trafficking through acidified vesicles (Figure 4-15). Co-staining with suitable markers e.g. a lysosomal-associated membrane protein antibody would be required to confirm the route of this transition.

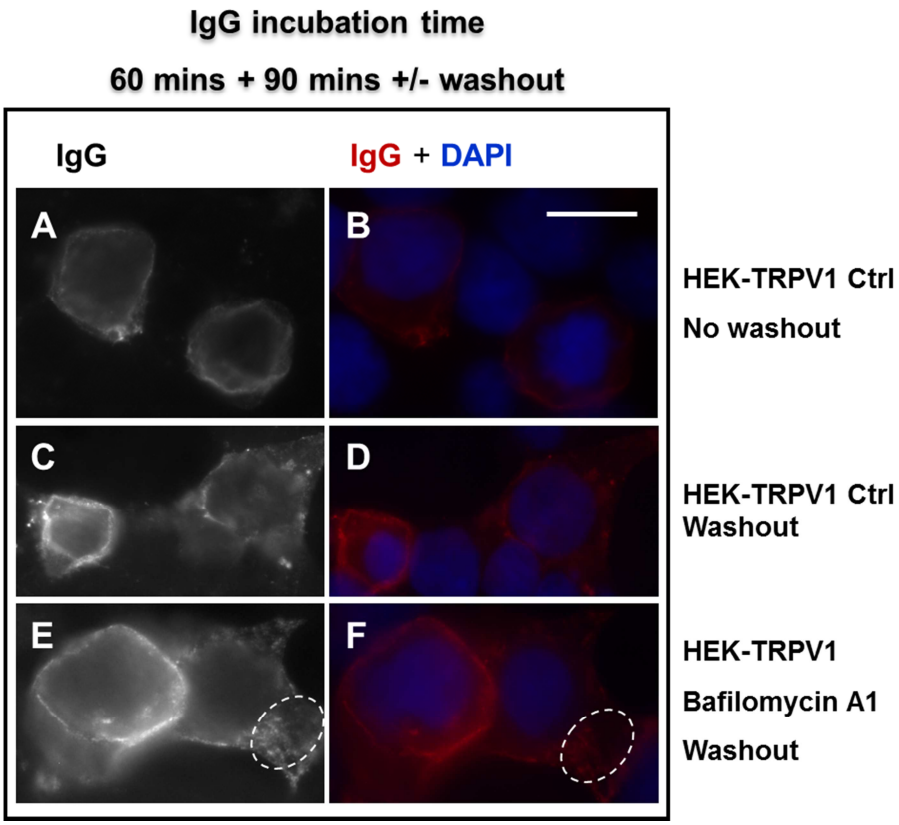

Figure 4-15 hTRPV1-A IgG cell staining with or without washout or bafilomycin A1.

Cells were incubated with 10 µg/mL of hTRPV1-A antibodies, with or without bafilomycin A1 (100 nM) for 60 mins. This was followed by either washout or no washout and incubation for an additional 90 mins. Additional method details can be found in section 2.4.1.4.

4.3.9. Pre-treatment with filipin blocked endocytosis of the antibody indicating that it utilises lipid rafts

Pre-treatment with 6 µg of filipin per well (an inhibitor of lipid rafts), followed by antibody incubation overnight resulted in intense plasma membrane staining without labelling of vesicles; endocytosis of the antibody was prevented by filipin, suggesting that TRPV1-A utilises lipid rafts (Figure 4-16).

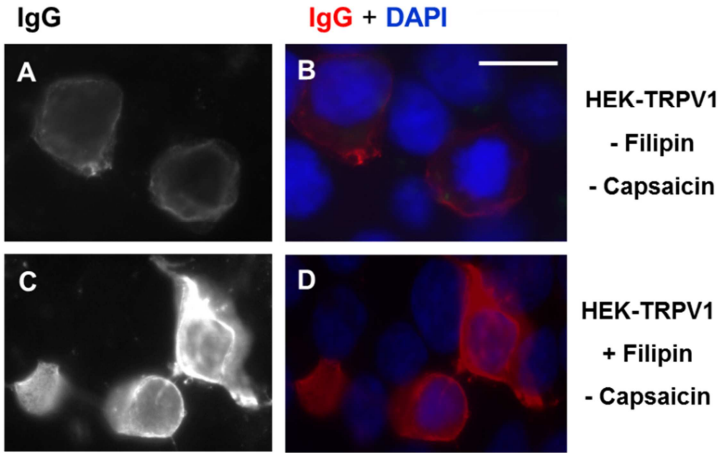

Figure 4-16 Pre-treatment with filipin followed by α-hTRPV1 antibody binding.

HEK-TRPV1 transfected cells were pre-treated with 6 µg filipin/well followed by 10 µg/mL IgG/well. Objective X 60, Bar 100 µm, Exposure red- 500 ms, blue- 200 ms. Further details can be found in section 2.4.1.4 of the Materials and Methods section.

4.3.10. Capsaisin stimulated antibody uptake and yielded more 'vesicular like' staining

HEK-TRPV1 transfected cells were incubated with hTRPV1-A antibodies (10 µg/mL) for 90 mins with 1 µM of capsaicin. Cells were then washed and incubated for an additional 6 hrs. Vesicular α-hTRPV1-A staining was observed in transfected HEK-TRPV1 cells (Figure 4-17), however, No staining was observed in the untransfected HEK-WT cells (not shown).

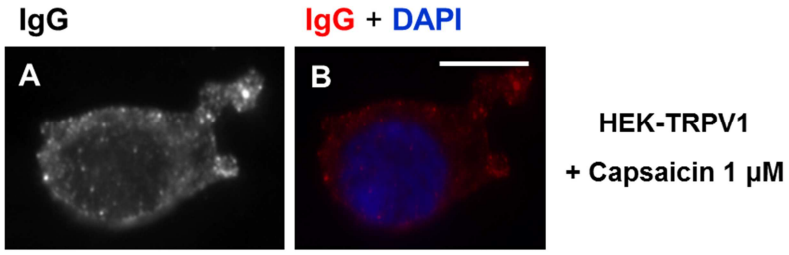

Figure 4-17 Capsaisin stimulated antibody uptake.

Antibody binding (90 mins), followed by washout and a 6 hr follow up period; 10 µg/mL IgG/well, 1 µM capsiacin, HEK-TRPV1 cells. Objective X 60, Bar 100 µm, Exposure red- 500 ms, blue- 200 ms. Further details can be found in section 2.4.1.3 of the Materials and Methods chapter.

4.3.11. An *in vitro* HEK cell culture model expressing SNAP-25 pIRES GFP was established

HEK cells were transiently transfected with pcDNA3 encoding pIRES GFP or left untreated for 48 or 72 hrs. GFP reactive cells were observed at 48 and 72 hours; reactivity decreased with incubation time; this could be explained by SNAP-25 turnover in the cell or alternatively, SNAP-25 GFP signal could be degraded due to cell division (Figures 3-18).

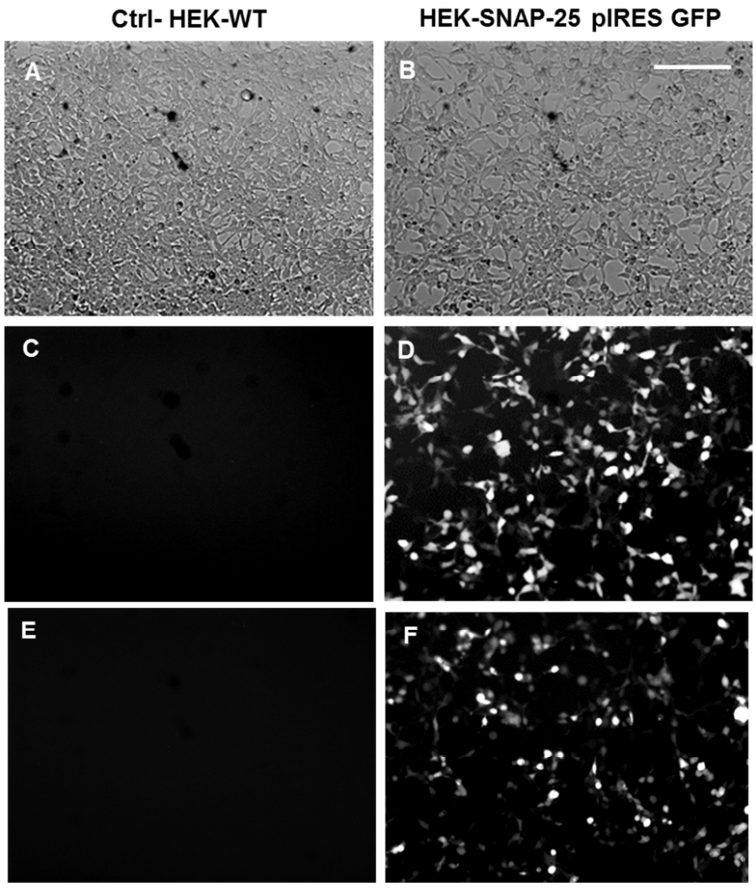

Figure 4-18 SNAP-25-WT pIRES GFP expression.

HEK cells were transiently transfected with pcDNA3 encoding pIRES GFP or left untreated for 48 or 72 hrs. No pIRES-GFP expression was detected in the HEK-WT untransfected cells -C, brightfield image, A. Transiently transfected HEK cells displayed positive expression of pIRES-GFP at 48 hrs post transfection panels B and D. Positive expression was also observed at 72 hrs F, with absent signal in the non-transfected control E.

4.3.12. Transient expression of SNAP-25 in HEK cells was greater when transfected with the construct lacking the fluorescent tag compared to that with the GFP tagged construct

HEK cells were transiently transfected with either SNAP-25 pIRES-GFP or pcDNA3-SNAP25-WT (a kind gift from Prof. Herbert Gaisano, University of Toronto) or left untreated for 48 or 72 hrs, respectively. Subsequently, the cells were lysed with SDS sample buffer and separated by SDS-PAGE and Western blotted for reactivity to an internal control α-actin and α-SNAP-25 SMI-81 antibodies. Greater expression was observed with the construct lacking the fluorescent tag compared to the GFP tagged construct at 72 hrs (Figure 4-19, 72 hrs, lanes 1 vs. 3).

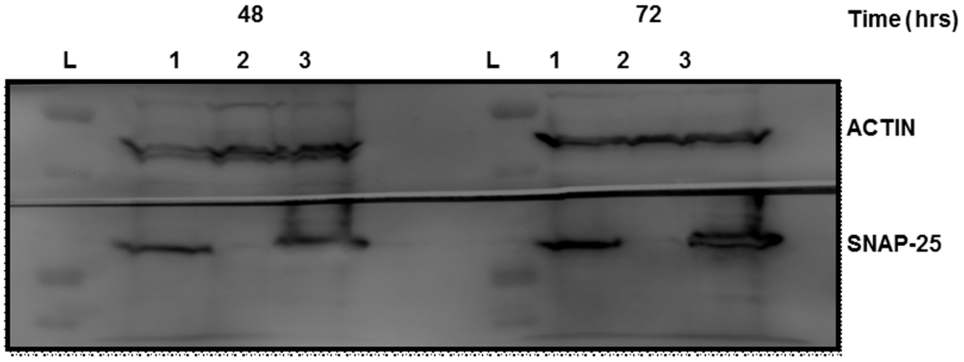

Figure 4-19 Western blot of SNAP-25-WT expression at 48 and 72 hrs.

HEK cells were transiently transfected with pcDNA3 encoding SNAP-25-WT pIRES GFP (lane 1) or SNAP-25-WT without the fluorescent tag (lane 3) or left untreated for 48 or 72 hrs (lane 2) prior to lysis in SDS sample buffer. Each sample 10 µl was separated by SDS-PAGE and Western blotted. Membranes were probed with the following antibodies: α-actin and α-SNAP-25 SMI-81 antibodies.

4.4. Discussion and conclusions

Antibodies to human TRPV1 were generated by immunisation with a peptide synthesised to a selected amino acid sequence region of human TRPV1. The immunised peptide (hTRPV1-A) shares 69% identity of amino acids with rat TRPV1, and 63% identity of amino acids with mouse TRPV1. Immunocytochemistry data revealed that these antibodies specifically detect

TRPV1 in a transiently over-expressed culture of HEK cells used as a screening assay (permeabilised, unpermeabilised and live cell staining); positive staining was blocked by competition with the control blocking peptide (100-fold molar excess) and no staining was observed in the non-transfected HEK-WT control cells. Western blotting and immunocytochemistry data confirmed that detection with this antibody is dose-dependent and that antibody binding increases over time. Unfortunately, α-TRPV1 polyclonal antibodies did not detect rat TRPV1 when it was transiently transfected in HEK cells. One of the main limitations of using HEK cells as the primary platform for this study is that they do not endogenously express SNAP-25, which is an essential requirement to investigate if antibodies conjugated to LC.H_N.H_{CN}/A are capable of cleaving its substrate. To overcome this obstacle, HEK cells were transiently transfected with SNAP-25 using two different plasmids, a model over-expressing SNAP-25 was established and may be utilised to screen potential BoNT-based bio-therapeutics *in vitro*. α-hTRPV1-A antibodies have now been characterised and may be utilised as a valuable tool to target BoNT-based therapeutics in the future or, alternatively, could be used for more elegant immunocytochemistry/immunohistochemistry studies.

4.5. Future work

One of the main limitations of these hTRPV1-A polyclonal antibodies is that they can only be investigated in a human TRPV1 expressing model; this, significantly limits their usefulness. For antibodies to be used as a therapeutic targeting agent, they would ideally be firstly evaluated in a primary sensory neuronal cell culture model before moving to a suitable pre-clinical *in vivo* model. Rabbits that were immunised produced an immune response to TRPV1-A-BSA, but were not reactive to rat TRPV1, suggestive of a lack of immunogenicity towards the TRPV1-B peptide as it shares 100 % identity to human and rat and would therefore be expected to detect both. An immune response to this epitope would be advantageous, as it could have been evaluated in both rat and human models. Interestingly, although the TRPV1-A peptide does not recognise rat TRPV1, it shares 100 % identity to guinea pig TRPV1. Thus, it could be further investigated in guinea pig sensory neurons and, subsequently, in a guinea pig

pre-clinical pain model. Although, guinea pigs would provide a model that would more closely mimic the human system, they generally have small litter sizes (1-4), longer gestation periods and require much larger housing than rats which limits their use for this study. The TRPV1-B peptide is currently being resynthesized for immunisation, this would provide α-TRPV1 antibodies with reactivity to both human and rat which could be evaluated in the already established rat sensory neuron cultures and *in vivo* SNL model of neuropathic pain in rat (Chapter 3).

5. DEVELOPMENT OF SINGLE CHAIN ANTIBODIES FOR FUTURE TARGETING OF THE LC.H_N.H_{CN}/A TO TREAT CHRONIC PAIN

5.1. Background

The primary purpose of producing antibodies against TRPV1, is that these could be used to target therapeutics specifically to sensory neurons. Ideally, single chain antibodies would be generated as the genes encoding TRPV1 recombinant antibodies could be gene ligated onto a modified BoNT therapeutic and could be expressed in large quantities for targeting. An alternative targeting strategy would be to chemically conjugate the purified polyclonal antibodies onto the BoNT based therapeutic.

5.1.1. Single chain antibodies as tools for targeting BoNT Zn2+-dependent light chain proteases to sensory neurons

In collaboration with Dr. Arman Rahman[1] and Prof. John McCafferty[2] of DCU[1] and Cambridge University[2], 48 rabbit clones were isolated from the TRPV1-A rabbit library using phage display; these fall into 13 different groups based on the variability of their gene sequences. Initially, RNA was extracted from rabbit spleen cells following immunization with the TRPV1-A peptide conjugated to BSA. This RNA was reverse transcribed into cDNA and used as a template for building the rabbit antibody library. The heavy and light chains were amplified using primers, specially designed at Cambridge University, and assembled into a single gene. PCR reactions were carried out with selected primers to add restriction sites to facilitate cloning into the phagemid vector and to amplify the scFv DNA fragment. The scFv ligated vector was then transformed into competent BL21 *E.coli* cells and grown before infecting with a helper phage; this produced recombinant phages displaying the TRPV1-A scFv fragments fused to the phage coat proteins. Bio-panning was used to screen and enrich the antigen specific TRPV1-A clones. The benefit of this approach is that the genes encoding these recombinant antibodies could be ligated onto that for a modified BoNT to target and deliver its light chain protease solely into sensory neurons.

5.1.2. Replacement of the binding domain of BoNTs with alternative moieties to allow therapeutic retargeting to sensory neurons

Substituting the binding domain of BoNT with an antibody, protein or peptide targeting moiety could generate a novel biotherapeutic that is capable of being retargeted to a region it is not physiologically designed to reach; this would provide immense therapeutic potential. Once the inserted domain binds to its new target, the H_N domain may be able to facilitate translocation of the LC to the cytosol by its usual mechanism. Evidence of BoNT retargeting to other cells was achieved when NGF was conjugated to the LH_N/A; although lacking the binding domain, it cleaved SNAP-25 and blocked noradrenaline release from PC12 cells (Chaddock et al., 2000a). Subsequently, wheat germ agglutinin was conjugated to the LH_N/A; it was capable of targeting to both neuronal and non-neuronal cells, cleaving SNAP-25 and inhibiting neurotransmitter release in cells that are not usually responsive to treatment (Chaddock et al., 2000b). Interestingly, LH_N/A has been conjugated to a lectin isolated from *Erythrina cristagalli* to target nociceptive afferents. Application of this novel conjugate blocked the release of substance P and glutamate from sensory cultured embryonic neurons (Duggan et al., 2002). This study was further supported by *in vivo* electrophysiology of the spinal cord which revealed that direct exposure to 100 µl of LH_N/A-ECL (4.5 µg/µl), reduced both C and Aβ fibre evoked activity by ~ 32 and 12 % respectively, while Aδ activity was not affected suggesting that it predominantly acts on the presynaptic peripheral sensory afferent (Duggan et al., 2002). The potential of this LH_N/A lectin conjugate to alleviate pain was further investigated in a pre-clinical mouse acute model of thermal pain where intrathecal administration of the conjugated biotherapeutic alleviated latencies in response to the hot plate for at least 30 days post treatment (Chaddock et al., 2004). Collectively, these exciting results prove that this strategy could be used to retarget BoNTs for new indications.

5.2. Aims and objectives

- To develop single chain antibodies that could be used to retarget BoNT-based therapeutics to sensory neurons.

- To characterise a panel of rabbit α-TRPV1-A single chain antibodies.
- To conjugate α-TRPV1-A purified polyclonal antibodies to the LC.H_N.H_{CN}/A (comprised of the light chain, translocation domain and N-terminal heavy chain of BoNT/A, but lacking the binding domain).

5.3. Results

5.3.1. Rabbit α-TRPV1-A scFv clones isolated by panning are reactive to TRPV1-A

All the panel of rabbit α-TRPV1-A scFv clones, isolated by panning by Dr. Arman Rahman, proved to be reactive with TRPV1-A-BSA but not BSA (Figure 5-1).

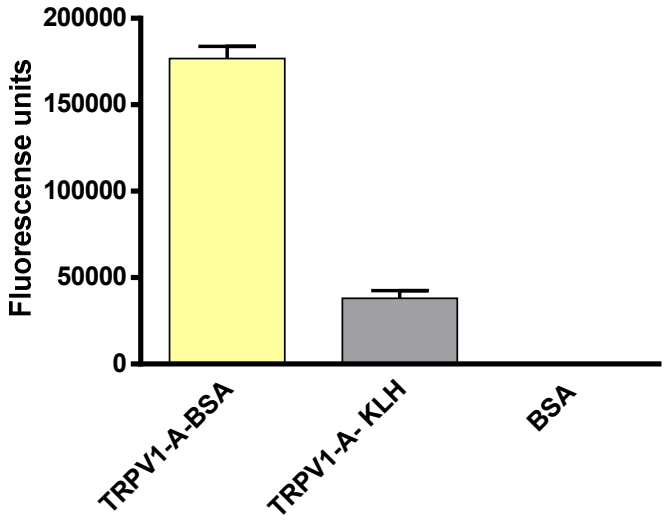

Figure 5-1 Reactivities of the isolated phage scFv clones.

Individual colonies were picked into 96 well plates in 150 µl medium (2TY plus glucose and kanamycin). After 24 hrs, plates were hedgehoged into new 96 well plates containing complete ZY medium and cultured for additional 20 hrs at 30^0C. Plates were centrifuged at 3200 g for 15 minutes, and the supernatant tested by ELISA onto a pre coated α-TRPV1-A antigen 96-well Nunc Maxisorb plate. The plate was blocked with BSA to eliminate BSA signal from the immunised carrier protein.

5.3.2. α-TRPV1-A scFv clones yielded high reactivities to hTRPV1-A

α-TRPV1-A rabbit scFv clones were analysed by direct ELISA (as described in the Methods section) against TRPV1-A-KLH (Figure 5-2). High absorbance values at 450 nm were obtained for supernatant (A) and periprep (B) rabbit scFv clones screened against the hTRPV1-A-KLH coated antigen plates (Figure 5-2 A and B). The panel of clones tested (supernatant or periprep) lacked reactivity to BSA (Figure 5-2 C and D).

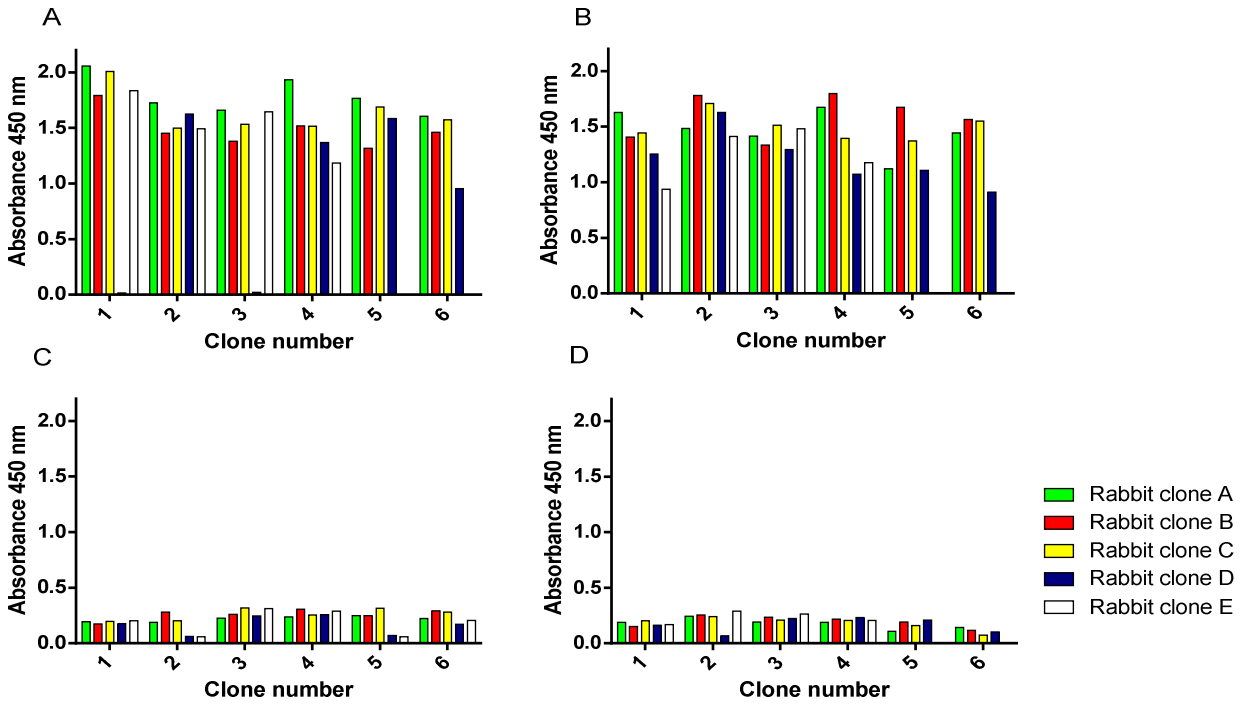

Figure 5-2 Reactivities of single chain α-hTRPV1 rabbit and human antibodies to the hTRPV1-A-KLH and BSA.

*scFv TRPV1-A rabbit antibodies present in either the supernatant **A and C)** or periprep **B and D)** were analysed by direct ELISA to determine their reactivities to either TRPV1 (A and B) or to BSA (C and D). For the supernatant ELISA, 50 µl of the overnight culture for each clone were analysed. For the periprep ELISA, 10 µl of crude periplasmic preparation was dissolved in 40 µl PBS and processed as described in the methods ELISA section 2.2.2.3. The following antibodies were employed; mouse monoclonal α-FLAG® 1^{O} (1/500 dilution), followed by, α-mouse HRP 2^{O} (1:5000 dilution).*

5.3.3. Free TRPV1 peptide competed with the α-hTRPV1-A scFv rabbit clones

A direct ELISA was performed to determine what dilution of each scFv would give an absorbance of 1 at 450 nm (Figure 5-3 A); these dilutions were subsequently used for the competitive ELISA in (Figure 5-3 B). Results revealed that free TRPV1-A peptide competes with each of the scFv TRPV1-A rabbit clones analysed giving ~ IC_{50} values of 2.66, 1.33, 0.26, 10.64, 2.66, 1.33 and 13.33 µM for clones 9, 16, 17, 59, 60, 61 and 63, respectively, Figure 5-3 B. Clones 17 and 63 had the lowest and highest IC_{50} values. These results are presented in Table 5-1 below.

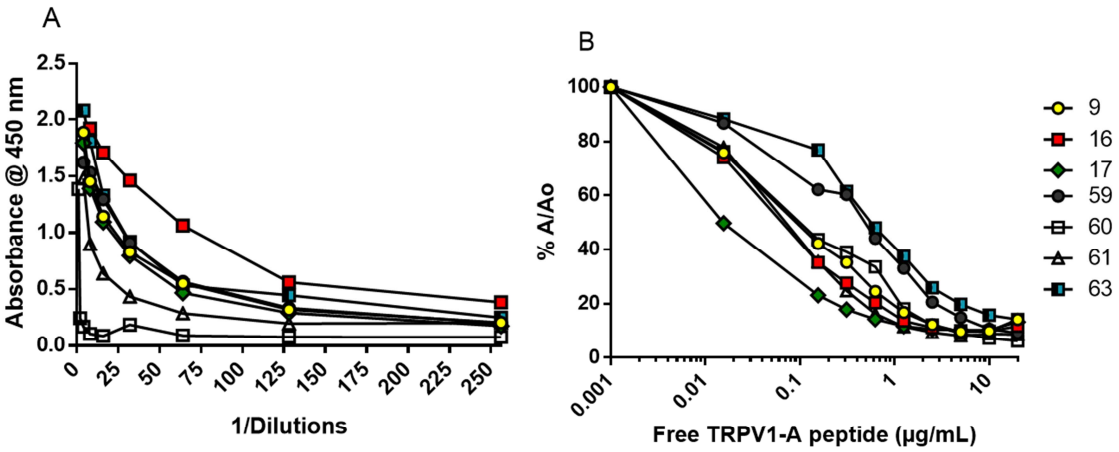

Figure 5-3 Direct and competitive ELISA of the scFv rabbit clones.

Plates were coated with the TRPV1-A-KLH peptide, 10 µg/mL overnight at 4^{O}C; 20 mL cultures were grown for each clone and the crude lysates analysed by direct and competitive ELISA. For the competitive ELISA, increasing concentrations of the control TRPV1-A non-conjugated peptide were incubated with the clone dilution that gave a direct ELISA A450 of 1. The following antibodies were employed; mouse monoclonal α-FLAG® 1^{O} (1/500 dilution), followed by, α-mouse HRP 2^{O} (1:5000 dilution).

Clones	~ IC_{50} values (µg/mL)	IC_{50} values (µM)
9	0.2	2.66
16	0.1	1.33
17	0.02	0.26
59	0.8	10.64
60	0.2	2.66
61	0.1	1.33
63	1	13.3

Table 5-1 Approximate IC_{50} values for rabbit TRPV1-A scFv clones

5.3.4. α-TRPV1-A scFv clones were expressed in *E. coli* and Western blotting confirmed the presence of the FLAG® tag

hTRPV1-A rabbit scFv clones were classified into 13 groups based on the variability of their gene sequences. All of the rabbit clones were seeded onto individual 2TY agar plates containing glucose and kanamycin and grown overnight at 37^{O}C. From each of these plates, a single colony was picked and seeded into a 5 mL starter culture (2TY medium, 2 % glucose, 100 µg/mL kanamycin) and grown overnight at 30^{O}C. A 1:1000 dilution of each of these starter cultures was inoculated into 2TY medium containing 2 % glucose and 100 µg/mL of kanamycin. This was grown until an A600 nm of 0.6-0.8 was reached, temperature was then reduced to 22^{O}C and 1 mM of IPTG added to induce the culture. After growing overnight for a further 16-20 hrs, cells were lysed and the expressed protein was purified by IMAC as described in the Materials and Methods section. Samples were collected from each of the stages of the IMAC process, separated by SDS-PAGE and protein stained; results confirmed that the product separated was of the correct size ~ 30 K (Figure 5-4 A). Western blot detected the presence of the FLAG® tag (this is an 8-amino acid peptide (Asp-Tyr-Lys-Asp-Asp-Asp-Asp-Lys) which was incorporated into the recombinant antibody production to facilitate screening) in the eluates (Figure 5-4 B).

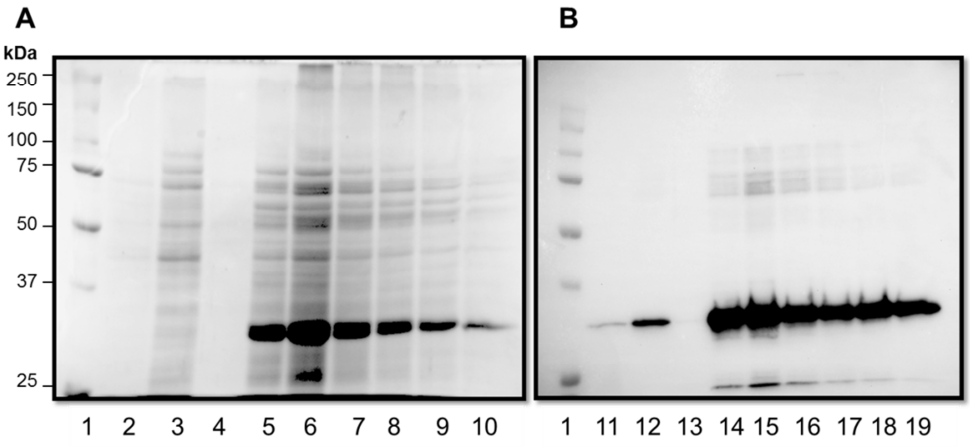

Figure 5-4 Protein expression and IMAC purification of single chain rabbit TRPV1 clone number 9.

Aliquots from each of the IMAC samples were collected and separated by SDS-PAGE followed by either Coomassie staining (A) or Western blotting for the FLAG® tag (B). Clone 9: 1= Precision plus markers; 2 = flow through, 1:10 dilution; 3 = wash 1, undiluted; 4 = wash 8, undiluted; 5-10 = elutes, undiluted, 11 = flow through, 1:20 dilution, 12 = wash 1, 1:5 dilution, 13 = wash 8, 1:5 dilution, 14-19 = elutes, 1:5 dilution. 1° antibody- mouse α FLAG® antibody 1:500; 2° antibody- donkey α mouse HRP 1:5000 dilution. Further details regarding the expression and purification of scFv antibodies can be found in sections 2.2.2.7 and 2.2.2.9.1.

5.3.5. No binding of the α-hTRPV1-A rabbit scFv crude lysates to a protein at 95 K was observed in TRPV1 transiently over-expressed HEK cells

Almost all (47/48) of the hTRPV1 scFv rabbit clones were screened for binding to human TRPV1. Each scFv was expressed in *E. coli* (50 mL cultures) from which crude lysates (5 mL) were prepared and shown by densitometric analysis of Western blotting (Figure 5-5) by Image J software to contain between 20 and 50 µg of over-expressed scFv. HEK cells over-expressing human TRPV1 and WT untransfected control cells were separated by SDS-PAGE; membranes were subsequently incubated with scFv lysates overnight at 4^{O}C. Unfortunately, none of the scFv clones tested to date were found to bind to TRPV1 at 95 K, despite the detection of over-expressed TRPV1 by the serum polyclonal antibody used as a positive control. Some scFv clones

demonstrated considerable binding to endogenous HEK proteins; however, these were present in both the negative and positive controls and migrated at sizes not representative of TRPV1 (Figure 5-6).

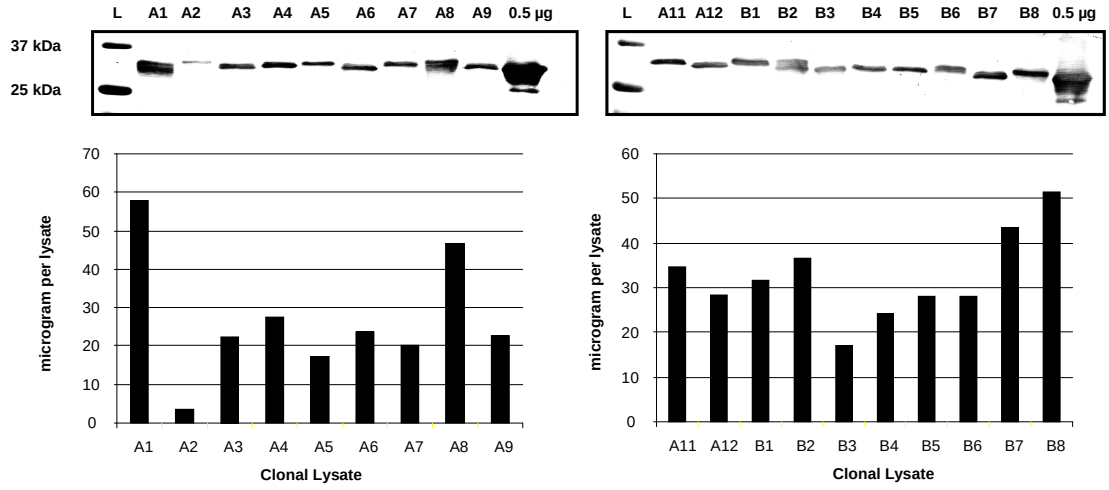

Figure 5-5 Protein concentration (µg/lysate) of the rabbit clonal lysates.

A single colony for each clone was selected and seeded into a 5 mL starter culture (2TY medium, 2 % glucose, 100 µg/mL kanamycin) and grown overnight at 30^{O}C. A 1:1000 dilution of each of these starter cultures was inoculated into 2TY medium containing 2 % glucose and 100 µg/mL of kanamycin. This was grown until an A600 nm of 0.6-0.8 was reached, temperature was then reduced to 22^{O}C and 1 mM of IPTG added to induce the culture. Subsequently, scFv clonal lysates were separated by SDS-PAGE and Western blotted for the presence of the FLAG® tag. Western blots were analysed by densitometric analysis using image J software and graphed. Antibodies employed include; 1^{o} - scFv clonal lysates; 2^{o} -mouse α-FLAG® antibody (1:500), followed by α-mouse AP (1:10000). Further details regarding the expression of scFv TRPV1 clones can be found in section 2.2.2.7 of the Materials and Methods chapter.

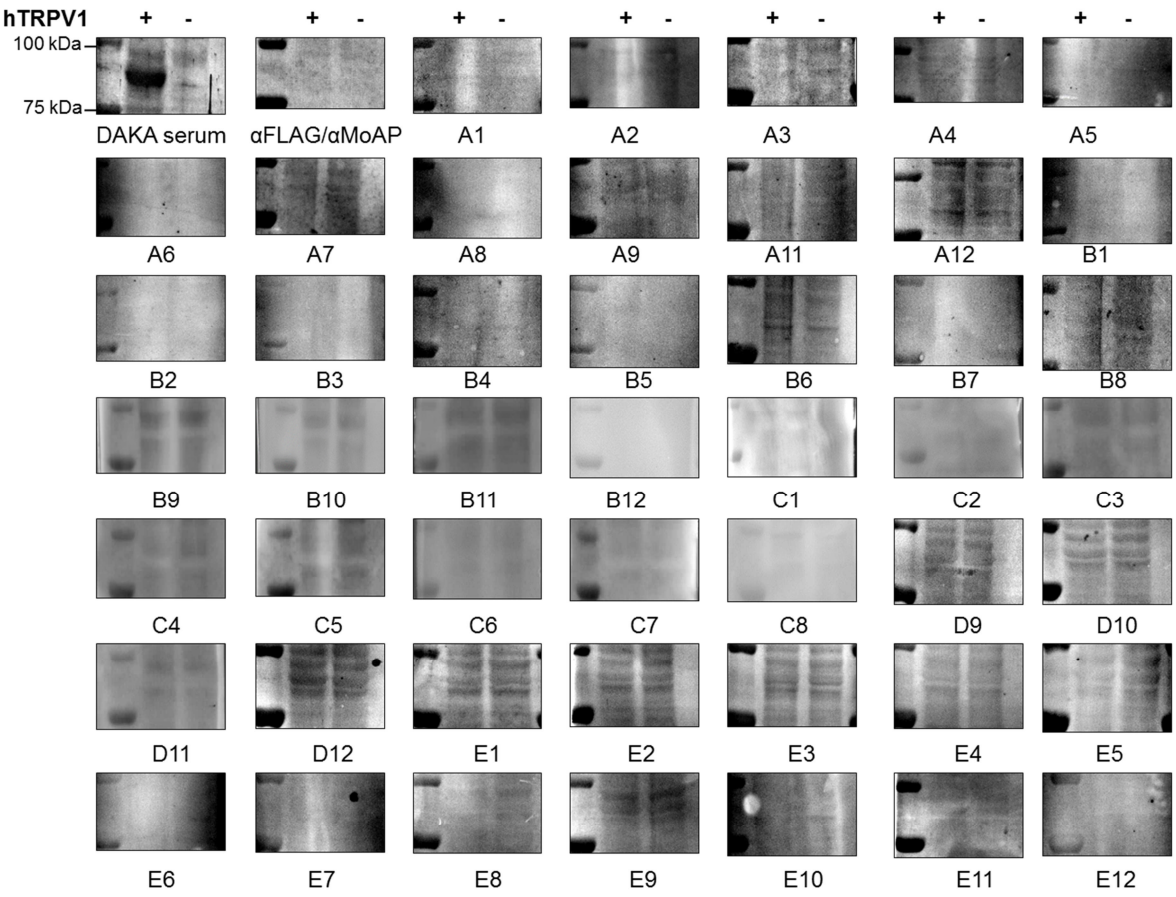

Figure 5-6 Specificity of the rabbit α-hTRPV1-A purified single chain antibodies to hTRPV1.

HEK cells were transiently transfected with pcDNA3 encoding either human TRPV1 or left untreated for 24 hrs prior to lysis in SDS sample buffer. Each sample (10 µl) was separated by SDS-PAGE and Western blotted. Membranes were incubated overnight at 4^{O}C with the α-hTRPV1 scFv clonal lysates or with the control DAKA polyclonal serum. Antibodies employed include; 1^{o} - scFv clonal lysates; 2^{o} -mouse α-FLAG® antibody (1:500), followed by α-mouse AP (1:10000). Method details for screening the panel of scFv clones can be found in section 2.2.2.11 of the Materials and Methods chapter.

5.3.6. LC.H_N.H_{CN}/A was expressed, purified and activated by nicking with thrombin

LC.H_N.H_{CN}/A was expressed and purified following standard laboratory established protocols which yielded a main protein band of 125 K on SDS/PAGE. Its purity was confirmed by the lack of contaminants. Incubation

with thrombin completely converted the single chain (SC) to the dichain (DC), confirmed by the expected HC and LC sizes after separation by SDS-PAGE in the presence of reducing agent, followed by Coomassie staining (Figure 5-7).

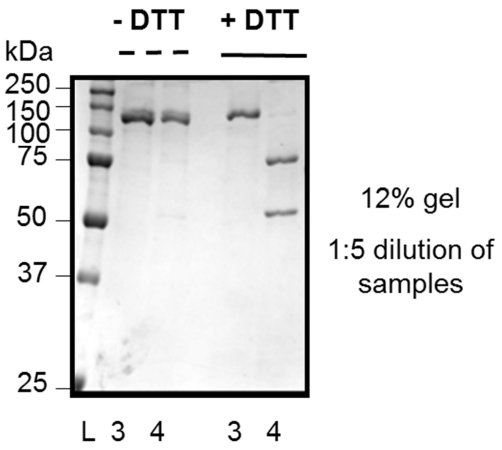

The buffer exchanged LC.H_N.H_{CN}/A sample was incubated with or without thrombin (1 mg toxin per unit of thrombin, for 1 hr at 22^{o}C) to activate the toxin. Subsequently, samples were separated by SDS-PAGE in the presence or absence of reducing agent, followed by Coomassie staining. Lanes 3 (- thrombin) and 4 (+ thrombin). In the presence of thrombin under reducing conditions (lane 4, + DTT), the SC was successfully converted to the DC active form.

Figure 5-7 Expression, purification and activation of the LC.H_N.H_{CN}/A.

5.3.7. Attempted chemical conjugation of the LC.H_N.H_{CN}/A hTRPV1 polyclonal antibodies did not reveal the expected size for the conjugated product

As the single chain antibodies were unable to detect hTRPV1 in the over-expressed cell culture model, there was a shift of focus to the purified polyclonal antibodies. Thus, it was decided to chemically conjugate these to the LC.H_N.H_{CN}/A (comprised of the light chain, translocation domain and N-terminal heavy chain of BoNT/A, but lacking the binding domain). Its conjugation to the Fc portion of α-hTRPV1 IgGs was attempted by oxidation of the carbohydrates present in the Fc region with periodic acid. This reaction cleaves bonds positioned between adjacent carbon atoms containing hydroxyl groups, resulting in the formation of two aldehyde groups that are reactive to both amine and hydrazide cross linking products. As the sulfhydryls present in the LC.H_N.H_{CN}/A may not be accessible, Trauts reagent (2-iminothiolane) (20, 40, 50 and 100-fold molar excess) was employed to introduce free sulfhydryls into the LC.H_N.H_{CN}/A by reacting with primary amines. Ellman's reaction was used to determine if sulfhydryl groups had been introduced into the LC.H_N.H_{CN}/A; results revealed an introduction of cysteines into the LC.H_N.H_{CN}/A. Following

confirmation that sulfhydryls had been introduced, the LC.H_N.H_{CN}/A was subsequently incubated with a hetero-bifunctional water-soluble, crosslinker namely 3, 3'-N-[e-maleimidocaproic acid] hydrazide trifluroacetic acid salt (EMCH- 10 and 20-fold molar excesses) containing a sulfhydryl reactive maleimide group and a functional carbonyl hydrazide group at either ends of a 6-carbon spacer the LC.H_N.H_{CN}/A. The maleimide group present in the linker reacts with sulfhydryl groups and the hydrazide group reacts with oxidised carbohydrates; together these reactions should form the α-hTRPV1-LC.H_N.H_{CN}/A conjugate by the formation of hydrazone bonds (Figure 5-8). Ellman's reaction revealed that incubation with the EMCH linker decreased the number of cysteines that were initially introduced by Traut's, suggesting that cysteines were being modified by the linker. Finally, the oxidised antibody was incubated with the Trauts and EMCH reacted LH.H_N.H_{CN}/A in a range of molar ratios of antibody to toxin including 2, 3 and 5:1, for varying times including 2 hrs at room temperature, and 4 and 16 hrs at 4^{o}C. To date, attempts of this conjugation have been unsuccessful, as the conjugated produced size was not observed when separated by SDS-PAGE (Figure 5-9 A).

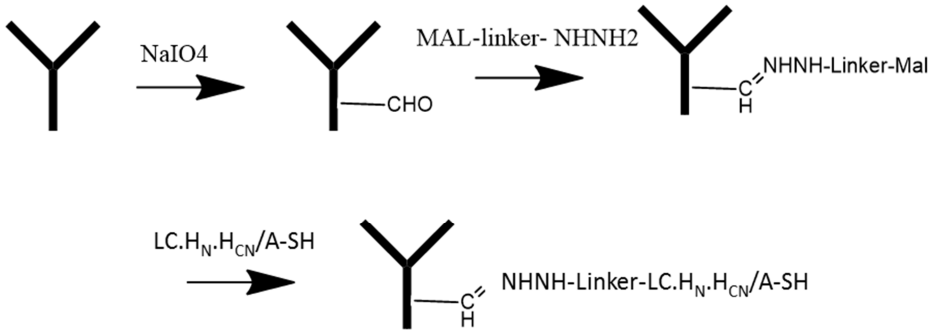

Figure 5-8 Schematic of the chemical conjugation strategy to join the α-hTRPV1 antibodies to the LC.H_N.H_{CN}/A.

The Fc portion of the antibody is reacted with periodate to oxidise the carbohydrates present and to produce reactive aldehyde groups. The LC.H_N.H_{CN}/A is reacted with Traut's reagent to introduce free sulfhydryls; this is subsequently reacted with the Mal-linker-NHNH2 which contains a sulfhydryl reactive maleimide group and a carbonyl reactive hydrazide group at either ends of a 6 carbon spacer arm. The oxidised antibody is incubated with the reactive LC.H_N.H_{CN}/A for the required time to create the LC.H_N.H_{CN}/A antibody conjugate. Figure prepared by Dr. Om Prakash.

5.3.8. Application of the LC.H_N.H_{CN}/A-antibody conjugated mixture onto A549 cells cleaved SNAP-25, presumably due to the free toxin

Samples from each of the conjugation steps (described above) were collected and subsequently separated by SDS-PAGE and stained by Coomassie. The expected conjugated product size was not visualised (Figure 5-9 A). Nevertheless, the antibody-LC.H_N.H_{CN}/A mixture from the final step was applied to A549 cells which express SNAP-25; its cleavage was observed, however, this was presumably due to the presence of the free toxin (Figure 5-9 B).

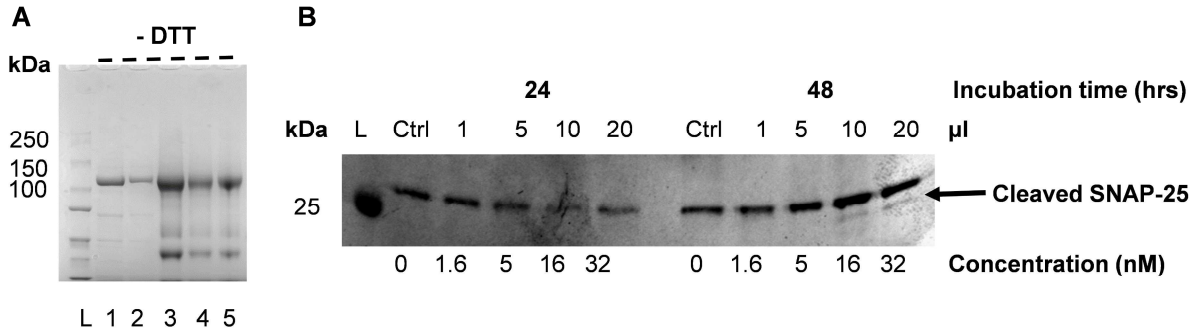

Figure 5-9 Unsuccessful chemical conjugation of the LC.H_N.H_{CN}/A to α-hTRPV1-A IgGs.

Samples (2 µg) from each step of the conjugation process were separated by SDS-PAGE, followed by Coomassie staining. 1. Nicked toxin (LC.H_N.H_{CN}/A sample was incubated with thrombin (1 mg toxin per unit of thrombin, for 1 hr at 22^{o}C) to activate the toxin by converting the SC to the DC active form), 2. Toxin + EMCH linker, 3. Antibody (Ab) concentrated, 4. Ab oxidised, 5. The final conjugated mixture- Ab + Toxin (Figure 4-10 A). The final product (lane 5) was applied to A549 cells, in varying concentrations and incubation times. Following incubation, the cells were lysed, separated by SDS-PAGE and Western blotted for SNAP-25 using the SMI-81 1^o antibody. Further details regarding the chemical conjugation method can be found in section 2.2.2.10 of the Materials and Methods chapter.

5.4. Discussion and conclusions

Characterisation of the polyclonal α-TRPV1-A antibodies in Chapter 3 confirmed its specificity for hTRPV1. However, recombinantly-produced scFv antibodies would be more useful as they could be gene ligated onto the LC.H_N.H_{CN}/A to

direct its Zn^{2+}-dependent light chain proteases into sensory neurons. Single chain antibodies are smaller in size (~ 30 K) and would have greater accessibility to their target epitope. Encouragingly, the scFv antibodies analysed were highly reactive to hTRPV1-A, and yielded low direct ELISA absorbance values to the immunised carrier protein BSA. Competitive ELISA revealed that free TRPV1-A peptide competes with ~ IC_{50} values of 2.66, 1.33, 0.26, 10.64, 2.66, 1.33 and 13.33 µM for clones 9, 16, 17, 59, 60, 61 and 63, respectively Figure 4-4 B. When the rabbit scFv clones were screened in the established HEK cell model over-expressing human TRPV1, no band was detected at the expected size for TRPV1 (~ 95 K), although, TRPV1 was detected by the polyclonal DAKA α-TRPV1-A antibody at the correct size. Given the lack of reactivity to human TRPV1 with the panel of scFv clones isolated, it was decided to chemically conjugate the purified polyclonal antibody to the LC.H_N.H_{CN}/A. Review of the literature verified that chemical conjugation strategies have been used to conjugate a variety of agents to the LC.H_N/A. Samples from the conjugation process were analysed by SDS-PAGE (2 µg of each to verify if the product was of the correct size), reaction with Ellmans (to determine if sulfhydryls had been introduced into the LC.H_N.H_{CN}/A by Traut's reagent and if these had been modified by the EMCH linker) and by Schiff reaction (to confirm antibody oxidation). Although, oxidation, introduction and modification of sulfhydryls were all confirmed; when the oxidised antibody and reacted with the LC.H_N.H_{CN}/A, no conjugated product was separated by SDS-PAGE. Perhaps, if more starting materials were used, the conjugated product might be observed.

5.5. Future work

Although polyclonal antibodies proved promising, the chemical conjugation strategy was unsuccessful to date; this would require further optimisation. Additionally, scFv clones isolated did not bind to human TRPV1 at 95 K; to overcome this obstacle, the scFv library would need to repanned with greater stringency to isolate specific clones; however, these would again only recognise human TRPV1. Currently, both TRPV1-A and B peptides are being resynthesised. scFv clones isolated from the TRPV1-B library, would be

reactive to both human and rat. This would be advantageous for specific targeting to sensory neurons as it could be evaluated in existing sensory neuronal cultures and in an already established *in vivo* model. Additionally, assays (Western blotting and immunocytochemistry) have been established to allow fast screening and characterisation of future clones.

BIBLIOGRAPHY

AKBAR, A., YIANGOU, Y., FACER, P., WALTERS, J. R., ANAND, P. & GHOSH, S. 2008. Increased capsaicin receptor TRPV1-expressing sensory fibres in irritable bowel syndrome and their correlation with abdominal pain. Gut, 57, 923-929.

AOKI, K. R. 2003. Evidence for antinociceptive activity of botulinum toxin type A in pain management. *Headache,* 43 Suppl 1**,** S9-15.

AOKI, K. R. 2005. Review of a proposed mechanism for the antinociceptive action of botulinum toxin type A. *Neurotoxicology,* 26**,** 785-93.

AOKI, K. R. & FRANCIS, J. 2011. Updates on the antinociceptive mechanism hypothesis of botulinum toxin A. *Parkinsonism Relat Disord,* 17 Suppl 1**,** S28-33.

APOSTOLIDIS, A., POPAT, R., YIANGOU, Y., COCKAYNE, D., FORD, A. P., DAVIS, J. B., DASGUPTA, P., FOWLER, C. J. & ANAND, P. 2005. Decreased sensory receptors P2X3 and TRPV1 in suburothelial nerve fibers following intradetrusor injections of botulinum toxin for human detrusor overactivity. *J Urol,* 174**,** 977-82; discussion 982-3.

BACH-ROJECKY, L. & LACKOVIC, Z. 2005. Antinociceptive effect of botulinum toxin type a in rat model of carrageenan and capsaicin induced pain. *Croat Med J,* 46**,** 201-8.

BACH-ROJECKY, L., RELJA, M. & LACKOVIC, Z. 2005. Botulinum toxin type A in experimental neuropathic pain. *J Neural Transm,* 112**,** 215-9.

BACH-ROJECKY, L., SALKOVIC-PETRISIC, M. & LACKOVIC, Z. 2010. Botulinum toxin type A reduces pain supersensitivity in experimental diabetic neuropathy: bilateral effect after unilateral injection. *Eur J Pharmacol,* 633**,** 10-4.

BARON, R., BINDER, A. & WASNER, G. 2010. Neuropathic pain: diagnosis, pathophysiological mechanisms, and treatment. *Lancet Neurol,* 9**,** 807-19.

BARRIENTOS N & CHANA P 2003. Botulinum toxin type A in prophylactic treatment of migraine headaches: a preliminary study. *J Headache Pain,* 4**,** 146-151.

BASBAUM, A. I., BAUTISTA, D. M., SCHERRER, G. & JULIUS, D. 2009. Cellular and molecular mechanisms of pain. *Cell,* 139**,** 267-84.

BEGGS, S. & SALTER, M. W. 2006. Neuropathic pain: symptoms, models, and mechanisms. *Drug Development Research,* 67**,** 289-301.

BENNETT, G. J. & XIE, Y. K. 1988. A peripheral mononeuropathy in rat that produces disorders of pain sensation like those seen in man. *Pain,* 33**,** 87-107.

BINDER, W. J., BLITZER, A. & BRIN, M. F. 1998. Treatment of hyperfunctional lines of the face with botulinum toxin A. *Dermatol Surg,* 24**,** 1198-205.

BOVE, S. E., CALCATERRA, S. L., BROOKER, R. M., HUBER, C. M., GUZMAN, R. E., JUNEAU, P. L., SCHRIER, D. J. & KILGORE, K. S. 2003. Weight bearing as a measure of disease progression and efficacy of anti-inflammatory compounds in a model of monosodium iodoacetate-induced osteoarthritis. *Osteoarthritis Cartilage,* 11**,** 821-30.

BRIN, M. F. 2009. Development of future indications for BOTOX. *Toxicon,* 54**,** 668-74.

BRIN, M. F., FAHN, S., MOSKOWITZ, C., FRIEDMAN, A., SHALE, H. M., GREENE, P. E., BLITZER, A., LIST, T., LANGE, D., LOVELACE, R. E. & ET AL. 1987. Localized injections of botulinum toxin for the treatment of focal dystonia and hemifacial spasm. *Mov Disord,* 2**,** 237-54.

CAMPBELL, J. N. & MEYER, R. A. 2006. Mechanisms of neuropathic pain. *Neuron,* 52**,** 77-92.

CAMPRUBI-ROBLES, M., PLANELLS-CASES, R. & FERRER-MONTIEL, A. 2009. Differential contribution of SNARE-dependent exocytosis to inflammatory potentiation of TRPV1 in nociceptors. *FASEB J,* 23**,** 3722-33.

CATERINA, M. J., SCHUMACHER, M. A., TOMINAGA, M., ROSEN, T. A., LEVINE, J. D. & JULIUS, D. 1997. The capsaicin receptor: a heat-activated ion channel in the pain pathway. *Nature,* 389**,** 816-24.

CHADDOCK, J. A., PURKISS, J. R., ALEXANDER, F. C., DOWARD, S., FOOKS, S. J., FRIIS, L. M., HALL, Y. H., KIRBY, E. R., LEEDS, N., MOULSDALE, H. J., DICKENSON, A., GREEN, G. M., RAHMAN, W., SUZUKI, R., DUGGAN, M. J., QUINN, C. P., SHONE, C. C. & FOSTER, K. A. 2004. Retargeted clostridial endopeptidases: inhibition of nociceptive neurotransmitter release in vitro, and antinociceptive activity in in vivo models of pain. *Mov Disord,* 19 Suppl 8**,** S42-7.

CHADDOCK, J. A., PURKISS, J. R., DUGGAN, M. J., QUINN, C. P., SHONE, C. C. & FOSTER, K. A. 2000a. A conjugate composed of nerve growth factor coupled to a non-toxic derivative of Clostridium botulinum neurotoxin type A can inhibit neurotransmitter release in vitro. *Growth Factors,* 18**,** 147-55.

CHADDOCK, J. A., PURKISS, J. R., FRIIS, L. M., BROADBRIDGE, J. D., DUGGAN, M. J., FOOKS, S. J., SHONE, C. C., QUINN, C. P. & FOSTER, K. A. 2000b. Inhibition of vesicular secretion in both neuronal

and nonneuronal cells by a retargeted endopeptidase derivative of Clostridium botulinum neurotoxin type A. *Infect Immun,* 68**,** 2587-93.

CHAPLAN, S. R., BACH, F. W., POGREL, J. W., CHUNG, J. M. & YAKSH, T. L. 1994. Quantitative assessment of tactile allodynia in the rat paw. *J Neurosci Methods,* 53**,** 55-63.

CHUNG, J. M., CHOI, Y., YOON, Y. W. & NA, H. S. 1995. Effects of age on behavioral signs of neuropathic pain in an experimental rat model. *Neurosci Lett,* 183**,** 54-7.

CUI, M., KHANIJOU, S., RUBINO, J. & AOKI, K. R. 2004. Subcutaneous administration of botulinum toxin A reduces formalin-induced pain. *Pain,* 107**,** 125-33.

DALLENBACH, K. M. 1939. Pain: History and Present Status. *The American Journal of Psychology,* 52**,** 331-347.

DAVIS, M. P. 2007. What is new in neuropathic pain? *Support Care Cancer,* 15**,** 363-72.

DIXON, W. J. 1980. Efficient analysis of experimental observations. *Annu Rev Pharmacol Toxicol,* 20**,** 441-62.

DODICK, D. W., TURKEL, C. C., DEGRYSE, R. E., AURORA, S. K., SILBERSTEIN, S. D., LIPTON, R. B., DIENER, H. C. & BRIN, M. F. 2010. OnabotulinumtoxinA for treatment of chronic migraine: pooled results from the double-blind, randomized, placebo-controlled phases of the PREEMPT clinical program. *Headache,* 50**,** 921-36.

DOLLY, J. O. & AOKI, K. R. 2006. The structure and mode of action of different botulinum toxins. *Eur J Neurol,* 13 Suppl 4**,** 1-9.

DOLLY, J. O., LAWRENCE, G. W., MENG, J., WANG, J. & OVSEPIAN, S. V. 2009. Neuro-exocytosis: botulinum toxins as inhibitory probes and versatile therapeutics. *Curr Opin Pharmacol,* 9**,** 326-35.

DOLLY, J. O. & O'CONNELL, M. A. 2012. Neurotherapeutics to inhibit exocytosis from sensory neurons for the control of chronic pain. *Curr Opin Pharmacol,* 12**,** 100-8.

DOLLY, J. O., WANG, J., ZURAWSKI, T. H. & MENG, J. 2011. Novel therapeutics based on recombinant botulinum neurotoxins to normalize the release of transmitters and pain mediators. *Febs J*.

DOLLY, O. 2003. Synaptic transmission: inhibition of neurotransmitter release by botulinum toxins. *Headache,* 43 Suppl 1**,** S16-24.

DRAY, A. 1995. Inflammatory mediators of pain. *Br J Anaesth,* 75**,** 125-31.

DRAY, A. 2008. Neuropathic pain: emerging treatments. *Br J Anaesth,* 101**,** 48-58.

DUBUISSON, D. & DENNIS, S. G. 1977. The formalin test: a quantitative study of the analgesic effects of morphine, meperidine, and brain stem stimulation in rats and cats. *Pain,* 4**,** 161-74.

DUGGAN, M. J., QUINN, C. P., CHADDOCK, J. A., PURKISS, J. R., ALEXANDER, F. C., DOWARD, S., FOOKS, S. J., FRIIS, L. M., HALL, Y. H., KIRBY, E. R., LEEDS, N., MOULSDALE, H. J., DICKENSON, A., GREEN, G. M., RAHMAN, W., SUZUKI, R., SHONE, C. C. & FOSTER, K. A. 2002. Inhibition of release of neurotransmitters from rat dorsal root ganglia by a novel conjugate of a Clostridium botulinum toxin A endopeptidase fragment and Erythrina cristagalli lectin. *J Biol Chem,* 277**,** 34846-52.

DWORKIN, R. H. & KIRKPATRICK, P. 2005. Pregabalin. *Nat Rev Drug Discov,* 4**,** 455-6.

DWORKIN, R. H., O'CONNOR, A. B., BACKONJA, M., FARRAR, J. T., FINNERUP, N. B., JENSEN, T. S., KALSO, E. A., LOESER, J. D., MIASKOWSKI, C., NURMIKKO, T. J., PORTENOY, R. K., RICE, A. S., STACEY, B. R., TREEDE, R. D., TURK, D. C. & WALLACE, M. S. 2007. Pharmacologic management of neuropathic pain: evidence-based recommendations. *Pain,* 132**,** 237-51.

FIELD, M. J., BRAMWELL, S., HUGHES, J. & SINGH, L. 1999. Detection of static and dynamic components of mechanical allodynia in rat models of neuropathic pain: are they signalled by distinct primary sensory neurones? *Pain,* 83**,** 303-11.

GILCHRIST, H. D., ALLARD, B. L. & SIMONE, D. A. 1996. Enhanced withdrawal responses to heat and mechanical stimuli following intraplantar injection of capsaicin in rats. *PAIN,* 67**,** 179-188.

GILRON, I., JENSEN, T. S. & DICKENSON, A. H. 2013. Combination pharmacotherapy for management of chronic pain: from bench to bedside. *Lancet Neurol*.

GOPINATH, P., WAN, E., HOLDCROFT, A., FACER, P., DAVIS, J. B., SMITH, G. D., BOUNTRA, C. & ANAND, P. 2005. Increased capsaicin receptor TRPV1 in skin nerve fibres and related vanilloid receptors TRPV3 and TRPV4 in keratinocytes in human breast pain. BMC women's health, 5, 2.

GUAY, D. R. 2005. Pregabalin in neuropathic pain: a more "pharmaceutically elegant" gabapentin? *Am J Geriatr Pharmacother,* 3**,** 274-87.

HARGREAVES, K., DUBNER, R., BROWN, F., FLORES, C. & JORIS, J. 1988. A new and sensitive method for measuring thermal nociception in cutaneous hyperalgesia. *Pain,* 32**,** 77-88.

HEMPENSTALL, K., NURMIKKO, T. J., JOHNSON, R. W., A'HERN, R. P. & RICE, A. S. 2005. Analgesic therapy in postherpetic neuralgia: a quantitative systematic review. *PLoS Med,* 2**,** e164.

JULIUS, D. & BASBAUM, A. I. 2001. Molecular mechanisms of nociception. *Nature,* 413**,** 203-10.

KIM, S. H. & CHUNG, J. M. 1992. An experimental model for peripheral neuropathy produced by segmental spinal nerve ligation in the rat. *Pain,* 50**,** 355-63.

LANDE, S., DOLLY, J. O. & WRAY, D. W. 1989. Abstr. 9th Nat. Mtg. Bayliss & Starling Soc.

LATREMOLIERE, A. & WOOLF, C. J. 2009. Central sensitization: a generator of pain hypersensitivity by central neural plasticity. *J Pain,* 10**,** 895-926.

LAWRENCE, G., WANG, J., CHION, C. K., AOKI, K. R. & DOLLY, J. O. 2007. Two protein trafficking processes at motor nerve endings unveiled by botulinum neurotoxin E. *J Pharmacol Exp Ther,* 320**,** 410-8.

LUO, Z. D. 2004. *Pain research: methods and protocols*, Springer.

LUVISETTO, S., MARINELLI, S., COBIANCHI, S. & PAVONE, F. 2007. Anti-allodynic efficacy of botulinum neurotoxin A in a model of neuropathic pain. *Neuroscience,* 145**,** 1-4.

LUVISETTO, S., MARINELLI, S., LUCCHETTI, F., MARCHI, F., COBIANCHI, S., ROSSETTO, O., MONTECUCCO, C. & PAVONE, F. 2006. Botulinum neurotoxins and formalin-induced pain: central vs. peripheral effects in mice. *Brain Res,* 1082**,** 124-31.

MARINELLI, S., LUVISETTO, S., COBIANCHI, S., MAKUCH, W., OBARA, I., MEZZAROMA, E., CARUSO, M., STRAFACE, E., PRZEWLOCKA, B. & PAVONE, F. 2010. Botulinum neurotoxin type A counteracts neuropathic pain and facilitates functional recovery after peripheral nerve injury in animal models. *Neuroscience,* 171**,** 316-28.

MARKENSON, J. A. 1996. Mechanisms of chronic pain. *Am J Med,* 101**,** 6S-18S.

MELZACK, R. & WALL, P. D. 1965. Pain mechanisms: a new theory. *Science,* 150**,** 971-9.

MENG, J., OVSEPIAN, S. V., WANG, J., PICKERING, M., SASSE, A., AOKI, K. R., LAWRENCE, G. W. & DOLLY, J. O. 2009. Activation of TRPV1

mediates calcitonin gene-related peptide release, which excites trigeminal sensory neurons and is attenuated by a retargeted botulinum toxin with anti-nociceptive potential. *J Neurosci,* 29**,** 4981-92.

MENG, J., WANG, J., LAWRENCE, G. & DOLLY, J. O. 2007. Synaptobrevin I mediates exocytosis of CGRP from sensory neurons and inhibition by botulinum toxins reflects their anti-nociceptive potential. *J Cell Sci,* 120**,** 2864-74.

MERCADANTE, S., ARCURI, E., TIRELLI, W., VILLARI, P. & CASUCCIO, A. 2002. Amitriptyline in neuropathic cancer pain in patients on morphine therapy: a randomized placebo-controlled, double-blind crossover study. *Tumori,* 88**,** 239-42.

MILLER, D., RICHARDSON, D., EISA, M., BAJWA, R. J. & JABBARI, B. 2009. Botulinum neurotoxin-A for treatment of refractory neck pain: a randomized, double-blind study. *Pain Med,* 10**,** 1012-7.

MILLIGAN, E. D. & WATKINS, L. R. 2009. Pathological and protective roles of glia in chronic pain. *Nat Rev Neurosci,* 10**,** 23-36.

MIRANDA, C., DI VIRGILIO, M., SELLERI, S., ZANOTTI, G., PAGLIARDINI, S., PIEROTTI, M. A. & GRECO, A. 2002. Novel pathogenic mechanisms of congenital insensitivity to pain with anhidrosis genetic disorder unveiled by functional analysis of neurotrophic tyrosine receptor kinase type 1/nerve growth factor receptor mutations. *J Biol Chem,* 277**,** 6455-62.

MONTAL, M. 2010. Botulinum neurotoxin: a marvel of protein design. *Annu Rev Biochem,* 79**,** 591-617.

MORAN, M. M., MCALEXANDER, M. A., BÍRÓ, T. & SZALLASI, A. 2011. Transient receptor potential channels as therapeutic targets. *Nature Reviews Drug Discovery,* 10**,** 601-620.

MORENILLA-PALAO, C., PLANELLS-CASES, R., GARCIA-SANZ, N. & FERRER-MONTIEL, A. 2004. Regulated exocytosis contributes to protein kinase C potentiation of vanilloid receptor activity. *J Biol Chem,* 279**,** 25665-72.

PARK, H. J., LEE, Y., LEE, J., PARK, C. & MOON, D. E. 2006. The effects of botulinum toxin A on mechanical and cold allodynia in a rat model of neuropathic pain. *Can J Anaesth,* 53**,** 470-7.

PATAPOUTIAN, A., TATE, S. & WOOLF, C. J. 2009. Transient receptor potential channels: targeting pain at the source. *Nat Rev Drug Discov,* 8**,** 55-68.

PECORARO, N., GINSBERG, A. B., WARNE, J. P., GOMEZ, F., LA FLEUR, S. E. & DALLMAN, M. F. 2006. Diverse basal and stress-related

phenotypes of Sprague Dawley rats from three vendors. *Physiol Behav,* 89**,** 598-610.

PERL, E. R. 2007. Ideas about pain, a historical view. *Nature Reviews Neuroscience,* 8**,** 71-80.

PERL, E. R. 2011. Pain mechanisms: a commentary on concepts and issues. *Prog Neurobiol,* 94**,** 20-38.

PUIG, S. & SORKIN, L. S. 1996. Formalin-evoked activity in identified primary afferent fibers: systemic lidocaine suppresses phase-2 activity. *Pain,* 64**,** 345-55.

RAFTERY, M. N., SARMA, K., MURPHY, A. W., DE LA HARPE, D., NORMAND, C. & MCGUIRE, B. E. 2011. Chronic pain in the Republic of Ireland--community prevalence, psychosocial profile and predictors of pain-related disability: results from the Prevalence, Impact and Cost of Chronic Pain (PRIME) study, part 1. *Pain,* 152**,** 1096-103.

RANG H.P., D. M. M., RITTER J.M., FLOWER R.J. 2007. *Rang and Dale's pharmacology*, Churchill livingstone elsevier.

RANOUX, D., ATTAL, N., MORAIN, F. & BOUHASSIRA, D. 2008. Botulinum toxin type A induces direct analgesic effects in chronic neuropathic pain. *Ann Neurol,* 64**,** 274-83.

RELJA, M. & TELAROVIC, S. 2004. Botulinum toxin in tension-type headache. *J Neurol,* 251 Suppl 1**,** I12-4.

ROBERTSON, C. E. & GARZA, I. 2012. Critical analysis of the use of onabotulinumtoxinA (botulinum toxin type A) in migraine. Neuropsychiatric disease and treatment, 8, 35.

ROSALES, R. L., ARIMURA, K., TAKENAGA, S. & OSAME, M. 1996. Extrafusal and intrafusal muscle effects in experimental botulinum toxin-A injection. *Muscle Nerve,* 19**,** 488-96.

SANZ-SALVADOR, L., ANDRES-BORDERIA, A., FERRER-MONTIEL, A. & PLANELLS-CASES, R. 2012. Agonist- and Ca^{2+}-dependent desensitization of TRPV1 channel targets the receptor to lysosomes for degradation. *J Biol Chem,* 287**,** 19462-71.

SCHANTZ, E. J. & JOHNSON, E. A. 1997. Botulinum toxin: the story of its development for the treatment of human disease. *Perspect Biol Med,* 40**,** 317-27.

SELTZER, Z. E., DUBNER, R. & SHIR, Y. 1990. A novel behavioral model of neuropathic pain disorders produced in rats by partial sciatic nerve injury. *Pain,* 43**,** 205-218.

SHIMIZU, T., SHIBATA, M., TORIUMI, H., IWASHITA, T., FUNAKUBO, M., SATO, H., KUROI, T., EBINE, T., KOIZUMI, K. & SUZUKI, N. 2012. Reduction of TRPV1 expression in the trigeminal system by botulinum neurotoxin type-A. *Neurobiol Dis,* 48**,** 367-78.

SHIR, Y., RATNER, A., RAJA, S. N., CAMPBELL, J. N. & SELTZER, Z. 1998. Neuropathic pain following partial nerve injury in rats is suppressed by dietary soy. *Neurosci Lett,* 240**,** 73-6.

SILLS, G. J. 2006. The mechanisms of action of gabapentin and pregabalin. *Curr Opin Pharmacol,* 6**,** 108-13.

SINDRUP, S. H., OTTO, M., FINNERUP, N. B. & JENSEN, T. S. 2005. Antidepressants in the treatment of neuropathic pain. *Basic Clin Pharmacol Toxicol,* 96**,** 399-409.

STEEDS, C. E. 2009. The anatomy and physiology of pain. *Surgery (Oxford),* 27**,** 507-511.

SZALLASI, A., CRUZ, F. & GEPPETTI, P. 2006. TRPV1: a therapeutic target for novel analgesic drugs? *Trends Mol Med,* 12**,** 545-54.

TOMINAGA, M. & TOMINAGA, T. 2005. Structure and function of TRPV1. *Pflugers Arch,* 451**,** 143-50.

VISSERS, K., DE JONGH, R., HOFFMANN, V., HEYLEN, R., CRUL, B. & MEERT, T. 2003. Internal and external factors affecting the development of neuropathic pain in rodents. Is it all about pain? *Pain Pract,* 3**,** 326-42.

WANG, J., MENG, J., LAWRENCE, G. W., ZURAWSKI, T. H., SASSE, A., BODEKER, M. O., GILMORE, M. A., FERNANDEZ-SALAS, E., FRANCIS, J., STEWARD, L. E., AOKI, K. R. & DOLLY, J. O. 2008. Novel chimeras of botulinum neurotoxins A and E unveil contributions from the binding, translocation, and protease domains to their functional characteristics. *J Biol Chem,* 283**,** 16993-7002.

WANG, J., ZURAWSKI, T. H., MENG, J., LAWRENCE, G., OLANGO, W. M., FINN, D. P., WHEELER, L. & DOLLY, J. O. 2011. A dileucine in the protease of botulinum toxin A underlies its long-lived neuroparalysis: transfer of longevity to a novel potential therapeutic. *J Biol Chem,* 286**,** 6375-85.

WHEELER-ACETO, H., PORRECA, F. & COWAN, A. 1990. The rat paw formalin test: comparison of noxious agents. *Pain,* 40**,** 229-38.

WIFFEN, P. J., MCQUAY, H. J., EDWARDS, J. E. & MOORE, R. A. 2005. Gabapentin for acute and chronic pain. *Cochrane Database Syst Rev***,** CD005452.

WOOLF, C. J. 2004. Pain: moving from symptom control toward mechanism-specific pharmacologic management. *Ann Intern Med,* 140**,** 441-51.

WOOLF, C. J. 2011. Central sensitization: implications for the diagnosis and treatment of pain. *Pain,* 152**,** S2-15.

XIAO, L., CHENG, J., ZHUANG, Y., QU, W., MUIR, J., LIANG, H. & ZHANG, D. 2013. Botulinum toxin type A reduces hyperalgesia and TRPV1 expression in rats with neuropathic pain. *Pain Med,* 14**,** 276-86.